

US Department of the Interior
National Park Service
National Center for
Preservation Technology and Training

TESTING THE ENERGY PERFORMANCE OF HISTORIC WINDOWS
IN A COLD CLIMATE

A Thesis Presented

by

Brad C. James

to

The Faculty of the Graduate College

of

The University of Vermont

In Partial Fulfillment of the Requirements
for the Degree of Master of Science
Specializing in Civil and Environmental Engineering

March, 1997

Accepted by the Faculty of the Graduate College, The University of Vermont, in partial fulfillment of the requirements for the degree of Master of Science, specializing in Civil and Environmental Engineering.

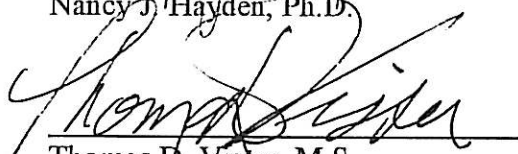
Thesis Examination Committee:



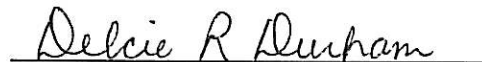
David R. Hemenway, Ph.D. Advisor



Nancy J. Hayden, Ph.D.



Thomas D. Visser, M.S. Chairperson



Delcie R. Durham, Ph.D. Dean,
Graduate College

Date: January 8, 1997

Abstract

A study was undertaken to determine the feasibility of renovating and upgrading an original condition window to the extent that its thermal performance would be equivalent to a window using replacement sash or window inserts. The study was funded by the State of Vermont Division for Historic Preservation based on a grant received from the National Center for Preservation Technology and Training of the U.S. National Park Service.

Thermal losses associated with a window are the result of infiltrative and non-infiltrative losses. Infiltrative thermal losses are a result of air infiltrating through and around a window whereas non-infiltrative thermal losses are due to conduction, convection and radiation through the materials of the window. Infiltrative thermal loss rates were based on fan pressurization data for total window and extraneous air leakage rates from 151 field-tested windows consisting of 64 original condition windows and 87 windows of varying upgrade types. Sash leakage characteristics for baseline typical, tight, and loose windows were assumed from the averaged original window data. The percentage of exterior air contained in the extraneous air volume was estimated during the test procedure based on temperature differences in the test zone during fan pressurization and added to the sash leakage for a total window leakage rate representative of the heating season. The Lawrence Berkeley Laboratory correlation model was used to convert leakage data to natural infiltration rates during the Vermont heating season. Non-infiltrative thermal losses were modeled using WINDOW 4.1, a fenestration computer simulation program.

Annual energy costs based on the combined infiltrative and non-infiltrative thermal loss rates for each upgrade category were estimated. A sensitivity analysis of the cost estimation method resulted in a variability of $\pm 25\%$. Each upgrade type was compared to the three assumed baseline windows to estimate annual energy savings in 1996 dollars. Also investigated were differing configurations of replacement storm windows and the effect double-glazing had on energy costs versus those associated with single-glazing.

Estimated annual savings per window due to renovations or upgrades ranged from zero to a high of \$3.60 as compared to a typical baseline window. Annual savings compared to a tight window ranged from \$0.05 to \$2.10 per window while savings compared to a loose window ranged from \$12.40 to \$16.60 per window. Pay-back period for any upgrade as compared to any of the typical windows was measured in decades.

A systematic upgrade of an original sash window can potentially approach the thermal performance of an upgrade utilizing replacement sash although decisions should not be based solely on energy considerations due to the similarity in savings between upgrades. It was found that approximately 85% of energy costs associated with thermal losses through and around a window were due to non-infiltrative losses. While tightening a window to prevent air infiltration around the sash and jamb and through the rough opening would reduce annual energy costs associated with a window, a more efficient use of time and resources would be to reduce non-infiltrative losses by using double- or triple-glazing and/or low-emission glass.

Acknowledgements

The final piece of writing has arrived at long last. It seems as though it began long, long ago in another building and another department. Without the assistance, support, encouragement, and words of advice from physicists extraordinaire, Dr. Robert Detenbeck and Dr. Kevork Spartalian, I would have been left floundering along the way many years ago. Their insight and humor kept me going through some tough times and they have my gratitude and respect. I would like to extend thanks to Dave Hammond, also of the physics department whose brand of humor (or lack thereof) was at least as twisted as mine. Dave kept me entertained and was also a fountain of information, some of which was even useful.

Upon becoming a convert to Environmental Engineering, I encountered a multitude of colorful characters. There were even some interesting graduate students. In no particular order, my thanks are extended to Dr. Olson and Dr. Downer for their advice on this project and their perceptions of life in general. I would like to thank Gail Currier for keeping me organized and for showing me how to use the fax machine - six or seven times. Many thanks to Dr. Nancy Hayden, whose five minute introductory discussion of the department with me took fifty minutes. She was instrumental in my decision to switch programs and was rewarded with the honor (?) of sitting on my committee. I enjoyed the many rambling discussions we had as well as her wit, a wit only surpassed by her singing ability which in turn was only surpassed by an as yet unnamed graduate student. And then of course, there was Dr. David Hemenway, my illustrious advisor and purveyor of fine (!?!) humor, a gentleman who kept me on track towards this end. Special thanks to him for his patience and guidance.

I would never have made it through the morass of computer programs and

accompanying glitches without the inestimable Dr. Patrick O'Shaughnessy. But more than that, his friendship and conversations were much appreciated, even though he never understood my allegiance to certain teams. The same holds true for Harry Linnemeyer and his melodious voice - the entertainment value of these two kept everything in perspective. Beth Live-in-the-woods Stopford, Parm Robusto Padgett, Chad No-respect-for-my-elders Farrell, Jennifer I-like-grad-student-life Bryant, and John G.C. Diebold were, if not necessarily helpful, always good for a laugh and a discussion way off topic. Then, there was the one familiar face of Bill McGrath, hearkening back to my first year of teaching. Those were the days when I knew more than he did. And let us not forget Mr. Ted Lillys, the one person whose morals were more questionable than mine.

In a serious vein, special thanks to Sylvia and Anders for bearing with me as I went through some trying times. I could not have done this without their support. I would also like to let Cyrus, the Wonder Dog, know that next year I will get him out in the woods - I have missed that companionship these last few years. It was for the three of you, my family, that I have attempted to better myself. Thanks to you all.

Table of Contents

Acknowledgements	ii
List of Tables	vii
List of Figures	ix
Glossary of Terms	xi
 Chapter	
1 Introduction	1
1.1 Objectives and hypothesis	4
1.2 Background and Significance	5
 2 Assumptions and Typical Parameters	 15
2.1 Typical affordable housing parameters	18
2.2 Typical parameters for existing windows	19
2.3 Original condition windows and window upgrades field tested	20
 3 Methodology	 24
3.1 Contribution of window thermal losses to whole house losses	24
3.2 Development of flow equations	26
3.3 Infiltrative thermal losses	30
3.3.1 Fan pressurization test method description	33
3.3.2 Environmental and window parameters recorded	34
3.3.3 Determination of percent exterior air in Q_e	36
3.4 Correlation of air leakage to natural infiltration rates	38
3.5 Non-infiltrative thermal losses	45
3.6 Total window thermal losses	45
3.7 Thermography	46
3.8 Energy savings due to window upgrades	47
 4 Results	 49
4.1 Appropriateness of flow model	49
4.2 Field test results - original condition windows	52
4.2.1 Air leakage characteristics of windows over time	54
4.2.2 Leakage characteristics of pin- versus pulley-type windows	56
4.2.3 Sash leakage reduction due to existing storm windows	57
4.2.4 Air leakage characteristics of single- versus double-hung windows	58
4.2.5 Correlation of descriptive physical parameters with air leakage rates	61
4.2.6 Original condition window summation	62
4.3 Field test results - window upgrades	63
4.3.1 Upgrades retaining the original sash	63

4.3.2	Replacement sash upgrades	70
4.3.3	Window insert upgrades	71
4.3.4	Storm window upgrades	72
4.3.5	Double- versus single-glazing upgrades	75
4.3.6	Window upgrades summation	76
4.4	Laboratory test window data	77
4.4.1	Leakage locations and reduction of leakage rates due to routine maintenance	78
4.4.2	Laboratory tests of Bi-Glass System upgrade	83
4.4.3	Laboratory testing summation	86
4.5	Natural infiltration rates	87
4.6	Thermography	91
4.7	Energy savings attributable to upgrades	98
4.8	Estimated costs for upgrade purchases and installation	101
5	Analysis and Discussion	105
5.1	Sensitivity analysis of cost estimation method	106
5.2	Correlating flow exponent to effective leakage area	107
5.3	Windows in heating season configurations	110
5.4	Infiltration reduction in windows tested pre- and post-upgrade	113
5.5	Improvements due to storm window upgrades	115
5.6	Infiltrative versus non-infiltrative thermal losses	116
6	Conclusions	119
6.1	Estimating savings in other locales	121
6.2	General observations	124
6.3	Further work	126
	References	127
Appendix		
A.	Anatomy of a double-hung window	131
B.	Calibration curve of fan pressurization unit	132
C.	Flow and regression data for field tested windows	134
1.	Sash air leakage (Q_s)	134
2.	Extraneous air leakage (Q_e)	137
3.	Total air leakage (Q_t)	140
D.	Numerical conversions and transformations	143
1.	Data standardization	143
2.	Standard cubic feet per minute per linear foot crack	143
3.	Standard cubic feet per minute per square foot of sash area	144
4.	Effective leakage area	144
E.	Field data sheets	146

1. Window data sheet	146
2. Physical condition check sheet	147
3. Physical condition criteria	148
F. Data sheet interpretation	150
1. Reference data sheet	152
G. Exterior air	153
1. Determination of percent exterior air in Q_e	153
2. Experimental data used to determine percentage exterior air	155
H. Equations for weather parameters based on psychrometric data	156
1. Determining dew point temperature and partial water vapor pressure	156
2. Determining relative humidity	158
I. Assumptions for using WINDOW 4.1	160
J. LBL correlation model computer printout	161

List of Tables

1: Site locations and ID's, showing numbers of original windows and upgrades tested	22
2: Window upgrades	23
3: Generalized shielding coefficients	41
4: Terrain parameters for standard terrain classes	42
5: Wind speeds equivalent to test pressure differentials	51
6: Assumed air leakage characteristics for original condition windows	53
7: $ELA_{RO \times 19}$ values for original condition pin- versus pulley-type windows with storms open	57
8: Comparison of 24 original condition windows with existing storms open and closed	58
9: Single- versus double-hung window sash leakage characteristics	60
10: Number of windows tested by general window upgrade category	63
11: Average leakage characteristics for upgrade types retaining original sash	65
12: Leakage characteristics for 11 replacement sash	70
13: Sash leakage characteristics for replacement window inserts	71
14: Comparison of exterior air volumes by upgrade type	72
15: Storm window upgrades by type	73
16: Percent reduction in extraneous leakage by interior storm window configuration	75
17: Non-infiltrative thermal loss rates for assumed windows and glazing replacements	75
18: Parameters assumed to be typical of Vermont, used in the LBL correlation model	87

19: Estimated natural infiltration flow rates (Q_{nat}) for the period October through April	90
20: Estimated first year annual savings in 1996 dollars due to window upgrades ($\pm 25\%$)	100
21: Estimated window upgrade costs as of August 1996, including materials and installation but excluding lead abatement costs	103
22: Averaged leakage characteristics of windows prior to and post renovation	114
23: Comparison of first year energy savings per window from double-versus single-glazed sash ($\pm 25\%$)	117
24: Estimated costs and first year energy savings ($\pm 25\%$) of categorized upgrades	120
25: Selected cities with heating degree-day units and conversion factors to estimate savings for other climates, based on the Burlington, VT data	123
26: Calibration data for the DeVac fan pressurization unit	133
27: Percentage of Q_{ext} in Q_e for 33 windows	154

List of Figures

1: Principle air leakage sites and construction features for a typical double-hung window	3
2. Schematic of the fan pressurization test set-up	33
3: Variability in R^2 values of a standard flow model fitted to the field data	50
4: Schematic of an original sash and jamb modified to accept a vinyl jamb liner and silicone bulb weatherstripping	67
5: Schematic of lower sash and vinyl jamb liner junction	68
6: Reproducibility of lab pressurization test results and test device over time	79
7: Lab window A leakage rates, original condition window versus routine maintenance	81
8: Lab window B, relative leakage reductions due to Bi-Glass System upgrade	85
9: Thermograph of sash infiltration reduction due to rope caulking	93
10: Thermograph of plexiglass interior storm window adjacent to window with interior storm removed	94
11: Thermograph of Robinson Hall window with no effective storm window attached	95
12: Thermograph of Robinson Hall window with aluminum triple-track storm window in place	96
13: Thermograph of Robinson Hall window with Bi-Glass System upgrade	97
14: Variability of flow exponent with ELA_{tot} for original condition windows	108
15: Variability of flow exponent with ELA_{tot} for window upgrades	108
16: Frequency distribution of flow exponent (x) for all windows	109

17: Frequency distribution of ELA_{tot} for all windows 110

18: Mean sash leakage flow exponents for eight general upgrade categories,
plus/minus one standard deviation 111

19: Mean whole window effective leakage area (ELA_{tot}) for eight general
upgrade categories, plus/minus one standard deviation 112

20: Comparison of costs due to infiltrative and non-infiltrative thermal losses
for selected window types, with and without storm windows 116

21: Anatomy of a double-hung window 131

22: Calibration curve for the DeVac fan pressurization unit 132

Glossary of Terms

Actual cubic feet per minute (acfm) - the volume of air at ambient conditions passing through the fan pressurization device per unit time

Air leakage - induced air flow through a building envelope or window when using fan pressurization. Induced air flow is a measure of building or window tightness.

Effective leakage area (ELA) - the area of a round orifice with a flow coefficient equal to one, allowing an air flow equivalent to the summed gaps around a window

Extraneous air leakage (Q_e) - the volume of air flowing per unit time through the rough opening and test apparatus when under pressurization by the testing device

Humidity ratio - mass of water vapor per mass of dry air. Essentially, the mass of water vapor contained within a volume of air as compared to the mass of that air if it were dry.

Infiltration - uncontrolled air flow through unintentional openings driven by pressure differentials induced by temperature differences and winds

Infiltrative heat load - thermal losses through a window from air moving around the sash and jamb as well as through any cracks or gaps associated with the window.

Linear foot crack (lfc) - the sum of all operable sash perimeter of a window, expressed in feet

Natural infiltration - uncontrolled air flow during the heating season through unintentional openings driven by pressure differentials induced by temperature differences and winds

Non-infiltration heat load - the thermal loss due to convection, conduction, and radiation through a window

R-value - thermal resistance ($\text{hr}\cdot\text{ft}^2\cdot^\circ\text{F}/\text{Btu}$). The steady condition mean temperature difference between two surfaces that induces a unit heat flow rate per unit area. Essentially, a measure of resistance to heat flow. R-value is the inverse of U-value.

Relative humidity - the ratio of the amount of water vapor in the air to the maximum amount of water vapor the air can hold at the ambient temperature.

Rough opening - the opening in a building envelope designed to accept a window

Sash air leakage (Q_s) - the volume of air flowing per unit time through the window exclusive of any air from the rough opening during the testing period

Standard cubic feet per minute (scfm) - the volume of air per unit time passing through the fan pressurization device, converted to standard conditions for reference and comparative purposes. Standard conditions for this study were defined as:

- standard temperature - 69.4°F (20.8°C)
- standard pressure - 29.92 inches of mercury (760 mm Hg)

Standard cubic feet per minute per linear foot crack (scfm/lfc) - standardized volume of air per unit time passing through one linear foot crack of operating window perimeter

Total air leakage (Q_t) - the volume of air flowing per unit time through the window system when under pressurization by the testing device

U-value - thermal transmittance (Btu/hr-ft²-°F). The rate of heat flow per unit time per unit area per degree temperature differential. Essentially a measure of thermal transmission through window materials and the boundary air films. U-value is the inverse of R-value.

Window - includes the jamb, sash, associated hardware but excludes the rough opening and any spaces between the jamb and rough opening

Window system - includes the window, any space between the window and rough opening, and framing members that form the rough opening

Nomenclature:

ELA_s /lfc - effective sash air leakage area per linear foot crack (in²/lfc)

ELA_{ext} /lfc - effective extraneous air leakage area per linear foot crack (in²/lfc)

ELA_{tot} /lfc - effective whole window leakage area per linear foot crack (in²/lfc)

ELA_{tot} - effective whole window leakage area (in²)

Q_{nat} - natural air infiltration rate during the heating season, due to pressure differentials induced by wind speed and direction, as well as interior/exterior temperature differences (scfm)

L_{inf} - whole window infiltrative thermal loss rates (Btu/hr-°F)

L_{non} - non-infiltrative thermal loss rates (Btu/hr-ft²-°F)

L_U - whole window non-infiltrative thermal loss rates (Btu/hr-°F)

L_{eff} - whole window thermal loss rates; infiltrative and non-infiltrative thermal loss rates combined (Btu/hr-°F)

L_{yr} - annual whole window thermal losses (Btu/yr)

C_{win} - annual energy costs per window (\$)

S_{win} - annual savings per upgrade (\$)

Chapter 1

Introduction

Windows serve a variety of integral roles in buildings, ranging from admitting light and ventilation to an expression of period technology and design. Windows also have a major impact on the energy consumption of a building as any thermal loss through a window must be replaced by the heating system. When historic buildings are to be renovated, the question of the existing historic windows is inevitably raised. The desire to retain the historic character of the windows and the actual historic material from which the windows are made is seen as competing with the desire to improve energy performance and decrease long term window maintenance costs. Replacement of window sash, the use of windows inserted inside existing jambs, or whole window replacement is often advocated in the name of energy efficiency, long-term maintenance cost reduction, ease of operation, and better assurance of window longevity. The renovation of historic windows to improve energy efficiency retains all or part of the existing sash and balance system and typically includes exterior triple-track storm window rehabilitation or replacement. To date, there is little data that quantifies the impact on estimated first year heating costs of these varied approaches or compares the estimated value of energy saved to installed costs. This study was undertaken to address the assumption that historic windows can be retained and upgraded to approach the thermal efficiency of replacement sash or window inserts. While window upgrades often improved other aspects of windows including ease of operation, reduction of lead hazard, and occupant comfort, only energy impacts were included in this study.

In December 1994, the State of Vermont Division for Historic Preservation of the

Agency of Commerce and Community Development issued a Request for Proposals to address the energy impacts of the rehabilitation versus replacement issue, based on a grant from the National Park Service and the National Center for Preservation Technology, and Training. The study was directed toward windows in historically significant buildings, including affordable housing and private residences. Major issues addressed were:

- energy savings attributable to existing window retrofits,
- estimating first year savings in heating costs attributable to field tested window retrofits,
- installation and materials costs for existing window retrofits, and
- the comparison of costs and savings from existing window retrofits to those incurred by replacement windows.

The decision to rehabilitate or replace a window is often based on factors other than long-term energy conservation, including the historical significance of a window, its role in a building's character, occupant comfort, and ease of operation. While some of these factors were often improved during window upgrades, only energy costs associated with reduced thermal losses due to infiltration and non-infiltration were studied. Infiltrative thermal losses are due to exterior air moving through and around the sash and rough opening. Infiltrative losses were investigated by field and laboratory pressurization testing. Figure 1 is a schematic diagram of a standard double-hung window, showing typical air leakage sites for that style window. Non-infiltrative losses include conduction, convection, and radiation through the materials of the window and were simulated using a computer model.

While historically significant buildings are found throughout Vermont, few were

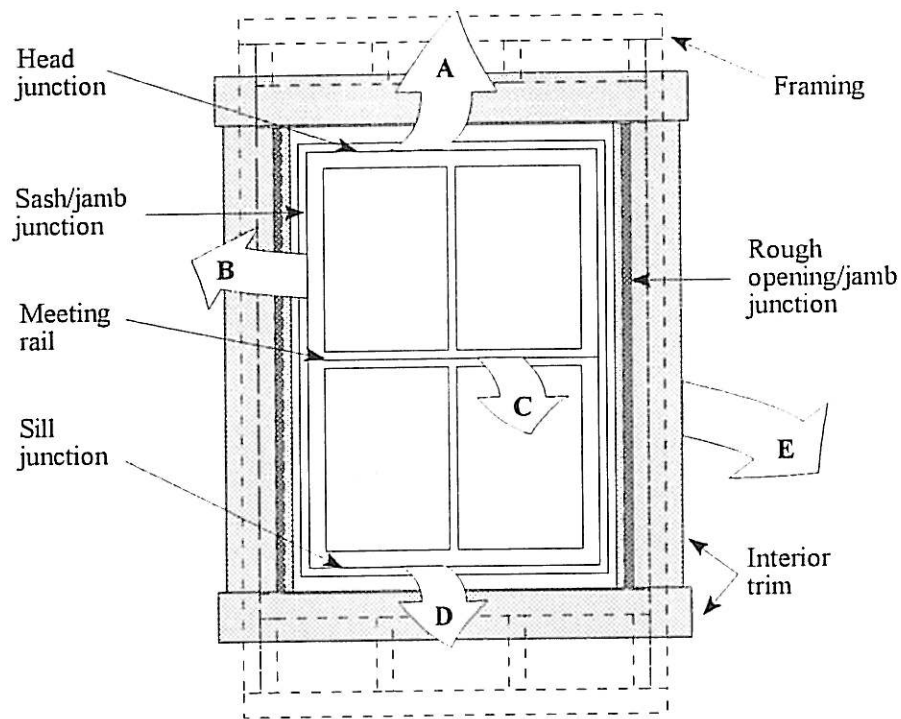


Figure 1: Principle air leakage sites and construction features for a typical double-hung window

- A - air infiltration through the head junction
- B - air infiltration through the sash/jamb junction
- C - air infiltration through the meeting rail
- D - air infiltration through the sill junction
- E - air infiltration through and around the jamb from the rough opening

scheduled for renovations during the time frame of the study. Many affordable housing buildings and private residences in Vermont are of the same nature as historic buildings and were scheduled for, or had undergone renovations during the required time period. Due to building similarities, windows in affordable housing and private residences consequently constituted the majority of field testing with the inclusion of some historical windows renovated during the course of the study.

This report contains the results of the study implemented to determine the effectiveness of various window rehabilitations in reducing infiltrative and non-infiltrative thermal losses. Those rehabilitations included windows utilizing existing sash as well as several replacement options. The results, gathered from 151 windows at 19 sites, estimate the first year energy impacts of upgrades associated with a reduction in heating cost requirements during an average Vermont heating season. No attempts were made to estimate either the contribution of solar gains during the heating season or energy impacts associated with reductions in cooling requirements due to window upgrades.

While not addressing all issues concerning window performance and operation, the results of this study concerning the energy performance of windows during the heating season will be beneficial to the historical preservation community as well as providers and developers of affordable housing and the general home-owner. This information will allow those organizations and individuals to make better informed choices about window rehabilitation and replacement strategies based on actual data as opposed to anecdotal evidence.

1.1 Objectives and hypothesis

The objectives of this study were to compare the thermal efficiencies of a variety of window renovations retaining the original wood sash to the thermal efficiencies of several replacement sash and window options. Knowing an estimate of the thermal efficiency of a window allowed for a calculation of the annual heat loss through a window, and thus the cost of energy associated with that window. As such, specific areas this study addressed include the following:

- energy savings attributable to existing window retrofits,

- estimating first year savings in heating costs attributable to field tested window retrofits,
- installation and materials costs for existing window retrofits, and
- the comparison of costs and savings from existing window retrofits to those incurred by replacement windows.

1.2 Background and significance

Energy costs are the result of infiltrative and non-infiltrative thermal losses, both of which were estimated during the study. Infiltrative losses through the sash and rough opening were estimated by fan pressurization and combined with non-infiltrative loss estimates, determined by a computer simulation model. Excessive natural infiltration may lead to a number of unwanted effects and problems in a building during the heating season. The addition of cold, infiltrative air represents an additional heat load for the building, unnecessarily increasing annual energy costs. Drafts from infiltrating air affect occupant comfort levels near windows or may preclude the use of entire rooms. Older buildings are subject to low relative humidity levels due to excessive infiltrative exterior air during the heating season. Exterior air has a low humidity ratio (mass of water vapor to mass of dry air), even though it has a high relative humidity. When the exterior air is heated, the humidity ratio remains constant but the relative humidity drops precipitously, giving rise to dry air.

As cold exterior air infiltrates a building during the heating season, warm interior air exfiltrates through wall and window openings as it is displaced. Prior to exfiltration, the warm air has increased its moisture content by accumulating water vapor from occupant respiration, cooking, and washing among other sources. As the warm air passes through the

building shell, temperature decreases and condensation may occur in insulation or on structural elements as the warmer air contacts the cooler surfaces. Condensation decreases the insulative value of insulation and may lead to wood rot.

A literature review was undertaken to determine the nature of previous work and findings relevant to the study.

One of the primary purposes of building renovation is to reduce energy consumption and costs via thermal losses due to air infiltration. A large body of pre- and post-renovation data for whole building energy consumption does not exist. However, a reduction in building energy requirements may be accomplished by reducing air infiltration through sills, walls, basements, attics, doors, and windows. Estimated energy costs associated with air infiltration range from 33% of total building energy costs (Sherman et al., 1986) to as much as 40% (Giesbrecht and Proskiw, 1986). Upon completion of whole building retrofitting, reductions in energy costs attributable to infiltration have been estimated to range from 19% based on a 55 house sample (Jacobson et al., 1986) to 50% for a single townhouse (Sinden, 1978). Most saving estimates fall between 30-37% (Giesbrecht and Proskiw, 1986; Harrje and Mills, 1980; Nagda et al., 1986). Giesbrecht and Proskiw also found two-story houses showed lower reductions in infiltration after renovations (24.4%) than single-story houses (36.9%), likely due to leakage between floors.

Of concern to this study was the portion of total house leakage attributable to infiltration through and around windows. Estimates of window contribution vary more widely than whole house leakage estimates. Two separate studies found the fraction of window leakage to be approximately 20% of whole house leakage (Tamura, 1975; Persily and

Grot, 1986). An estimated 37% of the total heat loss from a house may be due to infiltration through windows and doors (Lund and Peterson, 1952), while a 20 house survey showed these sources are unlikely to exceed 25% (Bassett, 1986).

The use of a mathematical model estimated 25% of heat loss through a loose fitting, nonweatherstripped window was attributable to infiltration with the remaining 75% of loss attributable to non-infiltrative losses (Klems, 1983). The modeled window was assumed to be typical of windows found in older housing (i.e., double-hung wood sash with single-glazing and a storm window). A reasonably tight double-pane window, typical of new construction, was estimated to have 12% of its thermal losses attributable to infiltration by the same model. Energy costs associated with infiltrative losses became a significant portion of total fenestration energy costs when air leakage rates exceeded 0.5 cubic feet per minute per linear foot crack (cfm/lfc) based on the Residential Fenestration (RESFEN) computer model developed by Lawrence Berkeley Laboratory (LBL, 1994a), University of California, Berkeley (Kehrli, 1995a). Various leakage rates at 0.30 inches of water pressure (75 Pa) were modeled with RESFEN, then reduced to total window energy losses at 0.016 inches of water pressure (4 Pa), the assumed average heating season interior/exterior pressure differential. Costs due to infiltration as a percentage of total window energy costs varied from 15% at 0.5 cfm/lfc to 41% at 2.0 cfm/lfc for a two story house, based on the RESFEN simulation.

The intent of weatherstripping a window is to reduce the amount of air infiltrating through the sash/jamb junctions and the meeting rails. Infiltrative losses were reduced from 37% to 17% of total house thermal losses when metal rib-type weatherstripping was installed

around the windows (Lund and Peterson, 1952). This corresponded to an approximate 24% reduction in building energy costs.

The installation of storm windows, either exterior or interior, presents its own range of advantages and disadvantages. In general, properly installed new storm windows in combination with existing single-glazed windows may achieve U-values comparable to insulating glass and reduce air infiltration while lowering maintenance costs and extending the life of the window (National Park Service, 1986). Thermal transmittance (U-values) refers to the amount of heat a one foot square section of window would lose per hour for every one degree Fahrenheit temperature differential and has units of $\text{Btu}/\text{ft}^2\text{-hr-}^\circ\text{F}$. Lower numerical values for thermal transmittance imply better thermal efficiency.

Disadvantages of exterior storm windows include visual obstruction of an historic window and its attendant details, while interior storm windows may increase condensation and cause moisture related problems to the primary sash (Park, 1982). The negative visual effect of exterior storm windows may be reduced by using single lite storm sash. Interior storm windows have avoided the problem of condensation by incorporating vent holes and a sealed fit (Park, 1982). The use of interior storm windows can also reduce infiltration by reducing air movement through the sash or rough opening into the building interior. Whole house energy consumption was reduced by 12% in a test house in England fitted with interior storm windows (Rayment and Morgan, 1985).

Many builders, contractors, and individuals purchasing new windows for either new construction or renovation are increasingly aware of energy considerations and choose windows based on rates of sash air leakage and thermal transmittance (U-values) as well as

appearance. These ratings are provided by window manufacturers and are the results of independent testing by accredited simulation laboratories. Laboratories are accredited by the National Fenestration Rating Council, with each accredited laboratory having one or more certified simulators. Air leakage tests are conducted according to ASTM E 283-91 (ASTM, 1994a), while thermal transmittance tests follow ASTM E 1423-91 (ASTM, 1994b; Kehrl, 1995b).

For sash air leakage, test results are generally provided as cubic feet per minute per linear foot-crack (cfm/lfc) at a differential of 0.30 inches of water pressure (75 Pa). National standards for sash air leakage at 0.30 inches of water (75 Pa) allow a maximum sash flow of 0.37 cfm/lfc for new windows in order to be certified (Warner and Wilde, 1996).

ASTM E 1423-91 is both a complex and expensive laboratory testing process, averaging \$1200 per test (Kehrl, 1995b). Researchers at the Lawrence Berkeley Laboratory have developed an interactive computer program to calculate the thermal transmittance of windows (LBL, 1994b). This program, WINDOW 4.1, is based on actual window testing following the ASTM E 1423-91 method and is consistent with the rating procedure developed by the National Fenestration Rating Council (NFRC, 1991). Test data listed by window manufacturers are the results of WINDOW 4.1, the LBL computer simulation program. Manufacturers provide a random sample of their higher and lower end window models to the accredited testing laboratories to ensure actual compliance with certifiable specifications (Weidt, 1995).

Should a renovation project be designed with replacement windows, a factor in the decision making process as to which windows are appropriate may be the results of the

manufacturers' infiltration test data. The maximum 0.37 cfm/lfc allowable sash flow for certification is often exceeded by windows, as shown by both field and production-line testing (Kehrli, 1995a). An on-site study of window leakage rates was done in the Minneapolis/St. Paul metropolitan area, comparing listed air leakage rates of 192 windows to actual measured leakage rates after installation in new residential constructions. Window models from sixteen manufacturers were tested, which included both double- and single-hung windows as well as casement and slider windows. Of all the window tested, 60% exceeded the manufacturers' listed performance specifications while 40% exceeded the 1979 industry maximum of 0.50 cfm/lfc for certifiable windows. More specifically, 79% of double-hung and 100% of single-hung windows exceeded the manufacturers' lab data. Installation technique, as performed by the various contractors, showed no significant effect on window performance (Weidt et al., 1979).

The Weidt study also showed double-hung windows had lower air infiltration rates per linear foot crack than did single-hung windows within any manufacturer. Infiltration rates expressed as cfm/lfc may be a misleading statistic when comparing different window types. As an example, a typical double-hung window has approximately 70% more operable linear crack per sash area than a single-hung window of identical size. If the two windows show equal air leakage rates per linear foot crack, more air is actually moving through the double-hung window due to its larger operable linear crack perimeter. When infiltration is expressed as cfm/sash area or cfm/ventilation area, single hung windows outperform double hung windows (Weidt et al., 1979).

Within the confines of how the predominant energy loss of a window occurs, there

is some debate. Those advocating non-infiltrative thermal losses being much greater than infiltrative losses, recommend all single-glazed sashes be replaced with double-pane insulating glass (Kehrli, 1995b). Energy losses due to direct heat transmission through a window were observed to be consistently greater than those due to air leakage, regardless of the leakage rate considered (Klems, 1983). In a comparison of energy requirements between a test house and an identical control, it was estimated that replacing single-glazing with double-glazing reduced losses via thermal transmission such that building space heating requirements were reduced by 9% (Rayment, 1989). If double-pane insulating glass is to be used and the original sash retained, there must be adequate wood thickness to accommodate the rabbeting necessary to insert thicker, double-pane glass. The wood must also possess the strength to support the extra weight of the double-pane glass (National Park Service, 1986). This has been done in some old single-lite sash but presents a more complicated problem in multi-lite sash where muntins are present. As compared to a single-lite window, the larger glass/wood edge perimeter of a multi-lite window will reduce the thermal improvements of double-pane insulating glass by allowing more conduction through the edges.

Others believe that air infiltration is a larger contributor to poor energy performance than single-glazing and any steps taken to reduce infiltration are nearly always cost effective (National Park Service, 1986). The Colcord Building in Oklahoma City reduced its space heating costs by 25% when its loose fitting, single glazed windows were renovated. Renovation included reglazing with new putty compound, painting, bronze V-strip spring weatherstripping, and the addition of removable interior acrylic storm panels (Park, 1982). It was undetermined what fraction of heating cost reductions were attributable to the interior

storm window and what fraction arose from the other renovations.

The addition of acrylic storm panels in the Colcord Building constituted a second glazing layer which served to decrease non-infiltrative losses through the windows. Acrylic panels were chosen over glass due to weight considerations, but provided the additional benefit of decreasing non-infiltrative losses by 15% as compared to ordinary glass storm panels. Storm windows in general provide a second glazing layer, reducing non-infiltrative thermal losses. Exterior storm windows provide the additional benefit of lowering window maintenance costs as well as prolonging window life by preventing accumulations of moisture (Fisher, 1985).

A significant source of infiltration may be the gap between the rough opening of the building and the frame of a window unit (Flanders et al., 1982). Estimates of infiltrative contributions through window rough openings range from 12% of whole building energy loads in loose construction (typical of affordable housing stock) to 39% in tighter construction (Proskiw, 1995a). Air leaking through the rough opening/frame juncture around an otherwise tight window will adversely affect the overall performance of the window unit (Louis and Nelson, 1995). The conventional method used to seal this gap in new construction is to insert fiberglass insulation between the rough opening and frame, even though fiberglass insulation is not intended to be an air barrier material. A laboratory study in Winnipeg, Canada, showed the conventional sealing method still allowed significant air leakage through the rough opening (Proskiw, 1995a).

The amount of air attributable to leakage through the rough opening was estimated for both loose and tight houses. A loose house was assumed to have 5 ACH₅₀ (5 air changes

per hour at 50 Pa, or 0.20 in. H₂O), typical of older houses. A tight house was assumed to have 1.5 ACH₅₀. Ratios of rough opening to whole house leakage were based on laboratory results, which gave estimates of 14% rough opening leakage for tight houses and 4% for loose houses. The two most efficient and cost effective methods for sealing rough openings were low expansion urethane foam and casing tape, reducing estimates of rough opening leakage to less than one percent of whole house leakage (Proskiw, 1995a). Casing tape is the tape normally used for taping joints between exterior sheets of insulated sheathing.

Older buildings often do not have any barrier between the frame and rough opening, allowing air access to the window unit with little impediment. Proskiw estimated 39% of total house air leakage was from rough openings in a loose house typical of older construction. The most effective means of reducing extraneous leakage require removal of both interior and exterior trim. Trim removal provides exposure and access to the window frame/rough opening junction, allowing thorough sealing. Care must be taken when using expandable foam to prevent overfilling, which could lead to window jamb distortion. It is possible to drill small holes in the jamb to insert foam, but three potential drawbacks exist. Insertion holes may be visible, but more importantly, there is a greater risk of overfilling the cavity with foam, which would cause distortion of the jamb. A complete seal also cannot be ensured without visual inspection. Removal of the trim provides this opportunity.

Relative humidity plays a significant role in infiltration through old wooden windows by influencing the fit of the sash to the frame. The physical change in wood dimensions as wood absorbs or releases atmospheric moisture affects the gap dimensions between the sash and frame, directly influencing infiltration. Temperature also affects wood dimensions but

relative humidity is a more important factor than wood temperature, with cold wood expanding more from absorption of outside moisture than from temperature changes (Lstiburek, 1995). While cold air in the winter does not carry a large amount of moisture, its relative humidity is approaching saturation due to the decreased amount of moisture the cold air may hold. Conversely, moisture migrating from the living space through the interior walls and gaps may condense on the cold wooden sash and jambs. This implies that some moisture absorption may occur in the winter with a corresponding degree of swell.

Significant reductions in infiltration may be accomplished by routine maintenance of an existing window while improving its integrity. Routine maintenance includes removing the glass, applying back putty, reinserting the glass, repointing and reglazing. Excess paint should be removed and any necessary sash or frame repairs done along with the installation of good quality weatherstripping (National Park Service, 1986). Repainting the sash, frame, and glazing will help provide a good seal against the elements.

The advantages of renovating existing windows versus replacement in an historic building include saving the historic value and design of the window as well as the interior/exterior appearance. For these reasons, it is advantageous to investigate methods of rehabilitation in an historic building. It has been shown in both the Colcord Building in Oklahoma City (Park, 1982) and the Delaware Building in Chicago (Fisher, 1985) that effective window rehabilitation can be accomplished at a lower cost than replacement windows while still resulting in significant energy savings.

Chapter 2

Assumptions and Typical Parameters

In order to test the hypothesis that renovated windows can approach the energy savings of replacement windows or sash, estimates of energy costs due to infiltrative and non-infiltrative thermal losses through and around a window were required. Infiltrative losses through the sash and rough opening were estimated by fan pressurization and combined with non-infiltrative loss estimates, determined by a computer simulation model. Data were normalized to an assumed standard window size (36 x 60 inches) with leakage characteristics of assumed baseline windows based on data from 64 original condition windows. First year energy savings achieved by upgrading existing windows were estimated as the difference between energy costs attributable to an assumed baseline window and those attributable to a window upgrade.

An estimate of typical heating season energy costs had to be made in order to estimate savings realized from any type of window upgrade. This necessitated the definition of a building typical of affordable housing from which a base line estimate of annual energy costs could be made. The windows in such a defined building were also to be typical of existing window stock. Although the focus of the study was to be residential historical windows, the decision was made to base estimated energy costs on a typical building used for affordable housing. The reasons for the decision were twofold - few historical windows were scheduled for renovation during the period of the study and affordable housing stock was representative of many Vermont residences, including many historical structures.

The relationship between thermal losses through typical windows to total house

energy costs was of concern in order to simplify these calculations. If a reduction in thermal loss through a single window due to energy improvements correlated directly to a reduction in whole building annual heating cost due to a window upgrade, then savings could be modeled for each window upgrade directly. If this were not the case, then a whole building simulation utilizing each upgrade type would be required. This required development of a typical building and baseline windows for the purposes of the study.

For whole buildings, pressurization data in terms of effective leakage area (ELA) has been correlated to natural infiltration by a fluid mechanical model developed by the Lawrence Berkeley Laboratory (LBL), also known as the Sherman-Grimsrud model (Sherman, 1980; Grimsrud et al., 1982). The LBL model uses a whole building ELA and a calculated coefficient to determine the seasonal average infiltration rate of a whole house (Grimsrud et al., 1982). This coefficient, specific to both house, climate, terrain, and shielding is the average heating season infiltration per unit ELA. Knowing the average seasonal infiltration rate, heating degree-days for the climate, heating system efficiency, and the cost of fuel allows an estimation of the heating costs attributable to the building.

For the purposes of this study, the use of the LBL correlation model was modified by using data from a single window rather than whole house data. The assumption was made that when using a window ELA, the results of the LBL model would have the same relative significance in predicting the average annual heating season natural infiltration rate for a window as the model would have when using a whole building ELA to predict the building heating season natural infiltration rate. It is recognized that this was not the intent of the model and as such, none of the derived values should be treated as absolutes. Rather,

numbers should be viewed only as relative values and used solely for comparative purposes with other values similarly derived in this study.

Air leakage characteristics for baseline windows were based on pressurization field testing of 64 original condition windows in older buildings and homes. These data were extrapolated to 0.016 inches of water pressure (4 Pa) and correlated to natural infiltration rates using the LBL correlation model.

A potentially significant source of thermal loss due to air leakage was around the window frame by way of the rough opening (Figure 1). The thermal loss may be of sufficient magnitude to significantly affect the thermal performance of an efficient window. A new test methodology cited in the literature has been proposed to segregate and quantify the amount of extraneous air leaking through the rough opening into the test chamber and window surround components (Louis and Nelson, 1995). The proposed methodology does not quantify the exterior air included in the extraneous air volume, but suggests several methods to estimate the exterior air volume using tracer gases, temperature, or air velocity probes.

One of the outcomes of the current study was a field method used to quantify the percentage of exterior air contained in the induced extraneous air entering the test chamber from the rough opening during pressurization testing. A simple method of estimating the volume of exterior air passing through the rough opening during fan pressurization is presented, based on temperature differentials (Section 3.3.3). The method, implemented in the spring of 1996, required an interior/exterior temperature differential and could only be applied during the pressurization testing of 33 windows due to a limited number of available interior/exterior temperature differentials.

The two infiltrative thermal loss rates based on field testing were combined for an overall window infiltrative thermal loss rate. The infiltrative loss rate was combined with the non-infiltrative thermal loss rate, derived from computer modeling, to give a total thermal loss rate for a window. First year energy costs associated with renovated windows or those associated with replacement sash or window inserts were estimated from these total thermal loss rates for any given window.

2.1 Typical affordable housing parameters

As previously mentioned, a typical affordable housing building was used to estimate energy costs although the focus of the study was on residential historical windows. Affordable housing provided a pool of old windows scheduled for renovation during the time frame of the study and was also representative of many Vermont residences. Affordable housing may be found in all manner of buildings, but in Vermont these buildings generally are two story structures with both an attic and basement. The following criteria were chosen to characterize a typical, historical affordable housing building:

- 30 x 50 foot rectangular building with a gable roof;
- two heated stories with an unheated attic having R-19 insulation;
- uninsulated basement, heated only by losses from the heating system and floor above;
- uninsulated basement walls, exposed 2 feet above grade;
- wood frame 2 x 4 walls, uninsulated;
- eight windows on each 50 foot side, four on each 30 foot side for a total of 24 windows;

- two wooden doors, 3 ft. x 6 ft. 8 in., without storm doors;
- oil-fired heating system, 65% efficient;
- 6,100 cfm infiltration rate at 0.20 in. water pressure (50 Pa), equivalent to an average 1.2 air changes per hour during the heating season; and
- leakage areas equally distributed between the walls, floor, and ceiling.

It was assumed for this study that the building would be renovated at the same time as the windows. Assumed typical post-renovation building parameters are listed below:

- walls insulated with dense-packed 4 inch cellulose (R-15);
- attic floor insulated to 12 inch settled depth (R-38);
- storm doors installed;
- infiltration rate reduced to 2,200 cfm at 0.20 in. H₂O (50 Pa) equivalent to an average 0.41 air changes per hour during the heating season; and
- heating system upgraded to 75% annual efficiency.

2.2 Typical parameters for existing windows

Typical windows found in affordable housing buildings were assumed to be single-glazed, wood double-hung windows, fitted with aluminum triple-track storm windows. Window dimensions of 36 x 60 inches were assumed, yielding 19 perimeter feet of operable linear crack. Sixty-four original condition windows were field tested for air leakage by a fan pressurization device prior to any retrofits. From these data, air leakage rates for a “typical” original condition window as well as both “loose” and “tight” windows were determined.

A typical window was assumed to have an aluminum triple-track storm window in the closed position. Air leakage characteristics of the typical window were assumed to be

equivalent to the averaged sash leakage of all original condition windows tested when storm windows were closed. The tight window was also assumed to have a storm window in the closed position but had leakage characteristics equivalent to one standard deviation lower than the field test average for windows with storms closed. The loose window was assumed to have no storm in place with leakage characteristics equivalent to the averaged sash leakage for original condition windows with storms in the open position. Thermal transmission characteristics for all baseline windows were based on wooden sash and frame with single-pane glass, with a storm window as a second glazing layer for the tight and typical windows. In all cases, a percentage of the averaged extraneous air was included with the sash leakage to account for the exterior air contribution.

2.3 Original condition windows and window upgrades field tested

For the study, 151 windows at 19 sites were field tested, with 87 of those windows being various upgrade types. Sites for pressurization testing were chosen by availability, timing of scheduled renovation, suitability as to window and upgrade type, and window accessibility. Several buildings were not typical of affordable housing, but all field tested windows were representative of windows found in affordable housing throughout Vermont.

Table 1 is a site list of windows field tested, showing the number of original condition windows and/or the number of upgrades tested at each site. Not all windows at a given site were tested due to accessibility or weather conditions, nor were all original condition windows retested after renovation. Occupancy and weather precluded retesting windows at some sites, while many other sites did not receive the expected upgrade within the allotted time frame of the study. Renovations sufficiently improved leakage characteristics of

windows at several sites to allow a greater number of upgraded windows to be tested. Also included in the last column are the number of windows tested prior to and post renovation at relevant sites.

A variety of window upgrades were field tested, ranging from minimal weatherstripping to replacement window inserts. Some windows had new aluminum triple-track storm windows installed while others retained the existing storm windows. Still others used interior storm windows as an upgrade option. In two instances, existing wooden storm windows were weatherstripped and retained. Table 2 lists locations and identification numbers of sites where window upgrades were tested as well as descriptions of the various upgrades encountered.

Table 1: Site locations and ID's, showing numbers of original windows and upgrades tested

Site ID	Location	Original Windows	Upgraded Windows	Windows Tested Pre- and Post-Upgrade
1	CVCLT Montpelier, VT	3	—	—
2	40 Nash Street Burlington, VT	3	3	3
3	133 King Street Burlington, VT	9	4	3
4	Congress Street Morrisville, VT	5	—	—
5	204 Pearl Street Burlington, VT	8	—	—
6	101 Fairfield Street St. Albans, VT	4	6	3
7	Sapling House Island Pond, VT	12	20	12
8	127 Mansfield Avenue Burlington, VT	6	—	—
9	6 Raymond Street Lyndonville, VT	6	—	—
10	124 Federal Street Salem, MA	4	4	4
11	76 Pearl Street St. Johnsbury, VT	—	6	—
12	12 Summer Street Morrisville, VT	—	10	—
13	George Street Morrisville, VT	—	10	—
14	Kidder Hotel Block Derby, VT	—	6	—
15	4 Oocom Ridge Hanover, NH	4	4	4
16	Irasburg Town Hall Irasburg, VT	—	7	—
17	605 Dalton Drive Fort Ethan Allen Colchester, VT	—	3	—
18	Brisson Residence South Hero, VT	—	2	—
19	40 Barre Street Montpelier, VT	—	2	—

Table 2: Window Upgrades

ID	Location	Upgrade
2	40 Nash Street Burlington, VT	Bi-Glass System: Existing sash routed to accept sealed double-pane insulating glass and vinyl jamb liners. Bulb weatherstripping at meeting rail, head, and sill junctions.
3	133 King Street Burlington, VT	Broscoe Replacement Sash: Single glazed, wood replacement sash with vinyl jamb liners. New aluminum triple track storm windows, caulked around frame.
6	101 Fairfield Street St. Albans, VT	Custom Gard: Vinyl frame and sash insert with vinyl replacement sash, installed inside existing jamb. Double-pane insulating glass.
7	Sapling House Island Pond, VT	19 Original Sash Retained: Sash routed to accept Caldwell DH-100 or 200 vinyl jamb liners. Bulb weatherstripping at meeting rail, head, and sill junctions. Weather Shield: One Custom Shield replacement window.
10	124 Federal Street Salem, MA	Storm Windows: Interior storm; aluminum triple track storm; low-profile, non-track, removable pane storm; new wooden storm window with primary sash weatherstripped.
11	76 Pearl Street St. Johnsbury, VT	Weather Shield: Custom Shield replacement wood frame and sash insert, installed inside existing jamb. Double-pane insulating glass.
12	12 Summer Street Morrisville, VT	7 Original Sash Retained: Sash routed to accept Caldwell DH-100 vinyl jamb liners. 3 Marvin Replacement Sash: Single-pane, wood replacement sash.
13	George Street Morrisville, VT	8 Original Sash Retained: Sash routed to accept Caldwell DH-100 vinyl jamb liners. Bulb weatherstripping at head and sill junctions. 2 Marvin Replacement Sash: Single-pane, wood replacement sash.
14	Kidder Hotel Block Derby, VT	Original Sash Retained: Windows reglazed and painted. New Harvey aluminum triple track storm windows caulked to exterior trim.
15	4 Occom Ridge Hanover, NH	Original Sash Retained: Interior plexiglass storm windows held by magnetic strips.
16	Irasburg Town Hall Irasburg, VT	Original Sash Retained: Caldwell coiled spring balances; bulb weatherstrip at sill junction. Wooden storm windows felt weatherstripped. Weather Shield: One Custom Shield replacement window.
17	605 Dalton Drive Fort Ethan Allen Colchester, VT	Original Sash Retained: Pulley seals; zinc rib-type weatherstripping along jamb; metal V-strip at meeting rail. Top sash painted in place. New aluminum triple track storm windows caulked to exterior trim.
18	Brisson Residence South Hero, VT	Marvin Tilt Pac: Double-pane insulating glass replacement sash with vinyl jamb liners utilizing existing frame.
19	40 Barre Street Montpelier, VT	Original Sash Retained: Top sash painted in place; bronze V-strip weatherstripping; old aluminum triple track storm window frame caulked in place.

Chapter 3

Methodology

Energy costs associated with existing windows in older housing must first be known in order to estimate savings from any type of window retrofit. Thermal losses accounting for these costs are attributable to natural infiltration through and around the window unit and non-infiltrative losses. Field testing and computer simulations were used to estimate associated energy costs due to infiltrative and non-infiltrative thermal losses.

A total of 151 windows at 19 sites were field tested for air leakage. These windows included 64 original condition windows used to determine baseline estimates for air leakage through assumed typical, tight, and loose windows. The remaining 87 windows consisted of a variety of window upgrades, ranging from minimal weatherstripping of the original window to the addition of new storm windows to total window replacement. Three windows in one location were tested over a period of eight months to investigate the correlation of air infiltration rates to environmental parameters. Extensive laboratory tests were also performed on two original condition windows to determine the precision of pressurization testing as well as primary leakage areas. Testing was repeated on one laboratory window after routine maintenance and on the other after an upgrade utilizing the existing sash.

3.1 Contribution of window thermal losses to whole house losses

Energy losses attributable to windows account for approximately 20% of whole house losses according to the literature. One of the goals of this study was to assess a change in whole house energy consumption on a per window basis due to a window upgrade. This required knowledge of how the cost of thermal losses due to windows affected the cost of

whole house losses. Calculations of energy savings could be simplified if the relationship was additive such that a decrease in energy costs for a window directly corresponded to an equivalent decrease in total building energy costs. Simplifications would arise from calculating savings based solely on energy cost reductions realized through window upgrades rather than modeling whole building performance for each type of window upgrade. This concept of an additive relationship for thermal loss is supported when leakage rates are expressed in terms of effective leakage area (ELA). Individual building components may be added together as ELA's to estimate a total building leakage area (Proskiw, 1995).

The relationship between window and whole house annual heating costs was investigated by utilizing two models, an ASHRAE static heat load model and REM/Design, a static model that estimates contributions of internal and solar heat gains. Based on surface area, actual blower door test data for both a tight and a loose house were scaled to the assumed typical affordable housing building. Surface area was chosen as the scaling factor based on the assumption that air leakage is proportional to surface area as increased surface area should allow for more leakage sites.

Both models were run using baseline typical, tight, and loose windows in loose and tight building configurations. Values for annual heating energy costs varied between the two models, but the incremental changes between window conditions were similar. Based on the similar incremental results of the two models, it was assumed that a reduction in energy costs due to window upgrades corresponded to an equivalent reduction in whole house energy loss.

The relative locations of leakage sites may play a large role in determining whether natural infiltration is the primary result of wind or temperature induced infiltration. Wind

induced pressures would be the dominant driving force for infiltration if most leakage sites were located in the walls of a building, as opposed to floors or ceilings. If that were the case, solely upgrading the windows to reduce air leakage would transfer a greater percentage of whole house leakage to floors and ceilings. The effect of this change in relative leakage location was investigated by running the LBL correlation model using typical Vermont temperature and wind speed data. Using the blower door data, tests with leakage sites relegated to varying percentage locations in walls, floors, and ceilings were run for loose and tight house configurations, as well as the scaled up buildings. It was found that relative location of leakage sites had little bearing on the results with an extreme case showing a difference of 4%. Distribution of leakage sites prior to modeling a window upgrade were assumed to be even for the purposes of this study (33% ceiling, 33% floor, 34% walls).

3.2 Development of flow equations

An understanding of the nature of the equations used to characterize air flow through windows is of value to understand the derivation of the effective leakage area (ELA). The ELA is a result of standard fluid dynamic formulas, as described in hydraulic textbooks (Streeter and Wylie, 1985).

The behavior of air as it flows through a gap in or around a window is determined from the fluid dynamics of pipe flow. Flow in a pipe has a linear dependence on pressure at low Reynold's numbers (laminar flow) and a square-root dependence on pressure for high Reynold's numbers (turbulent flow). This relationship has led to the use of a power model where the flow is proportional to the pressure differential raised to some power between 0.5 and 1, where 0.5 represents turbulent flow and 1 represents laminar flow (Kreith and

Eisenstadt, 1957):

$$Q = C \Delta P^x \quad (1)$$

where

Q = air flow rate

c = leakage constant

ΔP = pressure differential and

x = flow exponent.

For air moving through cracks, energy for the flow is supplied by the pressure drop across the window supplied by the fan pressurization unit. The Bernoulli equation for air flow moving across the window may be written as:

$$\frac{P_1}{\gamma} + \frac{V_1^2}{2g} + z_1 = \frac{P_2}{\gamma} + \frac{V_2^2}{2g} + z_2 + h_f \quad (2)$$

where

h_f = head loss due to friction.

Assuming the changes in height are negligible for distances through a window and the velocity heads are equal on both sides of the window, the above Bernoulli equation reduces to:

$$h_f = \frac{P_1 - P_2}{\gamma} \quad (3)$$

The sum of the forces in the horizontal direction (F_x) responsible for the air flow is equivalent

to:

$$\Sigma F_x = 0 = (P_1 - P_2)A - \tau LP \quad (4)$$

where

P = conduit wetted perimeter and

τ = shear stress.

For steady, uniform turbulent flow in a conduit of uniform cross-section, the shear stress is:

$$\tau = \lambda \frac{\rho}{2} V^2 \quad (5)$$

where λ is a dimensionless coefficient.

Dividing γA through equation 4 and then substituting equations 4 and 5 into equation 3 while using the relationships $\gamma = \rho g$ and $R = A/P$ (the hydraulic radius) yields:

$$h_f = \lambda \frac{V^2 L}{2g R} \quad (6)$$

For turbulent flow in pipes, when $\lambda = f/4$ and $R = D/4$, equation 6 becomes the Darcy-Weisbach equation:

$$h_f = f \frac{L V^2}{D 2g} \quad (7)$$

where f is the friction number.

Solving the Darcy-Weisbach equation for velocity and using the relationship $\Delta P = \rho g h_f$

yields:

$$V = C_f \sqrt{\frac{2\Delta P}{\rho}} \quad (8)$$

where C_f is the discharge coefficient, equal to:

$$C_f = \sqrt{\frac{D}{L_f}} \quad (9)$$

Since the friction factor is nearly constant for turbulent flow, the discharge coefficient will also be constant (ASHRAE, 1993). Virtually all cracks and openings in and around a window are short with low crack length to entrance length ratios, leading to turbulent flow. It has been shown that the required hydraulic radius of a crack to ensure laminar flow through a typical wall crack (critical length = 1 cm) is much less than 2 millimeters (Sherman, 1980). Turbulent flow through and around a window is thus proportional to the conduit area and the square-root of the pressure differential, regardless of the Reynold's number:

$$Q = A C_f \sqrt{\frac{2\Delta P}{\rho}} \quad (10)$$

Assuming the flow coefficient to equal one (Sherman, 1987), equation 10 may be rewritten in a form expressing the leakage area in terms of pressure and leakage characteristics by substituting equation 1 for Q . This is known as the effective leakage area (ELA) which is defined as the area of a round, sharp-edged orifice having a flow exponent equal to one that

allows the same total air flow as the window under a reference driving pressure (ASTM, 1994c):

$$ELA = c * P^{(x-0.5)} * \left(\frac{\rho}{2}\right)^{0.5} \quad (11)$$

where c and x are coefficients derived from linear regression of equation 1 using fan pressurization data.

When using inch-pound (IP) units, equation 11 becomes:

$$ELA = 0.18547 * c * P^{(x-0.5)} * \left(\frac{\rho}{2}\right)^{0.5} \quad (12)$$

where 0.18547 is the required conversion factor for the IP units.

3.3 Infiltrative thermal losses

Losses due to natural infiltration through a window are primarily the result of interior/exterior temperature differentials and wind induced pressure. Natural infiltrative losses were estimated from measurements of air leakage at a set range of pressure differentials. These data were the results of field testing existing window stock based on a modification of ASTM E 783-93 (ASTM, 1994d), the modification arising from the leakiness of the original window stock. Current industry standards for new windows list an air leakage rate of 0.37 scfm/lfc at 0.30 inches of water pressure (75 Pa), the recommended reference pressure cited in ASTM E 783-93. Many original windows were in poor condition, precluding the attainment of 0.30 inches of water pressure. A range of pressures was

systematically employed to characterize the leakiness of the windows according to the flow model presented in equation 1.

Using a range of pressures has also been shown to produce results having a higher degree of precision than when using a single point measurement as specified by ASTM E 783-93. Theoretically, multi-point testing is not as precise as two point testing but does allow for more robust results as it may reveal changes in leakage characteristics caused by pressure (Sherman and Palmiter, 1995).

Equation 1 as written mathematically describes half a parabola, requiring a natural logarithmic transformation in order to linearize the data. Linear regression was then used to determine the leakage constant (c) and flow exponent (x) for a window, based on leakage results from fan pressurization. These data were used to extrapolate air leakage rates at 0.30 and 0.016 inches of water (75 and 4 Pa, respectively). The latter pressure (0.016 in. H₂O or 4 Pa) was assumed to be the average heating season interior/exterior pressure differential that drives natural infiltration. The driving force is a result of pressure differences induced by building interior/exterior temperature differentials and those from wind speed and direction. However, pressure readings may fluctuate at lower pressure differentials due to variations in wind speed and direction. These fluctuations give rise to greater uncertainties in readings at lower pressure differentials. The logarithmic transformations necessary for regression analysis tend to decrease the weight of the more accurate high pressure differential readings, thereby giving the readings with larger degrees of uncertainty a greater impact on the extrapolated flow value. The end result is the uncertainty in the extrapolated air flow value is dominated by the low pressure point (Murphy et al., 1991; Sherman and Palmiter, 1995).

The effective leakage area (ELA) was used to characterize the total air flow moving through all openings and was calculated at 0.016 inches of water (4 Pa; ASTM, 1994c). As discussed previously, the ELA is equivalent to the area of a round orifice that allows the same total air flow as the window under a driving pressure differential of 0.016 inches of water (4 Pa). Using an ELA value allowed air openings in and around a window to be expressed as one total area for comparative purposes.

Pressurization data in terms of effective leakage area (ELA) were correlated to natural infiltration by the fluid mechanical model developed by the Lawrence Berkeley Laboratory. As stated previously, for the purposes of this study use of the LBL model was modified by using data from a single window rather than whole house data. It should be repeated that this modification was not the purpose for which the LBL correlation model was designed and any results should not be viewed as absolutes. Values obtained from this modification should be used only for comparative purposes with other values from this study.

A portable air test unit, manufactured by DeVac, Inc. of Minneapolis, Minnesota, was used to induce pressure differentials testing. The unit is a self-contained device, consisting of a blower motor capable of producing an approximate air flow of 40 cfm, low and high volume Ametek flow meters (1.2-11.6 cfm and 10-80 cfm respectively), and a Dwyer slant-tube manometer used to measure pressure differentials. The unit may be used to produce a positive or negative test pressure. An earlier study of 196 houses showed no systematic difference between pressurization and depressurization although significant uncertainty was associated with any individual measurement (Sherman et al., 1986). A negative test pressure was chosen for the purposes of this study, primarily for safety considerations. Any pressure-

induced glass breakage would have been directed inwards toward the interior plastic sheet.

3.3.1 Fan pressurization test method description

Polyethylene sheeting was taped to the inside trim of a latched window (if an operable latch was in place) and a series of negative pressures were applied (Figure 2). The amount of air flowing through the window unit was read from a flow meter calibrated in cubic feet per minute. The pressures applied ranged from a low of 0.03 inches of water pressure (7.5 Pa, equivalent to an approximate 8 mph wind impacting the building) to a high of 0.30 inches of water pressure if attainable (75 Pa, an approximate 25 mph wind). The applied negative pressure was uniform across the entire window so that each square inch was subjected to the

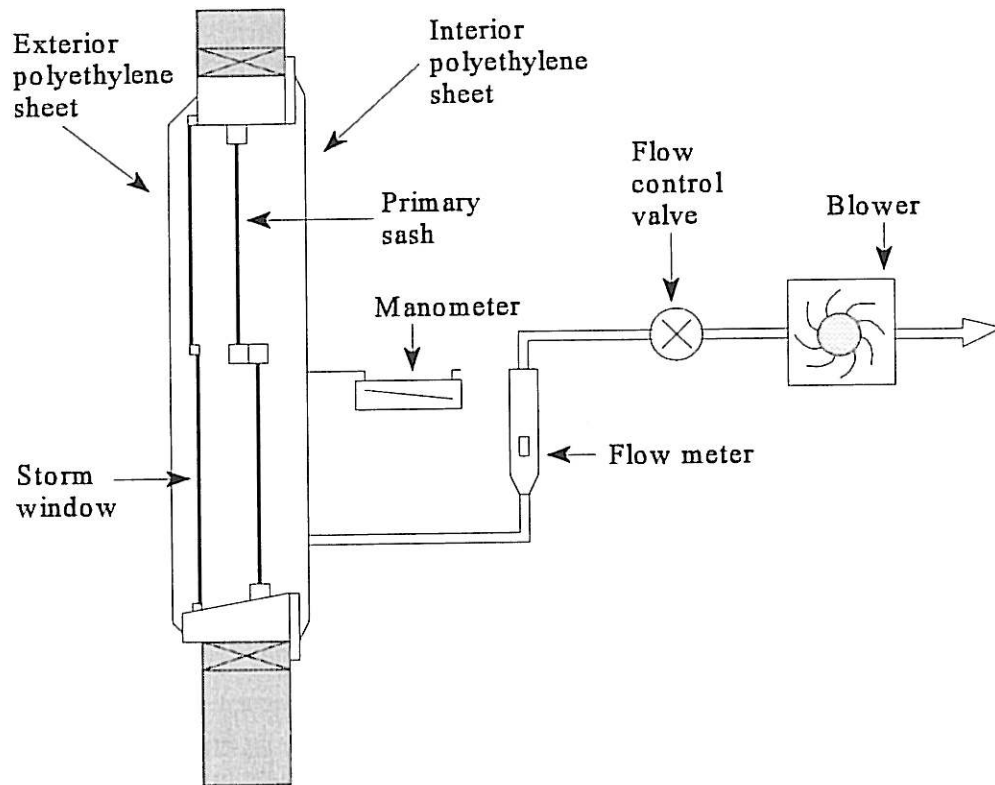


Figure 2: Schematic of the fan pressurization test set-up

same pressure.

The first set of readings represented the total flow (Q_t) of air passing through the window unit (through and around the sashes, jambs, and frame). A second sheet of polyethylene was then taped to the exterior trim of the window and the same pressure range was again applied to the window with corresponding flows recorded. The second set of readings was the extraneous flow (Q_e) and represented the air flow moving through the rough opening, frame, and jamb as the exterior sheet of plastic had isolated the area of the window within the jamb from any air passage. The difference between these two sets of readings was the sash flow (Q_s) and represented the amount of air passing through the sash area within the jamb:

$$Q_t - Q_e = Q_s \quad (13)$$

If the window was fitted with a working storm window, the procedure was repeated with the storm window in place.

3.3.2 Environmental and window parameters recorded

Interior/exterior temperatures and wind direction were recorded on-site for each window as per ASTM E 783-93 (ASTM, 1994d). Also estimated and recorded on-site were wind speeds based on the Beaufort Wind Scale, while barometric pressures were read and recorded in Burlington, Vermont. Relative humidities were determined using psychrometric charts and data from on-site readings of a sling psychrometer coupled with the on-site interior/exterior temperatures. Recorded also were various window dimensions (height, width, sash depth, etc.), window type (double- or single-hung; pulley- or pin-type), condition

and location of any locking mechanism, window orientation, and weather conditions for some of the latter tests where exterior air percentages were being determined. Appendix E 1 shows a field data sheet used for each window.

Left- and right-hand side gaps between the lower sash and jamb were measured as well as the distance the lower sash moved forward and backward at the meeting rail. Sash and meeting rail gaps were not measured for all original windows tested, as these measurements were deemed important after field testing began. For existing windows utilizing vinyl jamb liners as an upgrade, the distances between the sash/jamb liner bulb and the sash/jamb liner wall were measured on both sides of the lower sash.

It was an early goal to derive a means of visually examining a window and deciding whether to replace or renovate without resorting to pressurization testing. As a means towards that end, original windows were characterized by their general physical condition, utilizing a twelve parameter check list (Appendix E 2). These twelve parameters were reduced to several combination parameters, descriptive of the physical condition of the window. Two individual parameters were also investigated for significant correlations to air leakage. Combination parameters were weighted toward meeting rail and sash fit characteristics rather than glazing condition. It was assumed that any type of window renovation would include repair of existing glazing problems.

Along with the reduced physical descriptive parameter, window type was investigated for potential correlation with air leakage characteristics. Windows were categorized as single- or double-hung and as pin- or pulley-type windows for further clarification.

3.3.3 Determination of percent exterior air in Q_e

The method described above and used for this study failed to account for exterior air infiltrating through the rough opening. Infiltration of exterior air not only occurred through the window sash and sash/jamb junction (Q_e), but also through the rough opening (Q_{RO}), adding to the heating load. The amount of exterior air through the rough opening can have a significant effect on the infiltrative heating load of a tight window, where Q_e alone showed a small heat load. Determination of the amount of exterior air through the rough opening was therefore important.

A rough estimate of the volume of exterior air coming through the rough opening was calculated by knowing the exterior and interior air temperatures as well as the test chamber temperature (the temperature between the two sheets of polyethylene) while performing the test for extraneous air (Q_e). Knowing these three data points and any measured value of Q_e , a mass balance on temperature and air flow was performed to estimate the volume of exterior air in Q_e . The amount of exterior air in Q_e was determined by the following formula:

$$Q_{RO} = Q_e * \left[\frac{(T_{int} - T_{win})}{(T_{int} - T_{ext})} \right] \quad (14)$$

where

Q_{RO} = the flow rate of exterior air (acfm)

Q_e = the flow rate of air chosen from Q_e test data (acfm)

T_{int} = ambient interior air temperature (°F)

T_{win} = the temperature between the two plastic sheets during the test (°F)

T_{ext} = ambient exterior air temperature (°F)

The flow rate of exterior air (Q_{RO}) was converted to a percentage by dividing through by Q_e .

This method of estimating the percentage of exterior air entering the test zone during testing periods has limitations and values thus derived should not be assumed accurate. No attempt was made to determine the actual flow path of air as it entered the wall cavities while a window was under pressure. Exterior air likely increased its temperature and reached some equilibrium as it passed through walls warmer than the ambient exterior atmospheric temperature, raising questions as to the accuracy of the temperature readings in the test zone. The method was used to determine a rough approximation of the contribution of exterior air to the overall heating load and would be anticipated to underestimate the actual percentage of exterior air contained in the extraneous air.

Estimates of the amount of exterior air (Q_{RO}) entering a window as a percentage of extraneous air (Q_e) were made for 33 upgraded windows. Thirty-one of these windows retained the original sash with the other two being in-kind replacement sash with vinyl jamb liners. Based on the 33 windows, an averaged percentage of exterior air (Q_{RO}) was calculated. This percentage was multiplied by the average rate of extraneous air for each assumed and upgraded window type then added to the sash infiltrative rate measured while using the ASTM E 783-93 modification to provide a total infiltrative thermal loss for a window. Therefore, for a given window or upgrade type, the total infiltrative thermal loss was based on the total air flow:

$$Q_{tot} = Q_s + Q_{RO} \quad (15)$$

where

$$Q_{RO} = 0.30 * Q_e \quad (16)$$

3.4 Correlation of air leakage to natural infiltration rates

The air leakage rate of a window determined by fan pressurization data is a physical property of the window, dependent on the design, construction, and physical condition of the window at the time of the test. Natural infiltration rates on the other hand, are the result of pressures induced by winds, interior/exterior temperature differentials, internal appliances, and combustion devices (ASHRAE, 1993). Thus, window air leakage rates as measured by fan pressurization in the field do not directly correspond to natural infiltration rates through those windows during the heating season. A means of correlating leakage rates with average heating season natural infiltrative rates is necessary to make use of the pressurization data.

As previously stated, a widely accepted method of correlating whole building pressurization data in terms of effective leakage area (ELA) to natural infiltration rates is by using a fluid mechanical model developed by the Lawrence Berkeley Laboratory. The LBL correlation model uses a whole building ELA and a calculated coefficient to determine the heating season average infiltration rate (Q_{nat}) for the building (Grimsrud et al., 1982). This coefficient, specific to house configuration, terrain, shielding, and climate, is the average heating season infiltration rate per unit ELA.

The LBL model estimates natural infiltrative rates based on five measurable parameters (Sherman, 1980):

1. effective leakage area of the structure;

2. geometry of the structure (height, length, width);
3. interior/exterior temperature differential;
4. terrain class of the building; and
5. wind speed.

The LBL model uses these parameters to determine total infiltration due to the stack effect and a wind-driven infiltrative component which are treated as if independent of one another. The infiltration component due to the stack effect requires knowledge of the relative leakiness of the floor and ceiling, where the fraction of envelope leakage in the floor and ceiling is:

$$R = \frac{A_f + A_c}{A_o} \quad (17)$$

where

A_f = effective leakage area of the floor;

A_c = effective leakage area of the ceiling; and

A_o = effective leakage area of the building.

The effective leakage distribution is defined as:

$$X = \frac{A_c - A_f}{A_o} \quad (18)$$

and is used more often than the neutral level as the required parameters for X are the same as those for R . An approximation method was used to find an expression for infiltration in terms of X rather than the neutral level (Sherman, 1980; Sherman and Modera, 1986):

$$Q_s = A_o f_s \sqrt{gh \frac{\Delta T}{T}} \quad (19)$$

where f_s is the stack factor and is defined as:

$$f_s = \frac{(1+R/2)}{3} \left(1 - \frac{X^2}{(2-R)^2} \right)^{3/2} \quad (20)$$

Wind driven infiltration is the result of wind losing kinetic energy as it impinges on a building shell, creating a pressure differential. The change in the surface pressure on the building envelope is proportional to the local wind speed at ceiling height and the shielding coefficient of the building. Using wind-tunnel data, wind-induced infiltration was shown to be described by the following expression (Sherman, 1980):

$$Q_w = A_o v_1 C (1-R)^{1/3} \quad (21)$$

where

v_1 = wind speed at ceiling height and

C = generalized shielding coefficient.

Wind-induced infiltration is somewhat dependent on the amount of envelope leakage associated with both the floor and ceiling (R) as they are more heavily shielded from the wind than are the walls. The shielding coefficient (C) for Shielding Class I was determined from boundary layer wind tunnel data for an isolated structure, while the other shielding classes were approximated from the Class I value (Table 3).

Table 3: Generalized shielding coefficients

Shielding Class	C	Description
I	0.324	no obstructions or local shielding whatsoever
II	0.285	light local shielding with few obstructions
III	0.240	moderate local shielding, some obstructions within two house heights
IV	0.185	heavy shielding, obstructions around most of perimeter
V	0.102	very heavy shielding, large obstruction surrounding perimeter within two house heights

(Sherman and Modera, 1986)

Most wind data are not taken locally but rather from a weather tower (Sherman and Modera, 1986), necessitating transformation of the weather tower wind speed to the local free stream wind speed at 10 meters. This data transformation is accomplished by standard wind engineering formulae, resulting in the following expression (Sherman and Modera, 1986):

$$Q_w = A_o v f_w \quad (22)$$

where

v = measured wind speed and

f_w = the wind factor, defined as:

$$f_w = C(1 - R)^{1/3} \frac{\alpha_w \left(\frac{H_w}{10m} \right)^{\gamma_w}}{\alpha_t \left(\frac{H_t}{10m} \right)^{\gamma_t}} \quad (23)$$

where α and γ are terrain-dependent parameters (Table 4) and the subscripts w and t refer to local and weather tower data, respectively.

Table 4: Terrain parameters for standard terrain classes

Class	γ	α	Description
I	0.10	1.30	ocean or other body of water with at least 5 km of unrestricted expanse
II	0.15	1.00	flat terrain with some isolated obstacles
III	0.20	0.85	rural area with low buildings, trees, or other scattered obstacles
IV	0.25	0.67	urban, industrial, or forest areas or other built-up area
V	0.35	0.47	center of large city or other heavily built-up area

(Sherman and Modera, 1986)

The LBL model ignores the complex real-world interaction between wind- and stack-induced infiltration and instead uses the manner in which each affects the pressure differential to arrive at a total natural infiltration rate. Equation 10 assumed a square root dependence of flow on the driving pressure differential (i.e., turbulent flow), giving rise to flows adding in quadrature:

$$Q_{inf} = \sqrt{Q_s^2 + Q_w^2} \quad (24)$$

where

Q_{inf} = natural infiltrative rate.

The LBL model has been described as sacrificing accuracy for versatility and simplicity (Sherman, 1980). The model incorporates a series of simplifying assumptions to calculate the natural infiltration of a general structure (Sherman, 1987; Sherman and Modera, 1986):

1. The building is a single, well-mixed zone of simple, rectangular shape.
2. Air flow through gaps and cracks in the building envelope is turbulent.
3. All gaps and cracks are treated as simple orifices whose leakage characteristics can

be combined for a total leakage descriptive parameter.

4. Wind direction is averaged although it may strongly affect infiltration rates.
5. Areas of envelope leakage are grouped into three categories (ceiling, wall, and floor leakage areas) although actual leaks are distributed across the entire building envelope.
6. Within each leakage area, the actual leakage is assumed to be evenly distributed.
7. The air flows for each source (wind, temperature, or mechanically induced air flow) are combined in a simple quadrature manner based on the simplified leakage model (equation 10) although each flow may affect the pressure differential across the envelope differently.

For the purposes of the study, use of the LBL model was modified by using ELA data from a single window rather than whole house ELA data. The assumption was made that when using a window ELA, the results of the LBL model would have the same relative significance in predicting the average annual heating season natural infiltration rate for a window as the model would have when using a whole building ELA to predict the building heating season natural infiltration rate. It is recognized that this was not the intent of the model and therefore, the use of these results in determining annual costs allows for a degree of uncertainty. However, a sensitivity analysis of the cost estimation method revealed a maximum uncertainty of $\pm 25\%$ in annual energy costs per window when using extreme values in the LBL correlation model (Section 5.1).

Estimating the natural infiltration rate of a single window by using the LBL correlation model (as opposed to a whole building for which it was intended) further reduces the

accuracy of the results. This arises as a result of the data gathered from fan pressurization. During the extraneous air test (Q_e), there is a likelihood of air entering the walls through an adjacent window, similar to the hydraulic draw-down effect of adjacent wells. This uncertainty in the source of Q_e is carried over to the estimate of exterior air entering through the rough opening (Q_{RO}) which was used to determine a total infiltrative rate for the window (Q_{tot}). Any such flow between windows will thus serve to overestimate the total infiltrative rate for a window and the subsequent energy costs.

Also creating potential error is the relative importance of wind-induced infiltration versus stack-induced infiltration when using the correlation model. Leakage areas (*ie.*, the effective leakage areas the “floor”, “ceiling”, and “walls” of a window) were distributed evenly when using the model. It is likely that the wind-induced parameter is far more important than the stack-induced parameter for a window, a factor that decreases the estimated natural infiltration rate by approximately 2% when all of the leakage is assigned to the “walls”.

LBL values for natural infiltration rates (Q_{nat}) were based on whole window effective leakage areas (ELA_{tot}) which were defined to include a calculated volume of exterior air (Q_{RO}) with the sash leakage (Q_e) for the purposes of this study. Furthermore, low sample populations (n) for most window upgrades lend little statistical significance to estimated natural infiltration rates and therefore should not necessarily be regarded as typical of an upgrade category.

Other authors have compared LBL correlation model predictions of whole building natural infiltration rates to actual infiltration measurements based on single tracer gas decay

at fifteen sites (Sherman and Modera, 1986). The model was shown to predict infiltration rates to within 20% of those resulting from tracer gas measurements for well-characterized environments and slightly higher for less characterized environments when using short-term measurements. Using long-term averages, the model becomes more accurate, predicting to within 7% of measured values for well-characterized environments, rising to within 15% for those less characterized.

3.5 Non-infiltrative thermal losses

Non-infiltrative thermal losses were determined from simulations based on the computer model WINDOW 4.1 developed by the LBL Windows and Daylighting Group. User variable window parameters include window size and type, sash material, and type of glass among other parameters. The program calculated window thermal performance in terms of U-values (thermal transmittance), solar heat gain coefficients, shading coefficients, and visible transmittances. Only U-values were used for purposes of this study.

3.6 Total window thermal losses

Total window thermal loss was the result of non-infiltrative and infiltrative thermal losses through the window as well as thermal losses due to exterior air infiltrating via the rough opening. Sash infiltrative window losses were based on window air leakage characteristics while infiltrative losses due to exterior air were assumed to be the average of the 33 windows as discussed previously (Section 3.3.3). Sash and exterior air infiltrative losses were summed for a whole window infiltrative loss. The whole window infiltrative loss was correlated with natural infiltration rates by use of the LBL correlation model. Non-infiltrative thermal losses were based on WINDOW 4.1 modeling. The two estimates were

converted to common units and summed together for an “effective thermal loss”.

The validity of an “effective thermal loss” was not tested in this study and is subject to speculation (Klems, 1983). The aforementioned procedure adds the results of two very different methods of calculating heat losses, one based on infiltrative rates resulting from fan pressurization data (the LBL model) and the other the result of a computer model based on well understood thermodynamic principles (WINDOW 4.1). The concept of “effective thermal loss” was chosen for this study in order to provide an all encompassing parameter describing total thermal loss through a window.

3.7 Thermography

In February 1996, thermographs were taken of windows at two sites in Hanover, New Hampshire. Images of three windows were taken at Robinson Hall of Dartmouth College. Two of these windows were large, double-hung, pulley-type windows with conventional triple-track aluminum storm windows attached. The third window was a Bi-Glass Systems retrofit with vinyl jamb liners, double-pane insulating glass, and silicone bulb weatherstripping at the meeting rail, head, and sill junctions.

The second Hanover site was 4 Occom Ridge, where double-hung, pulley-type windows were fitted with conventional triple-track aluminum storm windows, as well as being caulked with rope caulking. One set of windows in the den was also fitted with an interior plexiglass storm window, attached by magnetic stripping.

These sets of thermographs were not used in a quantitative manner but were rather used as a means for visual comparisons between window upgrades.

3.8 Energy savings due to window upgrades

Savings in energy costs for a building were based directly on those savings attributable to energy reduction through window upgrades. This was a direct result of the apparent additive nature of the relationship between thermal losses due to windows and the remainder of whole house thermal losses as discussed previously (Section 3.1).

The following steps summarize the process used to calculate annual energy costs and savings due to a window upgrade, as compared to annual costs for typical windows:

1. convert typical sash leakage fan pressurization data (Q_s) as scfm/lfc to effective leakage area (ELA_s /lfc);
2. convert the volume of exterior air (Q_{RO}) as scfm/lfc to ELA_{RO} /lfc, based on a field derived percentage of average extraneous air leakage (Q_e);
3. add ELA_s /lfc to ELA_{RO} /lfc for a window ELA per linear foot crack due to infiltration (ELA_{tot} /lfc);
4. multiply ELA_{tot} /lfc by 19 lfc for a typical 36 x 60 inch double-hung window to determine the whole window ELA (ELA_{tot});
5. use ELA_{tot} in the LBL correlation model to predict the average heating season infiltration rate for the window (Q_{nat} - natural air infiltration rate);
6. multiply the average heating season infiltration rate (Q_{nat}) by the heat capacity of air (C_p) to determine total thermal loss rate through the window due to infiltration (L_{inf}):

$$L_{inf} = Q_{nat} * C_{p_{air}}$$
$$L_{inf} = Q_{nat} * \frac{0.018 \text{ Btu}}{\text{ft}^3 * ^\circ\text{F}} * \frac{60 \text{ min}}{1 \text{ hr}} \quad (25)$$

7. calculate non-infiltrative thermal loss rate (L_{non}) due to transmission (U-value) using WINDOW 4.1;
8. multiply the U-value (L_{non}) by 15 ft² for a typical 36 x 60 inch double-hung window to determine the total window non-infiltrative thermal loss rate (L_U);
9. add the infiltrative (L_{inf}) and non-infiltrative (L_U) thermal loss rates to determine the “effective thermal loss” of the typical window (L_{eff});
10. determine the annual window thermal loss (L_{yr}) in millions of Btu’s (MMBtu) by multiplying the “effective thermal loss” (L_{eff}) by the average Burlington, Vermont degree-day units by 24 hours per day:

$$L_{yr} = L_{eff} * 7744 \text{ degree-days} * \frac{24 \text{ hr}}{\text{day}} * 10^{-6} \quad (26)$$

11. calculate the annual cost per window (C_{win} ; example based on number 2 fuel oil, price as of June 1996):

$$C_{win} = \frac{(\text{fuel cost per gal}) * (\text{annual heat required}) * 10^6}{(\text{fuel heat capacity per gal}) * (\text{furnace efficiency})} \quad (27)$$

$$C_{win} = \frac{\$0.90/\text{gal} * L_{yr} * 10^6}{(138,600 \text{ Btu/gal}) * \text{eff}}$$

12. repeat steps 1-11 for a given window upgrade; and
13. determine the annual savings per upgrade type (S_{win}) by subtracting step 12 from step 11.

Chapter 4

Results

One hundred fifty-one windows at 19 different sites were field tested for this study. Sixty-four windows were tested in their original condition with storms both open and closed when operable. The remaining 87 windows underwent some form of upgrade. Six sites had a total of 29 windows tested both prior to and after renovative work. Two other windows underwent detailed testing in the laboratory.

4.1 Appropriateness of flow model

The correlation of induced air leakage to natural infiltration rates was dependent on extrapolation of field data from the range of test pressures (0.03 - 0.30 in. H₂O; 7.5 - 75 Pa) down to 0.016 in. H₂O (4 Pa). Extrapolation was based on a standard mathematical flow model (equation 1) used to describe air flow where air leakage was a function of the pressure differential. The degree to which the model accurately described the field data was determined by the value of the coefficient of determination (R^2) for each test, as calculated by linear regression. The coefficient was defined as the proportion of variability in the dependent variable (Q) accounted for by the independent variable (ΔP). The maximum allowable value for R^2 is 1.000, meaning the model is a perfect fit to the field data, resulting in the data falling on a straight line on a log-log graph.

Coefficient of determination values for all windows with storms open and/or closed are shown in Figure 3. The black circle and square respectively represent the mean R^2 values for windows with storms open and closed ($R^2 = 0.844$ and 0.760 , respectively). The lines represent plus or minus one standard deviation from the means, encompassing 68% of the

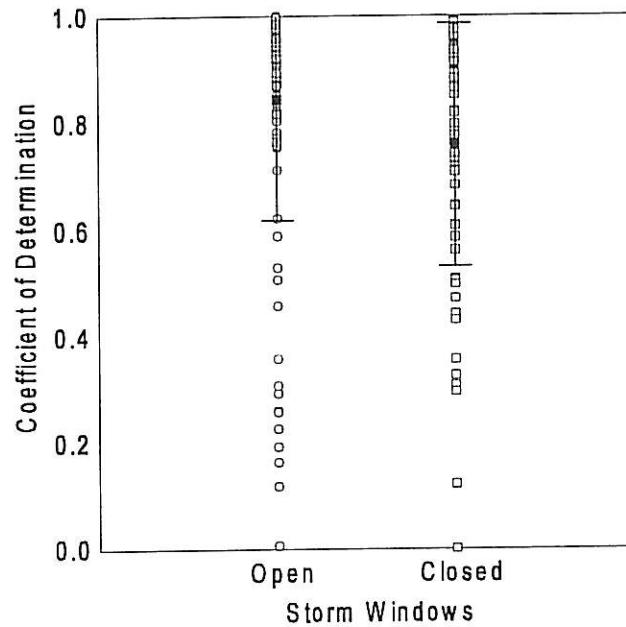


Figure 3: Variability in R^2 values of a standard flow model fitted to the field data

data points. As opposed to the mean R^2 values, the median \bar{R} value for windows with storms open was 0.921 while the median with storms closed was 0.838, thus indicating a distribution skewed to the right. The median represented the middle value of the ranked population, meaning half the population was above the median. In this case, the median values were more robust estimations of the central tendency than the means, since the mean is weighted towards lower R^2 values for a skewed population distribution. Based on the mean and median R^2 values, the field data showed a reasonable fit to the flow model chosen to represent the physical conditions, thus decreasing the uncertainty in the extrapolated values for air leakage at 0.016 inches of water (4 Pa).

Extrapolated values of air leakage were compared to measured air leakage rates at

0.30 inches of water pressure (75 Pa) for all windows able to attain the maximum pressure differential. Fifty-three original, renovated, and replacement windows with either an open storm window or no storm showed no significant difference between the measured air leakage rates and extrapolated rates ($p = 0.89$). When storm windows were in place, 38 original, renovated, and replacement windows also showed no significant difference between actual and extrapolated leakage rates ($p = 0.69$).

Some variation of R^2 was associated with gusting winds during some testing periods. Depending on direction, these winds had the effect of increasing or decreasing the pressure differential shown in the manometer. Wind induced pressure changes caused unnecessary adjustments of air flow rates to accommodate false pressure readings. Other windows and doors were opened in attempts to ameliorate the effects of strong winds. A larger variation in R^2 values was observed for those windows allowing little induced air leakage. For tight windows, the effect of even moderate winds on test accuracy increased as both air flow rates and pressure differentials decreased, due to the larger relative effects of the wind. Table 5

Table 5: Wind speeds equivalent to test pressure differentials

Wind speed (mph)	ΔP (in. H ₂ O)	ΔP (Pa)
25	0.30	75
23	0.25	62.5
20	0.20	50
18	0.15	37.5
14	0.10	25
12	0.07	17.5
10	0.05	12.5
8	0.03	7.5
6	0.016	4

shows wind speeds equivalent to pressure differentials used in the test, with pressures being expressed in both conventional (Inch-Pound) and metric (SI) units. Winds in the 12 to 15 mph range were routinely encountered during field testing, making windows with low leakage rates susceptible to increased error as these winds were equivalent to 0.07 to 0.10 inches of water pressure (17.5 - 25 Pa).

4.2 Field test results - original condition windows

Sixty-four original condition windows were field tested for air leakage. These data were used to model leakage characteristics of typical, tight, and loose affordable housing windows for comparison with differing window upgrades. The typical double-hung window was assumed to have dimensions of 30 x 60 inches, giving an operable crack perimeter of 19 linear feet and a surface area of 15 square feet.

As previously discussed (Section 3.3.3), a portion of extraneous air leakage made a contribution to the heating load by requiring conditioning. During the latter half of the study, 33 windows were monitored for the percentage of exterior air contained in the extraneous air leakage during the test period (Appendix G). The average percentage by volume of exterior air entering the test zone as a portion of the extraneous air (*ie.*, Q_{RO}) was 29% as measured and estimated by temperature differences. This average percentage was approximated as 30% for this study, although no attempt was made to validate the exterior air estimation method during the course of the study. This estimate of Q_{RO} can only be considered an approximation based on the lack of alternative experimental validation as well as the assumptions inherent in the mass balance model used and discussed previously (Section 3.3.3).

Field data for each window were converted to sash (Q_s) and extraneous (Q_e) leakage rates, expressed as standard cubic feet per minute per linear foot crack (scfm/lfc) with the Q_e value being converted to Q_{RO} . Based on the physical dimensions of each window, these results (Q_s and Q_{RO}) were in turn converted to effective leakage areas per linear foot crack (ELA/lfc) at 0.016 inches of water pressure (4 Pa), the assumed driving force for natural infiltration. After summing the two infiltrative ELA's/lfc, a whole window effective leakage area (ELA_{tot}) for the standard sized window was calculated by multiplying the summed rates by 19 feet, the operable window perimeter of the baseline double-hung window.

Table 6 shows assumed air leakage characteristics for typical affordable housing windows based on the field research. Total sash leakage ($ELA_{s \times 19}$ - i.e., $ELA_s/lfc \times 19$ lfc) for the baseline typical window was the averaged sash leakage rates of all original condition windows with operable storms in place (35 windows). Both the tight and typical windows were assumed to have storm windows in place, with the tight window having sash leakage characteristics one standard deviation less than the typical window. The loose window was assumed to have no storm in place and was the average of all original condition windows with storms open or missing (47 windows). As previously discussed, the contribution of Q_{RO} was expressed as a whole window exterior air effective leakage area ($ELA_{RO \times 19}$) and summed

Table 6: Assumed air leakage characteristics for original condition windows

Window Category	$ELA_{s \times 19}$ (in ²)	$ELA_{RO \times 19}$ (in ²)	ELA_{tot} (in ²)	Diameter (in)
Tight Window	0.27	0.59	0.86	1.04
Typical Window	0.89	0.59	1.48	1.37
Loose Window	2.19	0.59	2.78	1.88

with the sash flow ($ELA_{s, x 19}$) to determine a total effective leakage area (ELA_{tot}) for each baseline window.

The column labeled "Diameter" in Table 6 was included to facilitate visualizing ELA_{tot} . It refers to the diameter of the round orifice on which ELA is modeled. As previously stated (Section 3.2), ELA is the size of a round orifice passing the same air flow as the cracks associated with a window.

The significance of the exterior air contribution to the infiltrative heating load associated with a window may be seen from the above data. Exterior air contributes approximately 20% of the loose window infiltrative load, but rises to 40% and 70% of the total infiltrative heat load for typical and tight windows respectively.

4.2.1 Air leakage characteristics of windows over time

Air leakage characteristics of three windows at the Central Vermont Community Land Trust (CVCLT) in Montpelier, Vermont, were measured periodically over a time span of eight months, from March until October 1995. The purpose of this long term monitoring was to observe how air leakage responded to environmental factors as the seasons progressed. Seasonal variations in air leakage ranging from 20% to 25% higher in the winter months have been reported for several houses (Levin et al. 1995).

Wooden windows often become more difficult to operate during the summer season as wood swells in response to an uptake in moisture. The expansion and contraction of the wood affects gap sizes in a window, thereby influencing the rate of infiltration. An understanding of how leakage characteristics changed with long-term weather conditions was desired to determine when field testing was to begin and end so as to maintain similar test

conditions. Potential environmental parameters influencing moisture uptake by wooden windows (and thus potentially affecting air leakage rates) included exterior dry-bulb temperature, relative humidity, dew point temperature, and partial water vapor pressure, defined as follows:

- Exterior dry-bulb temperature - the current ambient air temperature as measured by a thermometer.
- Relative humidity - the ratio of the amount of water vapor in the air to the maximum amount of water vapor the air can hold at the ambient temperature.
- Dew point temperature - the temperature at which the ratio of water vapor pressure to atmospheric pressure is equal to the mole fraction* of water vapor in the air. This is the temperature at which water vapor condenses from the air to form liquid water (dew).
 - * Mole fraction - the ratio of the number of moles of a component (water) to the total number of moles of all components in the mixture (air).
- Partial water vapor pressure - that component of the atmospheric pressure exerted solely by the water vapor contained in the air mass.

The relative humidity, dew point temperature, and partial water vapor pressure are all related as they are dependent on the mole fraction of water vapor in air and the dry-bulb temperature (Appendix H).

Water vapor pressure was assumed to be the likely driving force in the uptake or release of moisture by wooden windows. The wood in windows of historical buildings was assumed to be air dried to the extent it exhibited a lagged response to changing atmospheric

moisture conditions by swelling or shrinking. An increased amount of moisture in the air would increase atmospheric water vapor pressure, thereby increasing the water vapor pressure differential between the air and wood. It was the pressure differential between atmospheric water vapor and wood moisture content that was assumed to be the driving force for dimensional changes in wooden windows, which in turn would affect rates of air leakage.

The assumption concerning air infiltration rates, wooden windows, and increased atmospheric moisture content during the summer season was that air infiltration would decrease as the summer season progressed, as wood swell would decrease the size of any gaps in the windows, essentially reducing the effective leakage area (ELA).

Total window leakage rates (Q_{tot}) were converted to effective leakage areas for comparison over time. Windows 1A and 1B exhibited a general decline in ELA while the storm window was in place. This trend was not as apparent when observing data taken when storm windows were open. Window 1C showed no general trends, either with the storm window open or closed. No strong correlations were found between air leakage rates and running averages of the four parameters tested when using time periods of one to six weeks. Significant correlations likely required a longer monitoring period and more windows for a larger data base. Such an investigation was beyond the scope of this study.

Data from the CVCLT windows monitored over time were unclear as to general leakage trends with seasonal progression. Field testing was halted in May 1995 and resumed in October 1995, continuing through June 1996 when weather permitted.

4.2.2 Leakage characteristics of pin- versus pulley-type windows

Original condition windows were separated into pin- and pulley-type windows to

Table 7: $ELA_{RO \times 19}$ values for original condition pin- versus pulley-type windows with storms open

Window type	n	$ELA_{RO \times 19}$ (in ²)	Diameter (in)
Pin	23	1.39	1.33
Pulley	32	2.37	1.74

determine if pulley-type windows allowed more air leakage due to the window weight cavities. Leakage through the sash (Q_s) was expected to be equivalent between the two window types while exterior leakage (Q_{RO}) was expected to differ, with more exterior leakage expected in the pulley-type windows due to the window weight opening allowing more air leakage through the rough opening. A comparison of the mean sash leakage rates (Q_s) for the two window types when storm windows were open showed no significant difference in sash leakage rates ($p = 0.28$). Exterior air leakage rates through the rough opening (Q_{RO}) for pulley-type window were significantly greater than those for pin-type windows as expected ($p = 0.002$). Exterior air values, expressed as whole window exterior leakage areas ($ELA_{RO \times 19}$), are shown in Table 7 for the two window types.

The observed increase in air flow around pulley-type windows indicates the importance of window weight cavities as a pathway for air infiltration during the heating season. Isolating the window weight cavities from the rough opening has been shown to have a significant effect on efficient energy use (Proskiw, 1995a).

4.2.3 Sash leakage reduction due to existing storm windows

The effect of existing storm windows on reducing sash leakage (Q_s) through prime windows was investigated using data from the original condition windows. Of the 64 original condition windows tested, 24 had data for storm windows in both the open and closed

Table 8: Comparison of 24 original condition windows with existing storms open and closed

Storm Window Position	ELA_{s x 19} (in²)	Diameter (in)	Sash Leakage Reduction
Open	1.86	1.54	---
Closed	1.01	1.13	46%

positions. Many windows with attached storm tracks had missing or broken panes. Others were inaccessible due to both sash being painted shut on the interior side.

Sash air leakage characteristics for those original windows with operable storms were calculated with storm windows in both the open and closed positions with results being expressed as whole window effective sash leakage area (ELA_{s x 19}). Windows with existing storms in the open position allowed significantly more sash leakage than did those same windows when storms were in the closed position ($p < 0.001$). Results are found in Table 8, as well as the percentage reduction in sash leakage affected by storm windows in the closed position.

A reduction in sash air flow was expected due to a closed storm window but was not expected in terms of exterior air leakage. All existing storm windows encountered were exterior storm windows and thus had no effect on air leaking through the rough opening due to their placement on the exterior trim. When exterior leakage data were compared, no significant difference in exterior air leakage rates was observed between windows with storms in the open and closed positions ($p = 0.59$).

4.2.4 Air leakage characteristics of single- versus double-hung windows

The manner of a window's operation was investigated to determine its bearing on sash leakage characteristics. Thirteen of the original condition windows were single-hung, with

the other 51 being double-hung windows. Of the 13 single-hung windows, one (6B) was discounted as it had a wooden storm window caulked into place and could not be removed, preventing characterization of the window's sash leakage with the storm window open. An open storm window was the condition chosen to compare single- versus double-hung windows as it has been shown previously that the effect of storm windows was to reduce sash leakage, thereby masking any differences between the two window types (Section 4.2.3). Sash leakage characteristics with storm windows open were determined for 35 of the 51 original double-hung windows, the remainder having inaccessible storm windows in the closed position.

The upper sash of three of the twelve single-hung windows (6A, 6C, and 6D) were held in place by wooden stops, but were also caulked to the jamb. These three windows were considered to be true single-hung windows in terms of air leakage with sash flow passing through the window only between the jamb/lower sash junction, the sill junction, and the meeting rail. The remaining nine single-hung windows had the upper sash held in place by a wooden stop or nail with the upper sash loosely fitted in its frame. In these instances, the upper sash could be rattled by hand, indicating a loose fit that potentially allowed air leakage through the upper sash/jamb junction. Single-hung windows such as these nine were considered as double-hung in terms of calculating normalized air leakage rates (scfm/lfc) since air leakage sites in these windows were identical to those for a double-hung window (*ie.*, through the meeting rail, around the upper and lower sash/jamb junctions, and through the sill and head junctions), and thus no differences in sash leakage rates were expected. Operable window perimeter was therefore calculated as $(2 \times H) + (3 \times W)$ for these nine

Table 9: Single- versus double-hung window sash leakage characteristics

Window Type	n	ELA _{s, x 19} (in ²)	Diameter (in)
Single-hung	9	3.11	1.99
Double-hung	35	1.93	1.57

single-hung as well as all double-hung windows.

The single-hung windows were all pin-type, necessitating further sorting of the double-hung windows by holding mechanism as it has been shown previously that pulley-type windows allow more air leakage than pin-type windows (Section 4.2.2). Twelve of the 35 double-hung windows were pin-type windows. When sash leakage rates (ELA_{s, x 19}) of these 12 double-hung windows were compared to those of the nine single-hung, the double-hung windows allowed significantly less sash leakage than the single-hung ($p = 0.005$; Table 9). Lower sash leakage for double-hung windows was an unexpected result, considering single-hung windows were characterized not by operable crack perimeter, but by available leakage perimeter and were thus equivalent to double-hung windows. Due to this method of determining operable sash perimeter, no difference was expected between the effective sash leakage areas for single- and double-hung windows.

Normalized air leakage rates (scfm/lfc) for the three single-hung windows with caulked upper sash were based on an operable perimeter of $H + (2 \times W)$. These three windows were separated from the other single-hung windows as their leakage characteristics were determined using a different operable perimeter formula. When sash leakage rates of these three “true” single-hung windows were compared to the other nine single-hung, no significant difference in sash leakage rates was observed ($p = 0.44$).

It remained undetermined as to why single-hung, pin-type windows had greater sash leakage rates than double-hung, pin-type windows when operable sash perimeter for both window types was characterized identically. To determine whether a statistically significant difference in sash leakage actually exists between single- and double-hung windows a minimum sample population of 18 single-hung and 18 double-hung windows would need to be tested (Montgomery, 1991; Ott, 1993). As the two sample variances showed no statistical differences ($p = 0.358$), the projected sample size was determined using the means of the windows tested and the standard deviation of the single-hung windows ($\sigma = 0.904 \text{ in}^2$).

4.2.5 Correlation of descriptive physical parameters with air leakage rates

An early goal of the study was to investigate the possibility of visually inspecting a window and estimating if sash leakage rates were low or high. The physical condition of each field tested original condition window was categorized using a check list of 12 subjective parameters describing the general sash, sash/jamb fit, and the glazing (Appendix E).

Descriptive physical parameters were reduced to combined parameters describing overall sash condition (glazing and putty for both sash), sash/frame fit (tightness of sash in jamb and squareness), a combined sash/frame and meeting rail fit, and the total gap width between the lower sash and jamb. The meeting rail fit and squareness of the sash in the frame were also investigated as independent parameters. Correlations of these six parameters with sash effective leakage area ($ELA_{s \times 19}$) were investigated for those original condition windows with storms open or missing.

There were no significant correlations between $ELA_{s \times 19}$ and the six parameters although a weak correlation was observed with an increasing meeting rail gap ($R^2 = 0.48$, p

< 0.001). The strongest correlation between $ELA_{s \times 19}$ and a combination of parameters as revealed by a multivariate analysis had an $R^2 = 0.61$, representing 13% more predictive value of the $ELA_{s \times 19}$ than just the meeting rail alone. This combination of parameters included the sash/frame fit (ie., tightness of sash in jamb and squareness), the meeting rail gap, and the total gap distance between the left- and right-hand jambs and lower sash and is described by the following equation:

$$ELA_{s \times 19} = 0.253 - (0.0133 * A) - (0.0121 * B) + (0.00595 * C) \quad (28)$$

where

A = the frame fit (ie., tightness of sash in jamb and squareness);

B = the meeting rail gap; and

C = the total distance between the left- and right-hand jambs and the lower sash.

Using the above parameter combination to predict the relative leakiness of a window will account for only 60% of the infiltration through the window, although at a power of 0.9984 (ie., $1 - \beta$) when $\alpha = 0.05$. Although this is an accurate model based on the given data, it still does not account for 40% of the infiltration, implying an accurate estimation of a window's leakiness can not be obtained from the above parameters. However, an indication of the relative leakiness can be obtained by observing the meeting rail gap, the size of the gaps between the jamb and lower sash, how square the sash fits in the frame, and how loose the sash are in the jamb.

4.2.6 Original condition window summation

It was found that exterior air (Q_{RO}) can have a significant role in adding to the

infiltrative heat load of any window, whether it be tight or loose. Pulley-type windows were found to be significantly leakier than pin-type windows when using exterior air leakage rates, largely due to the presence of a window weight cavity providing greater potential for exterior air to infiltrate the window from the rough opening. Single-hung windows were found to have significantly more sash leakage than double-hung regardless of the method used to calculate operable crack perimeter. No significant correlations were found between leakage rates and four environmental parameters but a weak correlation was found between leakage rates and the meeting rail gap.

4.3 Field test results - window upgrades

The second round of field testing involved pressurization tests of a variety of window upgrades on eighty-seven windows. Upgrades ranged from retaining the original sash to window inserts utilizing the existing jamb. Table 10 summarizes the number of windows (n) tested for each general upgrade category, with some windows falling into two categories.

Table 10: Number of windows tested by general window upgrade category

General Window Upgrade Category	n
Retain original sash	62
Replacement sash with vinyl jamb liners	11
Replacement window inserts	12
Whole window replacements	2
Replacement storm windows	17
Double- versus single-glazing replacements	19

4.3.1 Upgrades retaining the original sash

Sixty-two renovated windows retained the original sash with 59 of those windows at

nine sites also retaining the original glazing by employing a variety of weatherstripping, vinyl jamb liners, and/or storm window upgrade options. Three other windows retained the original sash by undergoing the Bi-Glass System upgrade which replaced single-glazing with double-pane insulating glass while utilizing vinyl jamb liners (Section 4.2.2). Thirteen windows retaining the original sash had no improvement other than the addition of replacement storm windows and are discussed in the section concerning storm window upgrades (Section 4.3.4), leaving 49 renovated windows utilizing the original sash.

Upgrade options tested in the field are summarized in Table 11, along with the number of windows tested for each upgrade type. Average sash leakage characteristics for each upgrade type are also shown, expressed as sash effective leakage areas ($ELA_{s,19}$). Data for windows with any storms in place are not included, as the effect of storm windows would mask reductions due to sash upgrades as previously discussed (Section 4.2.3). Also listed is the average air leakage through the rough opening for each site ($ELA_{RO,19}$), accounting for exterior air contributions to whole window leakage. These two values are summed for a whole window effective leakage area (ELA_{tot}) for each upgrade type.

The six windows with Caldwell coiled spring balances (site 16) show no data in Table 11 as the average maximum pressure attained during total window testing (Q_t) averaged 0.025 inches of water (6 Pa). These windows were extremely leaky, exceeding the blower capacity at larger pressure differentials, largely due to nothing having been done to prevent air from passing through the old window weight cavities or the large gaps at the meeting rails. This is reflected in the high value for the rough opening effective leakage area (1.32 in²), which is based on only 30% of the extraneous air measured during the field tests.

Table 11: Average leakage characteristics for upgrade types retaining original sash

Site ID	Upgrade Description	n	Q _i (scfm/lfc)	ELA _{s,x19} (in ²)	ELA _{RO x19} (in ²)	ELA _{tot} (in ²)	Diam. (in)
12	Vinyl jamb liners; no weather stripping	7	1.80	2.49	0.56	3.05	1.97
13	Vinyl jamb liners; silicone bulb weatherstripping at sill and head junctions	8	1.40	2.23	0.56	2.79	1.88
7	Vinyl jamb liners; silicone bulb weatherstripping at sill, head, and meeting rail junctions	19	0.78	0.87	0.26	1.13	1.20
2	Bi-Glass System with vinyl jamb liners; silicone bulb weatherstripping at sill, head, and meeting rail junctions; double-pane insulating glass; new latch at meeting rail	3	0.48	0.71	0.33	1.04	1.15
16	Caldwell coiled spring balances with silicone bulb weatherstripping at sill and head junctions; some weatherstripped wooden storm windows	6	***	***	1.32	***	***
17	Zinc rib-type weatherstripping on lower sash; upper sash painted in place; V-strip weatherstripping at meeting rail; pulley seals; new aluminum triple-track storm windows, frames caulked in place	3	0.18	0.48	0.61	1.09	1.18
19	Bronze V-strip weatherstripping on lower sash, meeting rail, and sill junction; top sash painted in place; existing aluminum triple-track storm window caulked in place; no locking mechanism	2	0.49	0.54	0.17	0.71	0.95
10	Sash weatherstripped with Polyflex T-slot between sash face and parting bead; Polyflex at sill, head, and meeting rail junctions	1	0.10	0.29	0.42	0.71	0.95

The lowest sash whole window effective leakage area (ELA_{s,x19}) was the window with Polyflex weatherstripping. That value should not be considered typical of the upgrade type as only one example was tested. That specific window required major sash repair prior to weatherstripping, with the entire renovation process requiring twelve man-hours. It was not possible to determine how much sash leakage reduction was a result of sash repair as opposed to weatherstripping.

Both sites 10 and 19 showed equivalent values for whole window effective leakage area ($ELA_{tot} = 0.71 \text{ in}^2$) while having significantly different sash leakage rates ($ELA_{s \times 19} = 0.29$ and 0.54 in^2 , respectively), with the discrepancy arising from exterior air entering via the rough opening ($ELA_{RO \times 19}$). Site 10 had a significantly larger $ELA_{RO \times 19}$ than site 19 (0.42 versus 0.17 in^2 , respectively) which was assumed to be more an artifact of building construction rather than window renovation. While this further illustrated the significant contribution exterior air can have when determining the infiltrative heat load of a window, it also showed the effect differing $ELA_{RO \times 19}$ values can have in determining the total infiltrative heat load of a window. To view the effect of differing $ELA_{RO \times 19}$ values on heating costs, an average value for $ELA_{RO \times 19}$ was used to determine ELA_{tot} for all upgrades, thereby removing building variation as a factor. Average $ELA_{RO \times 19}$ values yielded statistically equal results.

Both the zinc rib-type and bronze V-strip weatherstripping upgrades ($n = 3$ and 2 , respectively) show relatively low values for $ELA_{s \times 19}$ (0.48 and 0.54 in^2 , respectively). The Bi-Glass System upgrade ($n = 3$) has an $ELA_{s \times 19}$ substantially greater than either the rib-type or V-strip weatherstripping (approximately 50% and 30%, respectively). The low number of samples for these three upgrades carries little statistical validity and comparisons of results should therefore be viewed with caution.

Field sash leakage rates expressed as $ELA_{s \times 19}$ for the three Bi-Glass System upgraded windows are slightly larger than results from the one laboratory window having undergone the Bi-Glass System upgrade ($ELA_{s \times 19} = 0.71 \text{ in}^2$ versus 0.65 in^2). Due to the nature of the lab set-up, no comparisons could be made for $ELA_{RO \times 19}$ or ELA_{tot} . It should be noted that the three field windows were pin-type windows while the lab window was a pulley-type. As

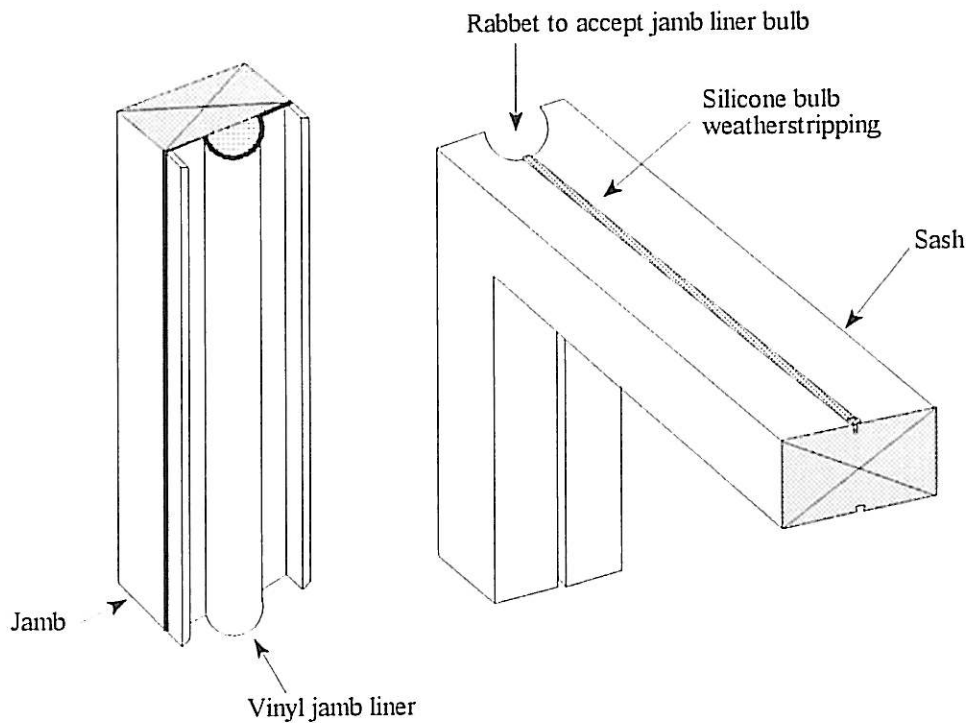
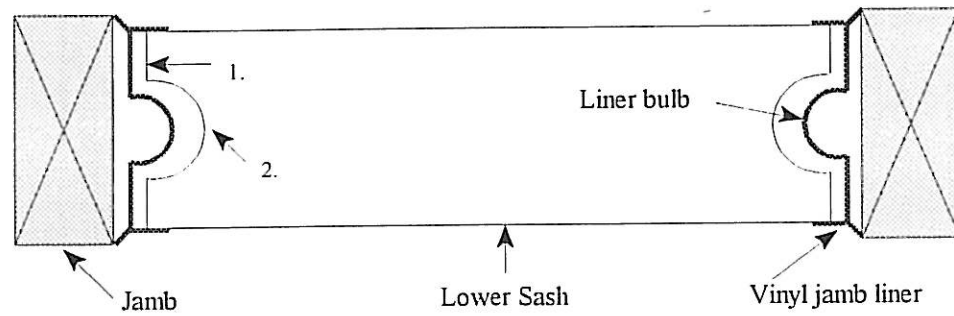


Figure 4: Schematic of an original sash and jamb modified to accept a vinyl jamb liner and silicone bulb weatherstripping

noted previously, pulley-type windows had significantly more exterior air leakage than pin-type but once again, caution should be taken when interpreting these results due to extremely low sample populations (Section 4.2.2).

Windows at sites 7, 12, and 13 used the same brand of vinyl jamb liner, with upgrade differences being found in the location of silicone bulb weatherstripping if it had been installed (Figure 4). Site 12 had no silicone bulb weatherstripping with the exception of the sill junction of one window. Site 13 had the same size and type windows as site 12, but had weatherstripping inserted into both sill and head junctions. The silicone bulb weatherstripping appeared to have little effect in reducing sash air leakage as no significant difference between



1. Sash to jamb distance
2. Sash to liner bulb distance

Figure 5: Schematic of lower sash and vinyl jamb liner junction

$ELA_{s \times 19}$ for the two sites was found (2.49 and 2.23 in², respectively; $p = 0.71$). The lack of a significant difference in sash leakage rates between sites 12 and 13 was somewhat unexpected as visually, the windows at site 12 appeared to have a poorer fit.

Site 7 had two window sizes, both larger than the windows at either site 12 or 13. These windows had silicone bulb weatherstripping inserted into the sill, head, and meeting rail junctions. There was a significant difference in $ELA_{s \times 19}$ between sites 7 and 13 (0.87 versus 2.23 in², respectively; $p < 0.001$), with the only difference between the two being weatherstripping at the meeting rail junction at site 7. The meeting rail gap had a very weak correlation with sash leakage as discussed previously ($R^2 = 0.48$, Section 4.2.5), so addition of weatherstripping at the meeting rail junction likely accounted for some but not all of the sash leakage reduction. To further investigate the difference, the jamb liner bulb/sash distance and jamb/sash distance were measured to see if a correlation existed between sash liner fit and sash leakage (Figure 5). A combined sash/liner parameter (consisting of the two measurements summed) was also tested for correlation to $ELA_{s \times 19}$. No significant correlations ($p = 0.08$) were found between sash/jamb liner measurements and $ELA_{s \times 19}$ for

any of the three sites.

Site 12 windows had significantly larger jamb liner/sash gaps than either site 13 or 7 ($p = 0.03$) while showing no statistical difference in $ELA_{s \times 19}$ as site 13 ($p = 0.71$). Routing of the sash to accommodate vinyl jamb liners was done by the same work crew at sites 12 and 13, while a different work crew performed the work at site 7. No significant difference in jamb liner/sash gaps was found between sites 7 and 13 ($p = 0.32$) although there was a significant difference in $ELA_{s \times 19}$ between the sites ($p < 0.001$). Based on the limited data, it is inconclusive as to whether differing work crews had a significant effect on installation quality and therefore, sash leakage rates, although the comparisons listed above suggest such an effect. In an earlier study, few significant differences in leakage rates were observed when differing contractors installed the same type windows in new residential housing in Minnesota (Weidt, 1992). However, that study concerned the installation of new windows whereas reworking original sash as in this study can allow more opportunity for differences in installation quality. It remained unresolved as to why site 7 window upgrades had better sash leakage characteristics than sites 12 and 13, although one contributing factor may be the locking mechanism and the amount of force it generates between the sash and jamb when closed.

New windows are characterized by sash leakage rates per linear foot crack and must meet or surpass the industry standard of 0.37 scfm/lfc at 0.30 inches of water pressure in order to be certified. Table 11 lists average extrapolated sash leakage rates (Q_s) at 0.30 inches of water for each upgrade type for comparative purposes with the industry standard. Actual sash leakage averages could not be used for comparative purposes as only 21 of the

49 original sash upgrades were of sufficient tightness to attain 0.30 inches of water pressure with the remaining 28 windows exceeding the blower capacity of the test unit.

Averaged sash leakage rates of the tightest original sash fitted with vinyl jamb liners and weatherstripping (site 7, 0.78 scfm/lfc at 0.30 in. H₂O) showed significantly more sash leakage than the certifiable industry standard window ($p < 0.001$). While other original sash upgrade options such as the Bi-Glass System and varied weatherstripping options appear to have large sash flow reductions, caution must be taken in drawing conclusions concerning those upgrades since the upgrade options had very population numbers ($n \leq 3$).

4.3.2 Replacement sash upgrades

Two makes of replacement sash utilizing vinyl jamb liners were encountered at four sites during field testing, accounting for eleven windows. Nine of the windows from both manufacturers were in-kind replacement units with single-glazing and utilized the existing jamb. Two other windows from one manufacturer had double-pane insulating glass. Table 12 presents leakage characteristics of these windows based on extrapolated values. Three of the eleven windows did not allow attainment of the maximum pressure (0.30 in. H₂O), although two (12B, 12D) allowed pressurization at 0.25 inches of water pressure. The third window (13I) was installed in an out-of-square frame, with 5 mm gaps at opposing upper and lower corners, attaining a maximum pressure of 0.07 inches of water (17.5 Pa). The average extrapolated leakage rate for the in-kind replacement sash ($Q_s = 0.31$ scfm/lfc) is significantly

Table 12: Leakage characteristics for 11 replacement sash

Q_s Ext. Avg (scfm/lfc)	$ELA_{1 \times 19}$ (in ²)	$ELA_{R0 \times 19}$ (in ²)	ELA_{int} (in ²)	Diameter (in)
0.31	0.45	0.30	0.75	0.98

less than the 0.37 scfm/lfc certifiable standard set by the window industry ($p = 0.002$), meaning the replacement sash were considered tight windows with low infiltrative rates.

The two sets of replacement sash with double-pane insulating glass (18A, 18B) were placed in visually out-of-square frames resulting in reported high levels of discomfort during the winter. After one heating season, these two windows underwent extensive sealing to reduce sash and extraneous air leakage prior to the pressurization testing. It was apparent from leakage characteristics of window 13I and occupant descriptions of air infiltration through 18A and 18B that squareness-of-frame was an important issue when using a replacement sash.

4.3.3 Window insert upgrades

Fourteen replacement window inserts at four sites, representing two manufacturers, were field tested during the study. All but one of these windows (16G) attained the maximum test pressure. The extraneous air leakage test (Q_e) for window 16G revealed a large volume of air leaking through the rough opening (0.07 in. H_2O maximum Q_e pressure attainable), an atypical result for other window inserts tested. Table 13 summarizes replacement window insert sash leakage data, both including and excluding window 16G. Window 16G illustrated the importance of sealing the rough opening to reduce exterior air infiltration. When data

Table 13: Sash leakage characteristics for replacement window inserts

	Q , Actual Avg (scfm/lfc)	Q , Ext. Avg (scfm/lfc)	$ELA_{s \times 19}$ (in ²)	$ELA_{RO \times 19}$ (in ²)	ELA_{int} (in ²)	Diam. (in)
16G excluded	0.14	0.13	0.12	0.09	0.21	0.52
16G included	---	0.17	0.13	0.16	0.29	0.61

Table 14: Comparison of exterior air volumes by upgrade type

Upgrade Category	Site Number(s)	n	Q _s (scfm/lfc)	ELA _{RO x 19} (in ²)	Diam. (in)
Window insert	6, 7, 11	13	0.13	0.16	0.34
Replacement sash	3, 12, 13, 18	11	0.29	0.30	0.62
Bi-Glass System	2	3	0.48	0.33	0.65
Original sash with vinyl jamb liners	7, 12, 13	34	1.14	0.39	0.70

from window 16G was included, the average ELA_{RO x 19} increased by approximately 75%. Window 16G also showed window inserts may not necessarily reduce exterior air infiltration significantly.

Replacement window inserts were expected to reduce extraneous air flow as they consisted of both sash and an integral frame. Table 14 compares the effective leakage area of the rough opening for window inserts (including 16G) to other upgrade categories and also shows extrapolated sash leakage rates at 0.30 inches of water pressure (Q_s). A significant reduction in ELA_{ex19} was achieved by the use of window inserts (0.16 versus 0.30 - 0.39 in²; p < 0.001), likely a result of the insert's integral frame sealing the existing jamb.

4.3.4 Storm window upgrades

Four different configurations of storm window upgrades were field tested, encompassing both new storm windows and upgrades of existing storm windows. General configurations of storm windows were aluminum triple-track, aluminum fixed sash with removable lower pane, fixed wooden sash, and fixed interior pane. Two aluminum triple-track storms were encountered that had been installed as interior storm windows. The number and type of each storm window tested are listed in Table 15 as well as the percentage

Table 15: Storm window upgrades by type

Upgrade Description		Site ID	n	Q _i Open (scfm/lfc)	Q _i Closed (scfm/lfc)	% Q _i Red.
New	Aluminum triple-track, replacement	10	1	1.80	0.93	50%
		14	4	1.16	0.27	75%
		17	3	0.18	0.11	35%
	Aluminum fixed sash, removable lower sash	10	1	1.10	0.48	55%
	Wooden sash, replacement	7	1	2.00	1.32	35%
	Interior mount, aluminum triple-track, replacement	14	2	1.11	0.04	96%
	Interior storm window, spring loaded metal frame	10	1	1.10	0.05	95%
	Interior storm window, plexiglass with magnetic stripping	15	4	0.90	0.01	98%
Original	Aluminum triple-track, existing frame caulked	19	2	0.49	0.35	30%
	Wooden sash, felt weatherstripping	16	4	***	***	***

*** No data available

reduction in sash air leakage when the storm window was closed. An overall improvement could not be determined for site 16 windows due to their extremely leaky nature.

Sash leakage reduction varied between the types of storm windows with interior storms providing the largest percentage reduction. This was clearly illustrated at site 14 where six windows were tested, four with aluminum triple-track storm windows mounted on the exterior and two with identical storm windows mounted on the interior. Interior installation of the two triple-track storm windows in this building was done to maintain the historic appearance of its front facade. All six storm windows had the aluminum trim caulked to the window trim with two one-inch slot weepholes left at the bottom. The four exterior storm windows reduced prime sash leakage by 75% while the two interior storms reduced

prime sash leakage by 96%.

A wide range of variability was observed in sash leakage reduction for windows fitted with new aluminum triple-track windows. The variability was dependent on site and was likely a result of installment procedures. Aluminum frames at site 14 were caulked to the exterior trim and were affixed to leaky prime windows (average extrapolated $Q_s = 1.14$ scfm/lfc). This was reduced to an average extrapolated sash leakage rate of 0.19 scfm/lfc for all six windows when the storms were closed. Site 17 frames had also been caulked in place but were three years old. Compared to site 14, the prime windows at site 17 were much tighter (average extrapolated $Q_s = 0.18$ scfm/lfc, reduced to 0.11 scfm/lfc with storms closed), an effect that decreases the importance of a reduction due to an effective storm window. Sample populations for all storm window types were too small to allow for valid statistical studies, but good quality storm windows can be seen to reduce sash leakage rates.

As well as reducing sash leakage (Q_s), interior storm windows provided the additional benefit of reducing extraneous air leakage (Q_e) by their installation within the interior window jamb, thus blocking air leakage to the interior from the rough opening. A drawback to interior storm windows as reported in the literature was the potential to cause moisture related problems from accumulated condensation (Park, 1982). Two sites (10 and 15) had fixed panel interior storm windows, while a previously discussed third location (site 14) had two aluminum triple-track storm windows installed on the interior window. Table 16 summarizes the reduction in extraneous leakage achieved by each interior storm window configuration. While reductions in extraneous air leakage are large, the small sample numbers should be noted.

Table 16: Percent reduction in extraneous leakage by interior storm window configuration

Interior Storm Window	Site ID	n	Q _e Open (scfm/lfc)	Q _e Closed (scfm/lfc)	Percent Q _e Reduction
Glass with metal frame	10	1	0.77	0.33	60%
Plexiglass with magnetic stripping	15	4	4.22	0.34	90%
Aluminum triple-track	14	2	1.13	0.46	60%

4.3.5 Double- versus single-glazing upgrades

Nineteen of the 87 window upgrades were fitted with double-pane insulating glass. Sixteen double-glazing upgrades were either replacement sash or window inserts, with the remaining three windows being original sash using the Bi-Glass System upgrade. Infiltrative differences were not expected between double- and single-glazed sash as glazing layers did not affect leakage in upgraded windows. However, thermal transmission differences due to a second glazing layer were expected as non-infiltrative loss rate changes and were modeled using WINDOW 4.1. Table 17 lists non-infiltrative loss rates for various glazing combinations

Table 17: Non-infiltrative thermal loss rates for assumed windows and glazing replacements

Site ID	Window Description	n	U-value (Btu/hr-ft ² -°F)	R-value (hr-ft ² -°F/Btu)
---	Typical and tight: single-glazed, storm windows	---	0.51	1.96
---	Loose: single glazed, no storm window	---	0.92	1.09
2, 7, 11, 16, 18	Double-glazed insulating wood sash, 1-over-1	13	0.49	2.04
6	Double-glazed insulating vinyl sash/ frame, 1-over-1	6	0.47	2.13
***	Single-glazed prime sash with low-e storm window	---	0.43	2.33
***	Low-e, single-glazed sash with standard storm window	---	0.37	2.70
***	Low-e, double-glazed insulating sash	---	0.35	2.86

***Not encountered in the field

as calculated by WINDOW 4.1 based on a double-hung wooden window with dimensions of 36 x 60 inches. Also included are non-infiltrative thermal loss rates for the baseline tight, typical, and loose windows.

The U-values for double-glazed windows and single-glazed windows with storms are relatively similar (0.49 versus 0.51 Btu/hr-ft²-°F, respectively), showing that storm windows are an effective second glazing layer when closed, reducing transmissive losses. Although not encountered during field testing, low-e glazing options were modeled using WINDOW 4.1 and are included in Table 17. It can also be seen that low-e glazing significantly reduces thermal non-infiltrative loss rates for any equivalent number of glazing layers.

Any possible effects of wind-driven infiltration moving into the storm window/prime sash space were not taken into account, that interaction being beyond the scope of the study. Such effects could change non-infiltrative thermal heat loss rates through a window.

4.3.6 Window upgrades summation

The importance of exterior air contributing to the overall infiltrative heat load of a window was seen throughout all upgrades. Exterior air leakage rates through the rough opening were often as great or greater than sash leakage rates. Window inserts generally reduced rough opening air leakage significantly by virtue of an integral frame. Replacement sash were shown to be effective in reducing sash leakage when placed in a square frame.

Second glazing layers reduced non-infiltrative losses significantly, whether the second layer was a result of a storm window or double-pane insulating glass. Low-e glass was shown to reduce non-infiltrative loss rates even further based on modeling results. Replacement

storm windows provided the benefit of a second glazing layer while also reducing prime sash leakage. Interior storm windows reduced prime sash leakage even further while also serving to reduce exterior air leakage rates.

Original sash utilizing vinyl jamb liners still allowed significant sash leakage, although no significant correlation was found between sash fit and leakage rates. It was inconclusive as to the effect installation practices had on these leakage rates.

4.4 Laboratory test window data

Two double-hung, pulley-type windows were purchased from a salvage warehouse to be used for laboratory testing. The purposes of testing windows in a laboratory were as follows:

1. to test the repeatability of the test procedure and equipment under controlled conditions;
2. to investigate the location of air leakage sites in detail;
3. to test improvements due to routine maintenance and various upgrades; and
4. to compare laboratory results of an upgrade to its field results.

These two windows appeared to be in better condition than many of the original condition windows encountered during field testing. Both lab windows had meeting rails that fit well with operable sash locks. Both windows also had a good sash to jamb fit, sitting squarely in their frames.

Walls were constructed of 2 x 6 lumber with quarter inch plywood facing to support the test windows. No effort was made to mimic older building styles as the intent was to prevent extraneous air leakage via the rough opening from entering the test zone, eliminating

a variable (ie., exterior air) that was difficult to quantify. Rough openings were sealed against air leakage from other wall areas with plastic and duct tape prior to installation of the windows to ensure measured air came solely through the window (ie., sash leakage, Q_s), removing the need for the exterior plastic sheet as required by ASTM E783-93. The effectiveness of the plastic was tested after window installation by running the fan pressurization test as performed under field conditions. At 0.30 inches of water (the maximum test pressure), a sash air leakage rate below the limits of resolution of the pressurization unit flow meter was observed for the entire window, meaning any leakage was below the measurement capabilities of the test unit. It was therefore assumed the rough opening had been effectively sealed.

4.4.1 Leakage locations and reduction of leakage rates due to routine maintenance

Lab window A was not immediately upgraded, being tested first in its original condition with missing putty, loose glass, and little paint to provide a baseline comparison for leakage reductions as a result of routine maintenance. Routine maintenance was considered to be application of new putty while replacing the glazing if necessary. The gap between the edge of the exterior trim and wall was also caulked, a step that would reduce extraneous air leakage in the field. These steps provided some idea of the efficacy of simple maintenance in reducing air infiltration as well as a baseline for comparison to other rehabilitation options.

Lab tests for window A were comprised of isolating and testing window leakage areas for respective sash leakage rates to gain a sense of where the majority of leakage occurred. Leakage sites were chosen on the assumption they would likely be addressed during window renovations. The exception is site F, the inside edges of the exterior trim. This site, along

with air from the outside edges of the exterior trim, was chosen to investigate the amount of air entering the test zone by way of the window weight cavity. Each leakage area was tested six times for statistical validation and was also used to check the reproducibility of the portable air test unit. Individual leakage sites of the window were identified as follows:

- A - the window as a whole unit;
- B - the meeting rail;
- C - the upper sash with the meeting rail sealed;
- D - the lower sash with the meeting rail sealed;
- E - the junction between the sill and the lower sash;
- F - the inside edges of the exterior trim; and
- G - the outside edges of the exterior trim.

Figure 6 shows reproducibility in terms of the test unit and day-to-day testing (i.e.,

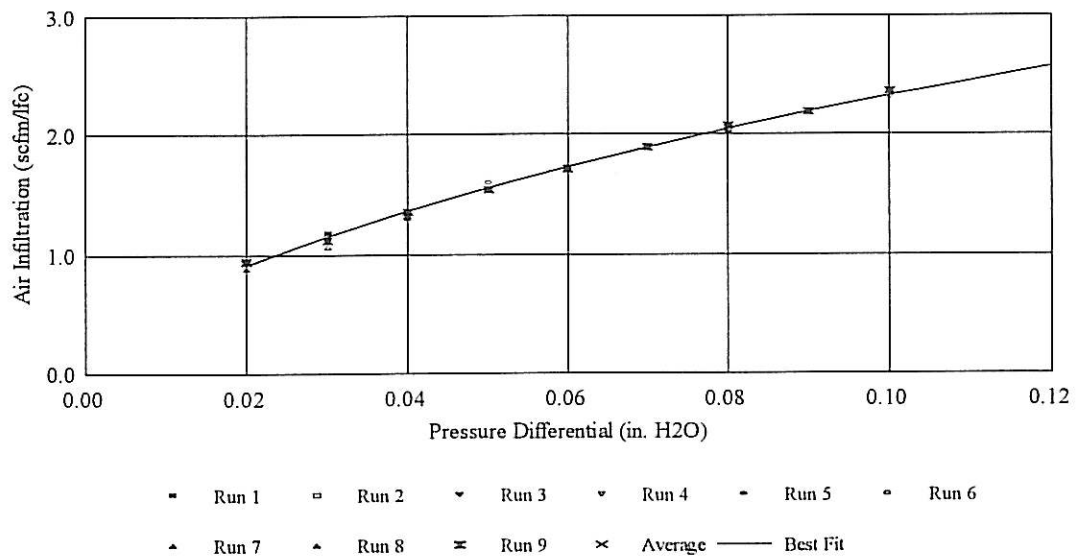


Figure 6: Reproducibility of lab pressurization test results and test device over time

reproducibility over time), questions specifically addressed during testing of the window as a whole unit (leakage site A). Three sets of three tests were run over the course of nine days to determine the reliability of test results. The air test unit was found to be reliable in terms of reproducibility, with the nine sets of data points falling on top of each other (Figure 6). These same sets of data also demonstrate the reproducibility of the test over a period of nine days, resulting in a high degree of confidence in the test procedure and the fan pressurization unit.

Each individual leakage site investigated using lab window A exceeded the certifiable industry standard for whole window sash leakage rates of 0.37 scfm/lfc at 0.30 inches of water pressure (75 Pa) for new window units (Figure 7). Both the total window (A) and lower sash (D) failed to attain the specified test pressure of 0.30 inches of water (75 Pa) due to limited blower capacity. Values shown in Figure 7 are those both measured and derived from extrapolations based on regression coefficients. Lab window A was considered to be an extremely leaky window as the maximum test pressure differential could not be attained for some individual sections, let alone the whole window.

The same leakage sites were retested after lab window A had new putty applied around the glazing of both sash and the exterior trim/wall junction caulked (i.e., routine maintenance). New putty was expected to decrease sash leakage (Q_s) while caulking was expected to decrease what would be exterior air leakage (Q_{RO}) through the window weight cavities in the field.

It can be seen from Figure 7 that significant reductions in sash leakage rates at 0.30 inches of water pressure (75 Pa) were observed ($p = 0.02$), but the lab window would still be

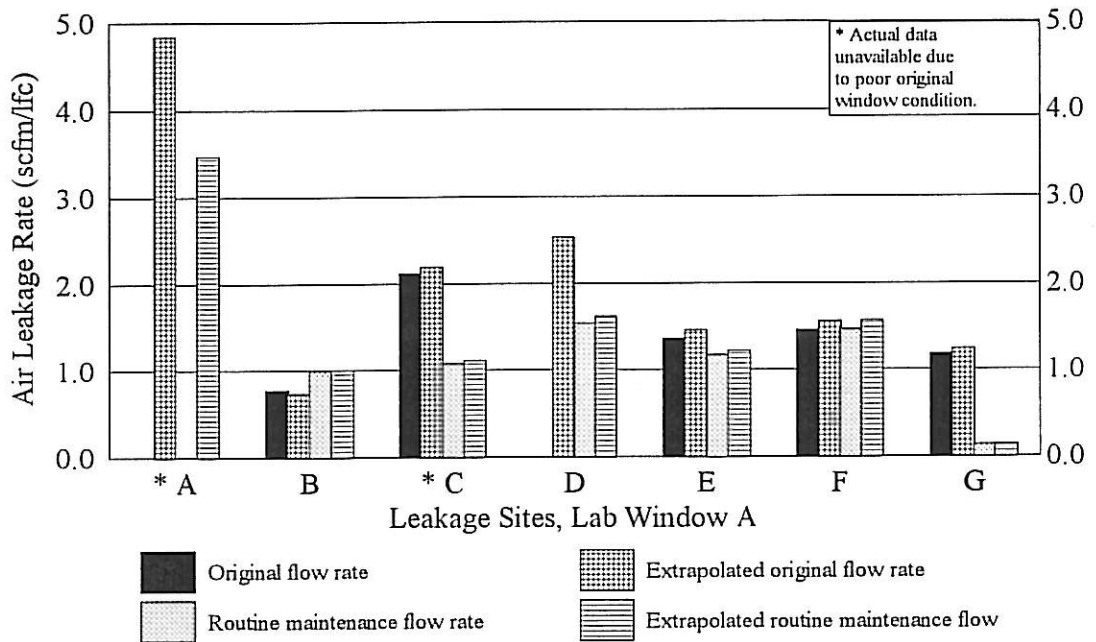


Figure 7: Lab window A leakage rates, original condition window versus routine maintenance

- A - Leakage rate through the total window
- B - Leakage rate through the meeting rail
- C - Leakage rate through the upper sash with the meeting rail sealed
- D - Leakage rate through the lower sash with the meeting rail sealed
- E - Leakage rate through the sill junction
- F - Leakage rate through the inside edges of the exterior trim
- G - Leakage rate through the outside edges of the exterior trim

classified as a loose window due to a whole window leakage rate over 3.4 scfm/lfc. Six of the seven individual leakage sites investigated were still above the certifiable industry standard for whole window sash leakage after routine maintenance. The one exception was site G, which allowed air leakage between the wall and outside edges of the exterior trim, allowing air infiltration through the window weight cavities. This site was the area receiving caulk, a procedure that would reduce exterior air infiltrating around a window in a building. Sash leakage rates (sites C, D) were reduced an average of 65% after routine maintenance, while leakage around the exterior trim/wall junction (site G) was reduced by 90%. An overall

leakage reduction of 35% was observed for the window as a whole. Simple window maintenance can significantly reduce air leakage for loose windows, but still allow significant leakage through and around the window. Leakage reduction would not be as significant for tight windows.

Examination of Figure 7 shows air leakage rates were not additive, as the total window leakage rate should have been equivalent to the summed leakage rates of other sites at equivalent pressures, excluding the sill junction (ie., $A = B+C+D+F+G$). The sill junction (E) was excluded from the summation as it was incorporated in the lower sash reading (D). Total window leakage rate was 4.8 scfm/lfc while the sum of the individual sites, physically identical to the total window leakage site, was 8.3 scfm/lfc. When added in quadrature, summed leakage rates more closely approximated the whole window rate (4.0 versus 4.8 scfm/lfc, respectively) as discussed by other authors (Sherman and Modera, 1986).

While the underlying cause of the resulting discrepancy when summing leakage rates was not investigated, it is possible that different masking combinations for differing leakage sites affected the mobility of window components, allowing or preventing valve action by one or more components. Changing mobility would allow a component to remain stationary under one masking combination while moving freely under another, affecting the air leakage rates.

It can be seen that for this one laboratory test window, the upper and lower sash separately accounted for approximately half the total window leakage when tested individually, both constituting major leakage sites. The above data are based on one window and should therefore not be considered representative of typical windows.

While leakage rates were not additive, effective leakage areas were expected to be (Proskiw, 1995a). Effective leakage areas for the laboratory test sites appeared more additive than leakage rates, overestimating the whole window value by an average of 30%, as opposed to a 65% overestimation when using leakage rates. An anomaly serving to increase overestimation based on ELA's was noted at the meeting rail (site B). Although air leakage was expected to remain relatively constant at sites B, E, and F, air leakage through the meeting rail increased by 25% after routine maintenance although remaining relatively constant at sites E and F. Routine window maintenance should not have affected those three sites as no changes were made to their physical nature. That increase in air leakage through the meeting rail after routine maintenance was not investigated further as the purpose was to check the approximate additive nature of ELA's, but may have been a result of a window component (or components) being held in a different position due to masking.

4.4.2 Laboratory tests of Bi-Glass System upgrade

Three windows at site 2 (all single-hung, pin-type windows) and one lab test window (a double-hung, pulley-type window) received the Bi-Glass System window upgrade. Lab window B treatment differed from the site 2 treatment by not inserting the double-pane insulating glass. The double-pane insert was excluded from the lab window as double-pane insulating glass should affect only non-infiltrative losses and not leakage rates, although in retrospect, the double-pane insulating glass may have affected window stiffness and thus the leakage rates. Non-infiltrative losses were investigated by computer simulation rather than lab testing.

The lab window was a pulley-type window with attached window weights. The Bi-

Glass System upgrade involved cutting window weight ropes while leaving the weights in the window weight cavity. Pulleys were removed from the jambs with fiberglass insulation then stuffed into the window weight cavities through the pulley openings. The pulley openings and window weight access panels were sealed with duct tape prior to installation of the jamb liners. Vinyl jamb liners were cut to length to fit the existing jamb and had an adhesive foam backing to reduce air movement between the jamb and jamb liner. The foam backing was compressed by the sash as well as three support screws on each jamb liner. The existing sash were routed to accept vinyl jamb liners and double-pane insulating glass inserts. Although existing muntins in the lab window were not an issue since double-pane insulating glass was not being installed, muntins present in a divided light would be trimmed to fit over the replacement glass, mimicking the look of a true divided light. The top rail of the upper sash and bottom rail of the lower sash were routed to accept a silicone weatherstripping bead intended to improve the seal at the head and sill junctions. A third silicone weatherstripping bead was inserted into the lower rail of the top sash to tighten the meeting rail junction, along with a new vinyl latch type lock attached near the meeting rail center.

Air leakage rates in terms of sash leakage (Q_s , as scfm/lfc) for various leakage sites of lab window B and its Bi-Glass System upgrade were compared (Figure 8). Sections A and C of the lab window in its original condition could not attain 0.30 inches of water pressure (75 Pa), but all sections were able to achieve the maximum test pressure after the Bi-Glass upgrade. Both Figures 7 and 8 show extrapolated and actual values where attainable, illustrating the proximity of extrapolated values to actual values.

The Bi-Glass upgrade made significant improvements to the efficiency of the lab

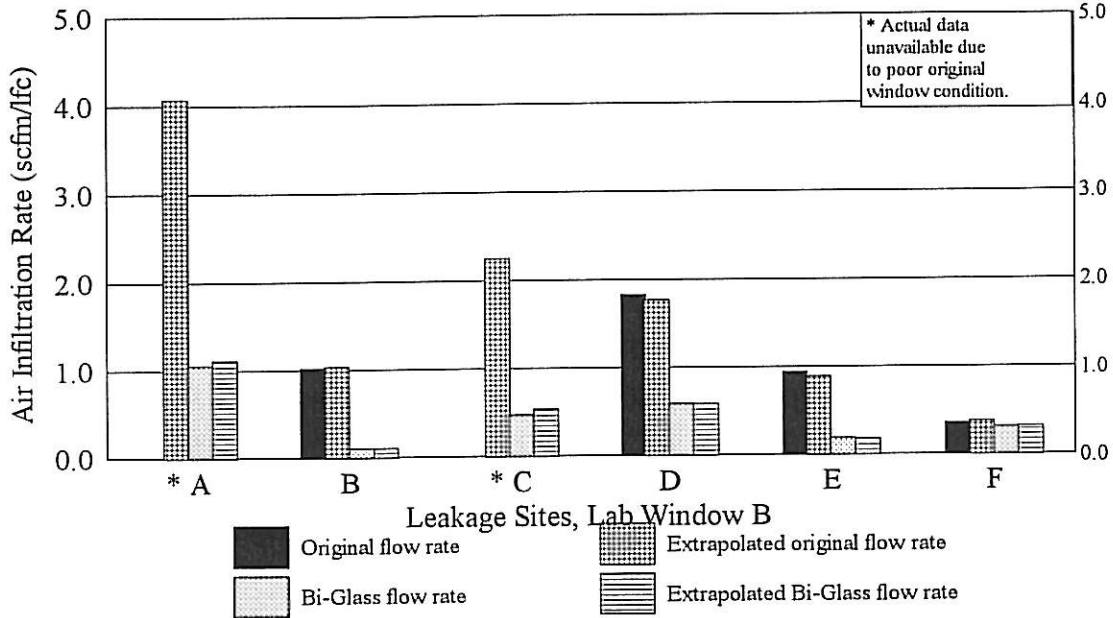


Figure 8: Lab window B, relative leakage reductions due to Bi-Glass System upgrade

- A - Leakage rate through the total window
- B - Leakage rate through the meeting rail
- C - Leakage rate through the upper sash with the meeting rail sealed
- D - Leakage rate through the lower sash with the meeting rail sealed
- E - Leakage rate through the sill junction
- F - Leakage rate through the outside edges of the exterior trim

window at all locations except through the outside edge of the exterior trim (F in Figure 8). This site represented extraneous air coming through the rough opening (Q_{RO}), passing into the test zone through the window weight cavities. As discussed previously, the Bi-Glass System window renovation stuffed fiberglass insulation into the window weight cavities to decrease air leakage through the rough opening (i.e., Q_{RO}), resulting in an approximate 10% reduction in leakage. The small decrease in air leakage through the rough opening supports the findings of an earlier Canadian study on the effectiveness of rough opening sealing methods (Proskiw, 1995a). That study showed fiberglass insulation stuffed into rough openings was a poor sealing method.

Extrapolated leakage rates for lab window B were over 4.0 scfm/lfc, based on regression coefficients for sash leakage at 0.30 inches of water pressure (75 Pa). The Bi-Glass System upgrade decreased the sash leakage rate to 1.1 scfm/lfc, a 360% reduction relative to the extrapolated value of 4.0 scfm/lfc. While the improvement was significant, the resulting air leakage rate was still well above the industry standard for new windows (0.37 scfm/lfc at 0.30 inches of water pressure).

A chemical smoke generator was employed to observe air currents to further identify leakage sites in the Bi-Glass System upgrade. Air was observed easily infiltrating the jamb/jamb liner junction, as well as the head/upper sash junction. Leakage through the jamb/jamb liner junction implied the failure of the jamb liner foam backing to perform as intended. The same was true for the silicone weatherstripping bulb in the head/upper sash junction.

4.4.3 Laboratory testing summation

Testing of the two lab windows revealed the perimeters of both sash to be major air leakage sites. Routine maintenance was shown to significantly reduce air leakage if the original condition window was in poor condition, but the result was still a loose window allowing substantial air leakage. The Bi-Glass System upgrade significantly reduced air flow for the whole window but did little to reduce air flow through the window weight cavity (i.e., a source of exterior air infiltration). Both the weatherstripping at the head junction and the foam backing on the jamb liners of the Bi-Glass System upgrade allowed air flow when viewed with a chemical smoke generator, implying a poor fit.

4.5 Natural infiltration rates

Window air leakage rates, as measured by fan pressurization in the field, do not directly correspond to natural infiltration rates through those windows during the heating season as discussed previously (Section 3.4). Natural infiltration rates vary over time largely as a result of a combination pressure differential, induced by wind speed and direction along with interior/exterior temperature differences.

The sash and extraneous air leakage rates for each window were used to extrapolate induced leakage rates at 0.016 inches of water pressure (4 Pa), the assumed heating season driving pressure for natural infiltration. Based on field measurements, 30% of the averaged extraneous air was assumed to be exterior air entering through the rough opening and was added to the sash leakage rate. This whole window infiltrative leakage rate was converted to a whole window effective leakage area (ELA_{tot}) at 0.016 inches of water pressure (4 Pa). The resulting value was used in the LBL correlation model to convert ELA_{tot} to a natural infiltration rate (Q_{nat}) for each type of window and upgrade. Parameters typical of the Vermont climate and affordable housing were used in the model (Table 18).

Table 18: Parameters assumed to be typical of Vermont, used in the LBL correlation model

Housing Parameters			Weather and Terrain Parameters		
Volume		30,000 ft ³	Terrain Parameters	γ	0.23
Roof Height		19 ft		α	0.73
Leakage area	ceiling	33%	Shielding Coefficient (Class III)		0.24
	floor	33%			
	walls	34%			
Interior Temperature		68°F			

The Vermont heating season was assumed to extend from the month of October through April. Mean monthly temperatures and wind speeds throughout the heating season for Burlington, Vermont were used to determine the overall heating season natural infiltration rate. The LBL model was placed in a spreadsheet and run using a personal computer with a sample print-out in Appendix J. Table 19 summarizes the predicted natural infiltration rates (Q_{nat}) based on results of the LBL correlation for each baseline window and window upgrade. Infiltration rates, expressed as ELA_{tot} , were based on whole window infiltration which includes the exterior air component. Most window upgrades have very low sample populations (n) and should not necessarily be regarded as typical of the upgrade type nor viewed as statistically significant but are helpful for envisioning potential trends and relationships.

Values for both ELA_{tot} and Q_{nat} for site 7, storm closed, should be viewed with a large degree of caution. The site had only one wood sash storm window (7B 2) in place with a poor fit to the exterior trim. The averaged site value for leakage with storm windows in place was based on the ratio of extrapolated sash leakage values for the one window tested with and without a storm at 0.30 inches of water pressure. This ratio (0.66:1) was multiplied by the average ELA_{tot} for storm windows open (off in this case) to estimate the effect of storms covering all site windows. The LBL correlation was run using these manipulated values and is therefore subject to speculation.

Replacement sash included two double-pane insulating glass windows not fitted with storms at site 18. The two data values in Table 19 reflect both the inclusion and exclusion of those windows from the group average. It can be seen that these two windows had a large

role in reducing average ELA_{tot} and Q_{nat} values for replacement sash with storm windows open. A large portion of the difference was in the volume of exterior air measured during the pressurization test that entered via the rough opening. Windows at site 18 had an excessive amount of work done to reduce exterior air leakage and were not considered typical renovations.

Window inserts also included one atypical window as discussed previously (Section 4.3.3). Again, two LBL correlation values are shown in Table 19 for replacement window inserts, one including window 16G and the other excluding it.

Table 19: Estimated natural infiltration flow rates (Q_{nat}) for the period October through April

Window	Site ID	n	Storm open		Storm closed		
			ELA_{int} (in ²)	Q_{nat} (scfm)	ELA_{int} (in ²)	Q_{nat} (scfm)	
Typical with storm window	—	—	—	—	1.48	2.07	
Tight with storm window	—	—	—	—	0.85	1.19	
Loose with no storm window	—	—	2.77	3.87	—	—	
Original sash; vinyl jamb liners; no weatherstripping	12	7	3.05	4.26	1.48	2.07	
Original sash; vinyl jamb liners; weatherstripping at sill, head junctions	13	8	2.79	3.90	1.74	2.43	
Original sash; vinyl jamb liners; weatherstripping at sill, head, meeting rail junctions	7	19	1.13	1.58	0.83*	1.16*	
Bi-Glass System	2	3	1.04	1.45	0.71	0.99	
Coiled spring balances; weatherstripping at sill, head junctions; wooden storm windows weatherstripping	16	2	—	—	3.43	4.80	
Rib-type weatherstripping; V-strip at meeting rail; pulley seals; top sash painted in place; new triple-track storm window frames caulked in place	17	3	1.09	1.52	0.91	1.27	
V-strip weatherstripping around lower sash; top sash painted in place; existing triple-track storm window frames caulked in place	19	2	0.71	0.99	0.60	0.84	
Polyflex T-slot weatherstripping around upper and lower sash	10	1	0.71	0.99	0.81	1.13	
Interior storm window with spring loaded metal frame	10	1	4.25	5.94	0.39	0.55	
Fixed aluminum storm window, removable pane	10	1	4.55	6.36	0.64	0.90	
Aluminum triple-track storm window, not caulked to trim	10	1	4.25	5.94	0.86	1.21	
Reglazed and painted with new aluminum triple-track storm windows	14	6	2.16	3.02	0.45	0.63	
Interior plexiglass storm windows held by magnetic strips	15	4	2.25	3.15	0.27	0.38	
Top sash painted in place; bronze V-strip weatherstripping; old aluminum triple-track storm frame caulked in place	19	2	0.71	0.99	0.60	0.84	
Replacement sash	Includes 18	3, 12, 13, 18	11	0.75	1.05	—	—
	Excludes 18	3, 12, 13	9	0.87	1.22	0.78	1.09
Replacement window inserts	Includes 16	6, 7, 11, 16	14	0.29	0.41	—	—
	Excludes 16	6, 7, 11	13	0.21	0.29	—	—

* Data based on one window with exterior wooden storm sash. See text for explanation.

4.6 Thermography

Thermographs were taken of two upgrade options in February 1996. Interior plexiglass storm windows at 4 Occom Ridge, Hanover, NH (site 15) were compared to an adjacent window with the plexiglass storm panel removed. This window also had rope caulking around the operable perimeter and pulleys to prevent drafts as well as an aluminum triple-track storm window in place. The caulking was partially removed to demonstrate its ability to reduce air infiltration. The resulting thermograph (Figure 9, page 87) showed the rope caulking reduced air infiltration, keeping the sill a minimum of 8°F warmer than the lower sash. The black corner at the sash/frame junction revealed cold air infiltration through the window. It can be seen that the caulking effectively prevents infiltration around the operable perimeter. Upon pressurization testing, these windows were discovered to be very leaky when the interior storm window and rope caulking were removed.

The second thermograph (Figure 10, page 88) shows the aforementioned window with an adjacent plexiglass interior storm window in place. The surface temperature of the window without an interior storm ranged from below 50°F to 62°F. The surface temperature of the interior plexiglass storm ranged from 58°F to 66°F, with the vast majority of its surface area being in the 60°F to 66°F range. The coldest section was at the storm window/sill junction where the effects of conduction would be seen.

Images of three other windows were taken in Robinson Hall of Dartmouth College. One of these was a Bi-Glass System upgrade while the other two windows were in their original condition. Both of the original condition windows had triple-track aluminum storm windows, but one window was missing the lower panel. Where the lower panel should have

been was a sheet of plexiglass resting against the window. Figure 11 (page 89) shows this window, with the warmest surface area (65°F) corresponding to the location of the plexiglass panel. The center of glass surface temperature for this window with effectively no storm window, was between 55°F and 60°F.

Figure 12 (page 90) shows the window with the operable triple-track storm panels in place. Its average surface area was approximately 65°F, warmer than the window with no effective storm window.

Figure 13 (page 91) shows the Bi-Glass System replacement with its double-pane insulating glass. The surface temperature of the glass ranged from 70°F near the sill to 85°F in the center of glass.

Any conclusions based on the Robinson Hall thermographs must consider the effect of unequal space heating. As in most old buildings, hot water radiators were situated beneath the windows. The temperature regimes of the radiators varied considerably from window to window with the coolest radiator being below the coolest window and the hottest radiator being directly beneath the Bi-Glass System upgrade. The radiators likely had a significant effect on the glass surface temperatures, but it is unlikely either of the other two windows would have achieved as high a center of glass temperature as the Bi-Glass window.

16.TIF

2/26/95 9:28:25 PM

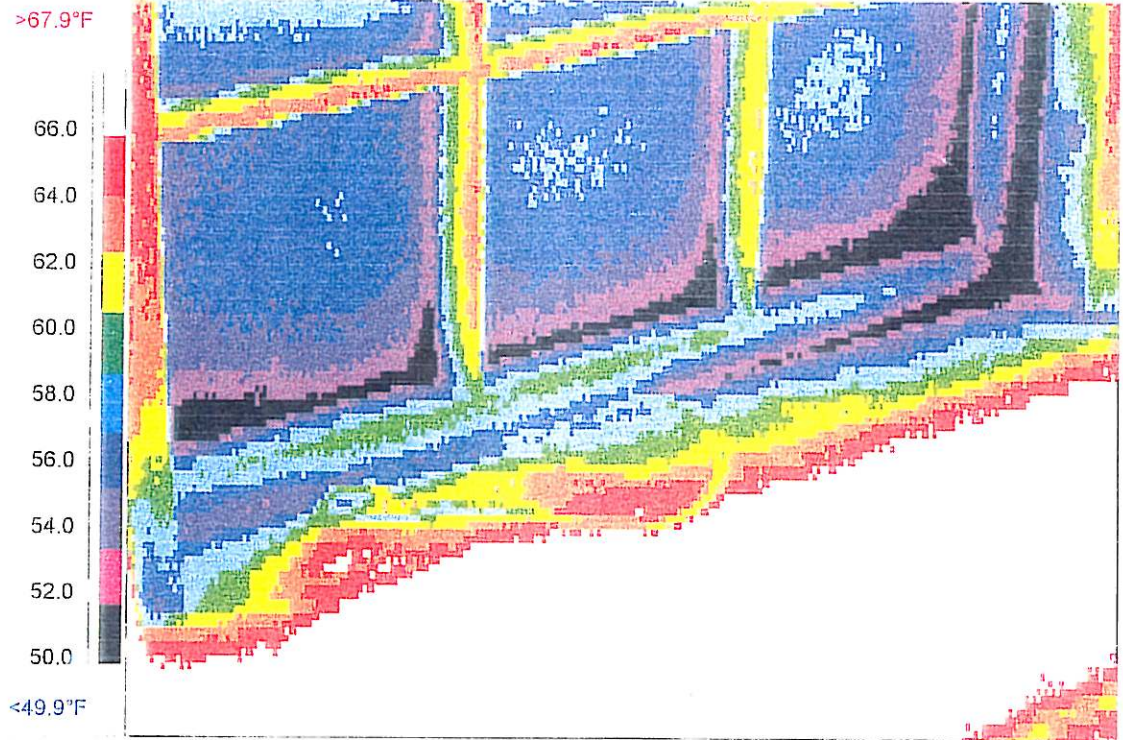


Figure 9: Thermograph of sash infiltration reduction due to rope caulking

15.TIF

2/26/95 9:24:12 PM

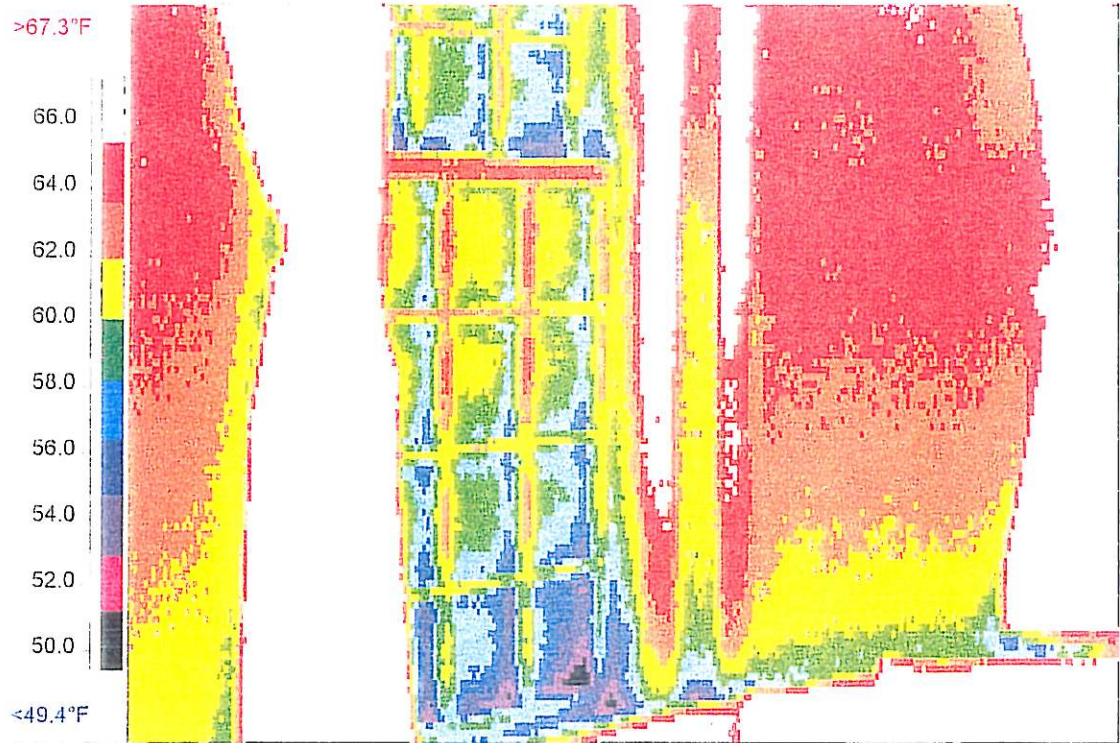


Figure 10: Thermograph of plexiglass interior storm window adjacent to window with interior storm removed

02.TIF

2/26/95 7:07:53 PM

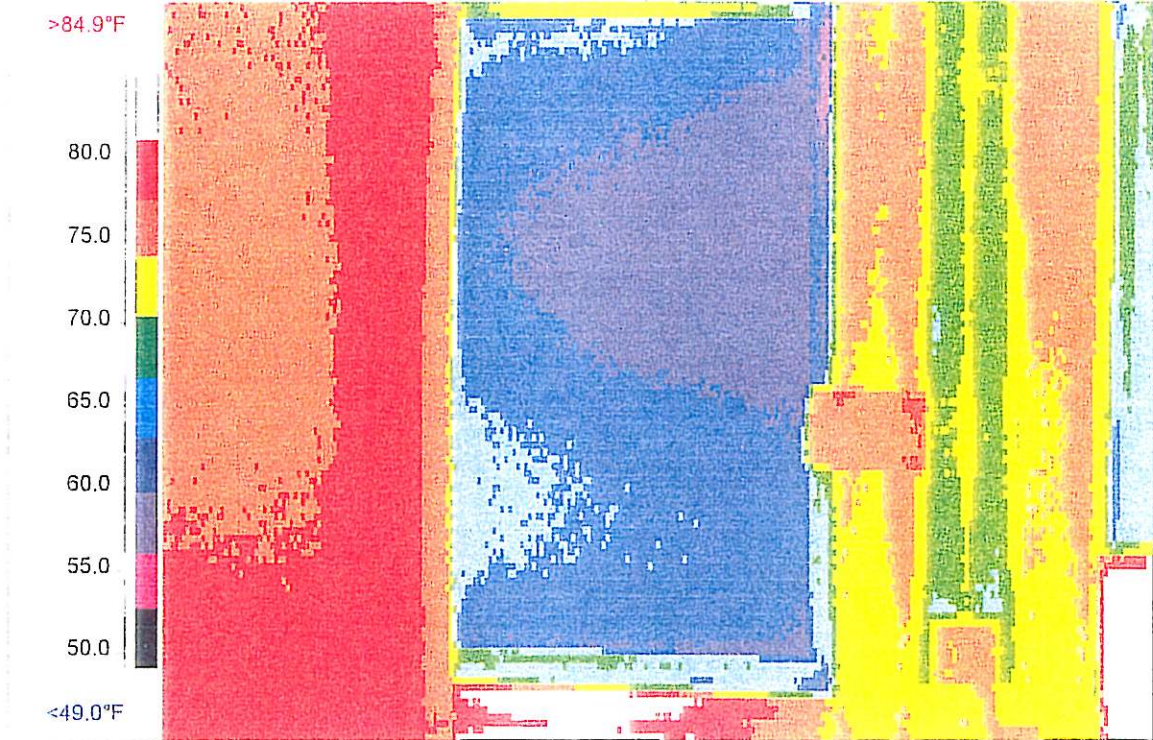


Figure 11: Thermograph of Robinson Hall window with no effective storm window attached

01.TIF

2/26/95 7:06:59 PM

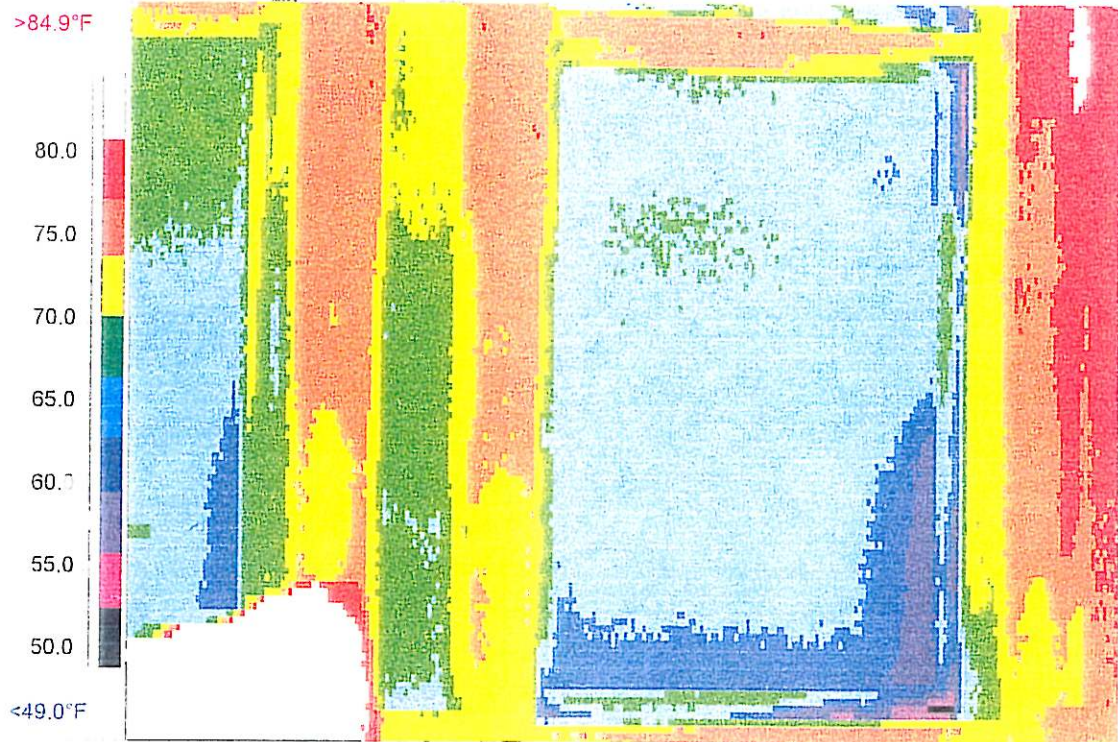


Figure 12: Thermograph of Robinson Hall window with aluminum triple-track storm window in place

05.TIF

2/26/95 7:12:40 PM

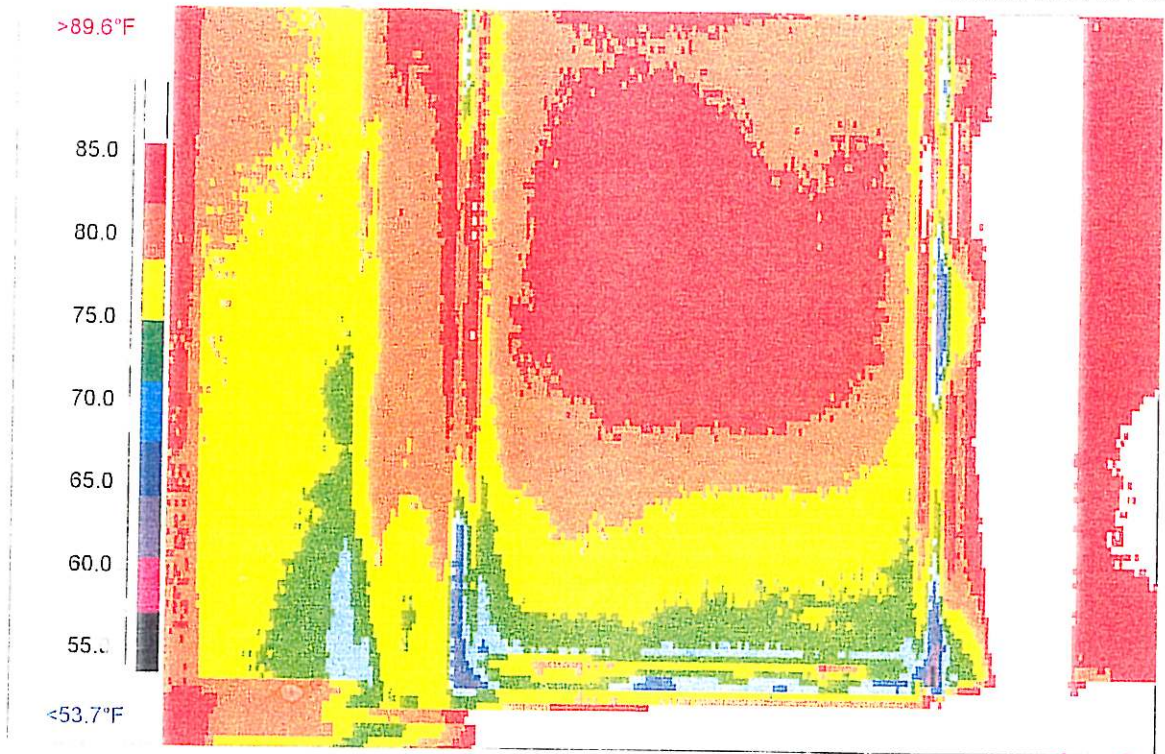


Figure 13: Thermograph of Robinson Hall window with Bi-Glass System upgrade

4.7 Energy savings attributable to upgrades

Average seasonal heating infiltrative rates (Q_{nat}) were converted to infiltrative thermal loss rates per window (L_{inf}) by multiplying Q_{nat} by the heat capacity of air:

$$\begin{aligned} L_{inf} &= Q_{nat} * C_{p_{air}} \\ L_{inf} &= Q_{nat} * \frac{0.018 Btu}{ft^3 * ^\circ F} * \frac{60 min}{1 hr} \end{aligned} \quad (29)$$

Non-infiltrative loss rates (U-values) were converted to non-infiltrative thermal loss rates per window (L_u) by multiplying the estimated U-value by the area of a baseline window (15 ft²). Whole window infiltrative and non-infiltrative loss rates were summed to determine the “effective thermal loss” of a window (L_{eff}):

$$L_{eff} = L_{inf} + L_u \quad (30)$$

Annual heat loss per window (L_{yr}) in millions of Btu’s (MMBtu) was calculated by multiplying the “effective thermal loss” (L_{eff}) by the average number of degree-day units in Burlington, Vermont:

$$L_{yr} = L_{eff} * 7744 \text{ degree-days} * \frac{24 hr}{day} * 10^{-6} \quad (31)$$

The annual heating cost per window in 1996 dollars was calculated by using fuel cost (as of June 1996), fuel heat capacity, burner efficiency, and annual heat loss per window (L_{yr}) in the following formula:

$$C_{win} = \frac{(fuel\ cost\ per\ unit) * (annual\ heat\ required) * 10^6}{(fuel\ heat\ capacity\ per\ unit) * (heating\ system\ efficiency)} \quad (32)$$

$$C_{win} = \frac{\$0.90/gal * L_{yr} * 10^6}{(138,600\ Btu/gal) * 0.75}$$

First year annual heating costs per window were based on number 2 fuel oil as an energy source at \$0.90/gallon (as of June 1996) with a 75% furnace efficiency. Table 20 shows estimated first year annual heating costs in 1996 dollars attributable to the assumed existing window types and each upgrade. Estimated first year annual heating costs for each upgrade were compared to those costs estimated for the baseline typical, tight, and loose windows with estimated savings for each upgrade in 1996 dollars also shown in Table 20.

It is important to note once again that in this study, the LBL correlation model was used for a purpose for which it was not intended. However, a sensitivity study of the method used to estimate energy costs revealed an accuracy of $\pm 25\%$ for the estimated energy costs when extreme measurements were used (Section 5.1). The values in Table 20 not only give a reasonable estimate of annual energy costs and savings but also give an indication of the relative savings attributable to each window upgrade as compared to energy costs associated with baseline windows.

Estimated first year annual energy savings realized from field tested upgrades ranged from zero to a maximum of \$3.60 per year per window by use of a replacement window insert when compared to annual energy costs for a typical existing window. Although not field tested, using a low-e, double-pane insulating window insert showed an estimated first year annual energy savings of \$7.00 per window per year, showing the importance of decreasing

Table 20: Estimated first year annual savings in 1996 dollars due to window upgrades ($\pm 25\%$)

Window Upgrade Description	Heating Cost per Window Upgrade ($\pm 25\%$)	Annual first year savings ($\pm 25\%$) per upgrade as compared to a:		
		Tight Window	Typical Window	Loose Window
Tight window with storm	\$14.38	---	---	---
Typical window with storm	\$15.91	---	---	---
Loose window with no storm	\$28.93	---	---	---
Original sash; vinyl jamb liners; no weatherstripping	\$15.91	***	0.00	\$13.00
Original sash; vinyl jamb liners; weatherstripping at sill, head junctions	\$16.53	***	***	\$12.40
Original sash; vinyl jamb liners; weatherstripping at sill, head, meeting rail junctions	\$14.33	\$0.05	\$1.60	\$14.60
Bi-Glass System	\$13.55	\$0.80	\$2.40	\$15.40
Rib-type weatherstripping; V-strip at meeting rail; pulley seals; top sash painted in place; new triple-track storm windows, caulked	\$14.52	***	\$1.40	\$14.40
V-strip weatherstripping around lower sash; top sash painted in place; existing triple-track storm windows caulked in place	\$13.77	\$0.60	\$2.10	\$15.20
Polyflex T-slot WS around upper and lower sash	\$14.27	\$0.10	\$1.60	\$14.70
Reglazed and painted with new aluminum triple-track storm, caulked to trim	\$13.40	\$1.00	\$2.50	\$15.50
Interior plexiglass storm window held by magnetic strips	\$13.00	\$1.40	\$2.90	\$16.00
Interior storm window with spring loaded metal frame	\$13.30	\$1.10	\$2.60	\$15.70
Replacement sash with storm window	\$14.20	\$0.20	\$1.70	\$14.70
Low-e replacement sash with storm window *	\$10.83*	\$3.55*	\$5.10*	\$18.10*
Replacement sash with low-e storm window *	\$12.27*	\$2.10*	\$3.60*	\$16.70*
Replacement sash with double-glazed insulating glass	\$13.65	\$0.70	\$2.30	\$15.30
Replacement sash with double-glazed low-e insulating glass *	\$10.27*	\$4.10*	\$5.60*	\$18.70*
Replacement window inserts with double-glazed insulating glass, excluding 16G	\$12.33	\$2.10	\$3.60	\$16.60
Replacement window inserts with low-e double-glazed insulating glass *	\$8.95*	\$5.40*	\$7.00*	\$20.00*

*** Denotes no estimated savings

* Denotes window upgrades not encountered during field testing

non-infiltrative losses. First year savings compared to a baseline loose window ranged from \$12.40 to \$16.60 for field tested upgrades and up to \$20.00 for low-e insulated glass replacement window inserts. Again, all values may vary by $\pm 25\%$ of the estimated values shown.

There was a large range of variation in estimated first year annual savings by upgrade, but a grouping of upgrades by glazing type revealed field tested double-glazed upgrades showed significantly larger savings than single-glazed upgrades with storm windows closed ($p = 0.01$). It should be noted that the double-glazed windows included 14 replacement window inserts which significantly reduced exterior air infiltration and therefore costs due to infiltrative thermal losses associated with those windows. Therefore, differences in savings as discussed below are not solely attributable to double-glazing.

All field tested double-glazed upgrades were averaged together yielding an estimated first year annual savings average of \$2.90 per year per window when compared to the assumed typical window versus a \$1.40 average per year per single-glazed window with a closed storm. When compared to the assumed loose window, averaged savings were \$16.00 per year per double-glazed window versus \$14.00 per year per single-glazed window with a closed storm. Greater first year estimated annual savings would be realized by the addition of low-e glass, based on computer simulations.

4.8 Estimated costs for upgrade purchases and installation

Along with estimated savings in first year energy costs, initial materials purchase and installation costs in 1996 dollars were considered for the upgrade options. Table 21 shows estimated costs associated with upgrade options as of August 1996, including labor priced at \$20 per hour. The estimated cost of a window upgrade and its installation may be compared to the relative size of estimated savings in first year energy costs as found in Table 20. Values in Table 20 may not properly be used to calculate payback periods for a window upgrade when combined with estimated costs from Table 21 as the Table 20 values are not

absolutes. No provisions were made in this study to investigate the life span of any window upgrade, nor were provisions made to estimate how energy savings change over time.

A further issue in window renovations was that of lead paint. In order to retain an original sash in a residential project, federal (Housing and Community Development Act of 1992) and Vermont regulations (Act 165) require the permanent containment, encapsulation, or removal of lead-based paint in most types of rental housing as of January 1, 1997. If abatement of lead paint is deemed necessary, an additional cost of \$125 to \$150 per window is typically required, sums that are not reflected in Table 21. The inclusion of this additional cost for original sash lead abatement would make the first four options approximately equivalent in price. Act 165 also proscribes specific methods for the stabilization of deteriorated lead-based paint in Vermont rental housing, followed by the application of a fresh coat of non-lead paint covering the lead-based paint. The installation of window well inserts, estimated to be no more than \$10 per window, is required when using this method. Labor costs associated with repainting are low, but if paint stabilization is required, labor costs rise as specialized cleaning of the work area is mandated by Act 165. These costs were not estimated due to the number of labor variables involved in paint stabilization and specialized cleaning processes.

Table 21: Estimated window upgrade costs as of August 1996, including materials and installation but excluding lead abatement costs

Upgrade option	Materials	No. Reqd	Unit Cost	Total	Labor Hours	Labor Cost @ \$20/hr	Total Cost	
V-strip + cam locks; fix upper sash in place; rehab storm	Bronze V-strip	1 set	\$5.00	\$5.00	0.50			
	Caulk			1.00	0.10			
	Cam Locks	2	1.00	2.00	0.25			
	Pulley seals	2	0.75	1.50	0.10			
	Rope for pulleys	8 ft	0.10	0.80	0.25			
	Window putty	0.25	3.00	0.75	0.50			
	Paint prep			0.50	0.50			
	Storm window rehab			10.00	0.50			
			Total		\$21.55	2.70	\$54	\$76
Vinyl jamb liners; rehab storm	Caldwell DH100 jamb liners	1	\$12.00	\$12.00	1.50			
	Silicone bulb WS	6	0.90	5.40	0.50			
	Sash lock	1	1.00	1.00	0.25			
	Foam for cavity	0.5	12.00	6.00	0.50			
	Int. trim adjustment	5	1.00	5.00	0.50			
	Int. trim paint			2.00	0.50			
	Window plow	0.2	12.00	2.40	1.00			
	Window putty	0.25	3.00	0.75	0.50			
	Paint prep			0.50	0.50			
	Storm window rehab			10.00	0.75			
		Total		\$45.05	6.50	\$130	\$175	
Brosco double-hung single-glazed	6/6	\$110	Sash lock	1	1.00	1.00	0.25	\$210
	2/2	\$114	Foam for cavity	0.5	12.00	6.00	0.50	\$214
with low-e glass	1/1	\$79	Int. trim adjustment	5	1.00	5.00	0.25	\$179
	6/6	\$174	Int. trim paint			2.00	0.50	\$274
	2/2	\$178	Storm window rehab			10.00	0.50	\$278
	1/1	\$143			Total	5.00	\$100	\$243
Marvin E-Z Tilt double-hung, double-glazed	6/6	\$520						\$615
	2/2	\$319						\$414
with low-e glass	1/1	\$168	Foam for cavity	0.5	12.00	6.00	0.50	\$263
	6/6	\$594	Int. trim adjustment	5	1.00	5.00	0.25	\$689
	2/2	\$372	Int. trim paint			2.00	0.50	\$467
	1/1	\$211	New screen or rehab storm			10.00	0.50	\$306
Marvin Tilt-Pac with low-e glass	6/6	\$499			Total	4.75	\$95	\$594
	2/2	\$396						\$491
	1/1	\$222					\$317	
Harvey Tru-Channel triple-track storm window	Standard glass	\$70						\$100
	Low-e glass	\$87			Total	1.5	\$30	\$117
Fixed upper, removable lower panel storm window	Standard glass	\$200						\$220
	Low-e glass	\$240			Total	1.0	\$20	\$260
Wood exterior storm window	Standard glass	\$110						\$125
	Low-e glass	\$140			Total	0.75	\$15	\$155
Allied Window magnetic interior storm window	Standard glass	\$110						\$125
	Low-e glass	\$150			Total	0.75	\$15	\$65
Alternative Window interior spring loaded storm window	Standard glass	\$115						\$125
	Low-e glass	\$150			Total	0.5	\$10	\$160
Bi-Glass System upgrade							\$200-\$250 depending on size	\$225
Weather Shield "Custom Shield" wood replacement window insert							\$350	\$500
Vinyl replacement window insert							\$200-\$300 depending on quality	250

Ancillary notes to Table 21

Window Rehab Option Costs

NOTES

- 1 Labor and materials do not include paint cost, as that is assumed to be the same for all treatments
- 2 For existing sash that are retained, 1 hour total assumed for putty and paint prep, and \$10 + 1/2 hour for storm rehab
- 3 Costs are as of August, 1996
- 4 Costs do not include the following, which may be required in some cases.

sales tax on materials	5% Vermont sales tax rate
lead paint abatement	\$135 typical cost
total reglaze of sash	\$25 assumes re-using glass
painting	Range from \$25 to \$50
Storm window glass or other repair	Varies
Contractor markup, OH & P	Range from 10% to 20%
Total interior trim replacement	\$25
If no pulley cavity for all options except #1.	(\$22) deduct if no window weight cavity
Additional adjustment of opening or trim	Varies

- [1] For added ~\$50, available with "Poly-Paint" 10-yr warranty, but can not trim window to fit. Price is for 5'-2" height-for custom size of 5'-0" add \$50.
- [2] Note: price includes prepainted sash&frame, 10-yr warranty paint, 1/1
- [3] Mark-up is applied to materials and to labor costs

Replacement Sash Costs		Sash Only with Channels	
Brosco single glass			
2-8*5-2 sash opening	6/6	\$95.09	110.39
	2/2	\$99.00	114.3 (special order)
	1/1	\$79.38	94.68
	Side channels	\$15.30	per pair
Brosco insulated glass	1/1	\$106.43	121.73
true divided lites	2/2, 6/6 not available		
Brosco energy panels			
low-e glass		\$63.20	
Marvin Tilt-Pack, low-e	8/8		
insulated glass	6/6	\$499.23	
2-8 x 5-2 sash opening	2/2	\$395.53	
true divided lites	1/1	\$221.33	
includes channels			
Interior spring-loaded storm			
Alternative Window Co.	\$115.00	wholesale price	(retail \$150)
low-e glass, add	\$35.00	wholesale price	
1/3 hour estimated labor	\$6.67		
TOTAL	\$156.67		
Allied Window Co	\$197.00	contractor's price	
Top fixed, bottom removeable	based on 10 or more windows, standard color		
Exterior storm, Model HOL	Low-e adds \$40		
Harvey Tru-Channel Storms	\$69.50	wholesale price	
low-e glass, add	\$17.00	wholesale price	
Weathershield (price from Huttig)		single	double low-e
3-0 x 5-0	6/6		
wood, primed	2/2		
with tilt-turn channels	1/1		
Magnetic interior storm window			
form Allied window		110	
U-channel at head	Low-e adds \$40		
V-strip weatherstrip at sill			

Chapter 5

Analysis And Discussion

Estimated savings for first year energy costs show little variability between upgrade options when compared to the estimated energy costs of a typical window. The cost variability of upgrade options decreases significantly if lead abatement of original sash needs to be included. Estimated first year savings are also of very small magnitude when compared with typical windows. It therefore does not appear to be worthwhile to base upgrade decisions solely or even primarily on energy considerations. Other non-energy considerations should play a greater role in deciding whether to upgrade or replace existing windows, although energy performance should be included as part of the decision making process. Life cycle costs of window upgrades should also be considered, including maintenance costs over time.

Visual examination of windows' apparent physical condition and fit gave no clear indication of their leakage classification as tight, typical, or loose windows. However, weak correlations were noted between window leakage characteristics and the sash/jamb fit, the meeting rail fit, and the total gap width between the lower sash and frame. Therefore, a cursory examination of those areas will give some indication as to a window's leakage characteristics. If this examination is combined with the type of window (*ie.*, single- versus double-hung and pin- versus pulley-type), a general idea of the window leakage may be determined. The study showed pulley-type windows were more prone to air leakage than pin-type, likely due to the window weight cavity acting as a conduit to the rough opening while a small sample of single-hung pin-type windows were leakier than double-hung pin-type

windows. However, the lack of an easy method of deducing air leakage rates for a window without resorting to fan pressurization was unimportant given the leaky nature of the majority of original condition windows field tested.

Fan pressurization data showed pulley-type windows allowed significantly larger rates of exterior air leakage than pin-type, illustrating the importance of reducing air infiltration through the rough opening. The significance of the exterior air contribution to a window's total heating load was revealed throughout the study, with exterior air accounting for a large percentage of the infiltrative thermal losses. Reducing exterior air infiltration should be a part of any window renovation, whether the renovation is an original sash upgrade or a replacement sash.

The inclusion of an exterior air component in window infiltrative thermal losses increased the estimated annual window energy costs for all upgrades, approximating actual thermal losses through a window and its surround more closely than thermal losses through the window sash alone. The contributing role of exterior air to the heat load of a tight window is more significant than to the heat load of a loose window as it represents a larger percentage of the overall infiltrative losses for a tight window. Any renovation will serve to reduce sash air leakage, thereby increasing the relative significance of exterior air infiltration unless steps are taken to simultaneously reduce exterior air infiltration.

5.1 Sensitivity analysis of cost estimation method

A sensitivity analysis of the method used to derive energy costs associated with a window resulted in $\pm 25\%$ of the calculated costs for an extreme case. An extreme case was considered as changing the effective leakage area by a factor of 2 and assigning 95% of the

relative leakage to the window “ceiling” as opposed to the window “wall”. As measuring the effective leakage area is a well established procedure, an error of 200% represented an extreme variability in the measurement range. In fact, repeated measurements of several windows over time showed changing the effective leakage area by a factor of 2 was beyond three standard deviations of the mean ELA’s. Relative locations for window leakage in the LBL correlation model (Section 3.4) were reversed from 95% wall leakage and 5% ceiling leakage to 5% wall leakage and 95% ceiling leakage. Since the majority of window leakage for this model is typically considered as “wall” leakage, assigning 95% of the leakage to the window “ceiling” represented an extreme value in the relative leakage locations and had little impact on the overall estimates ($\pm 4\%$).

5.2 Correlating flow exponent to effective leakage area

Based on the flow equation used to characterize air leakage through windows (equation 12), a trend should exist between flow exponents (x) and effective leakage areas (ELA’s) with flow exponents decreasing as effective leakage areas increase. Figures 14 and 15 are plots of flow exponents versus effective leakage areas for original condition windows and all upgrades respectively. Both figures show a very weak correlation of decreasing flow exponents with increasing effective leakage areas as expected from equation 12 ($R = -0.34$ and -0.33 for original condition windows and upgrades, respectively). The variability of the flow exponent increased as the effective leakage area decreased, an occurrence that tended to mask any strong trend. It is possible tight windows were dominated by small cracks and air flow through them behaved like laminar flow while loose windows were dominated by large cracks and behaved as turbulent flow. These results were similar to whole house

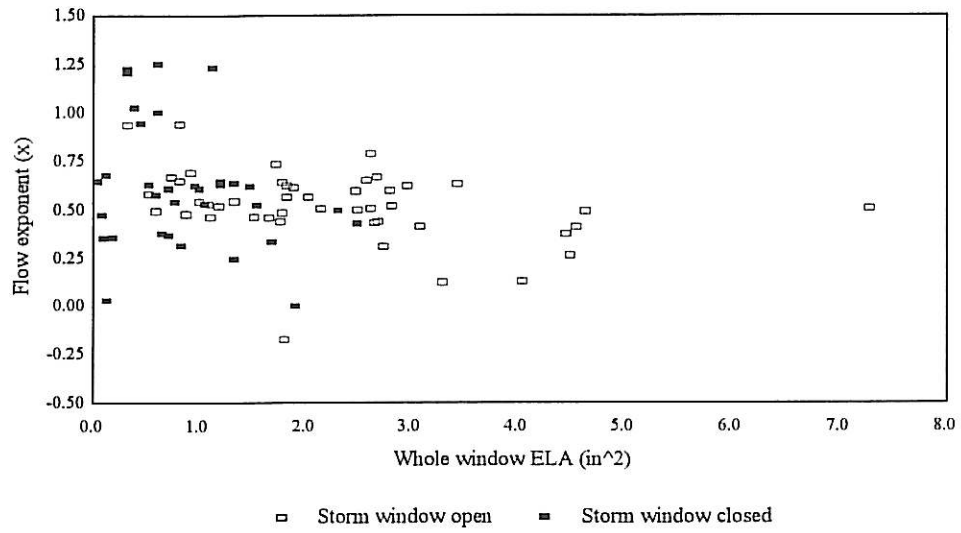


Figure 14: Variability of flow exponent with $ELA_{t,\alpha}$ for original condition windows

pressurization data for 711 samples which exhibited the same weak downward trend between flow exponents and effective leakage areas when using the same flow model as this study

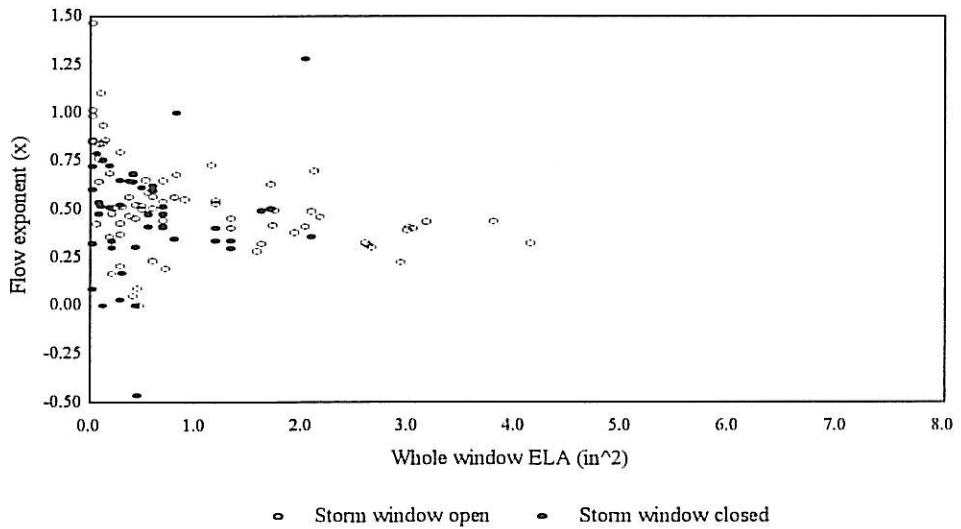


Figure 15: Variability of flow exponent with $ELA_{t,\alpha}$ for window upgrades

(Sherman et al., 1986).

Also of note was the comparison of the whole window leakage areas distribution between the upgrades and original condition windows. Upgraded windows had a much tighter grouping between the lower ELA_{tot} of zero and one square inch than did the original condition windows (Figures 14 and 15), illustrating the general improvement of window upgrades and renovations.

A frequency distribution of the flow exponents for sash leakage (Q_s) is shown in Figure 16. This figure represents 197 fan pressurization tests, counting windows with operable storms in open and closed positions as individual tests. While the data exhibits a slight right skew, it is fitted reasonably well by a normal Gaussian distribution with a mean equal to 0.52 ($\sigma = 0.30$). This mean value is well below the value of 0.65 widely assumed to be typical of air infiltration leakage sites, although 0.65 is well within one standard deviation

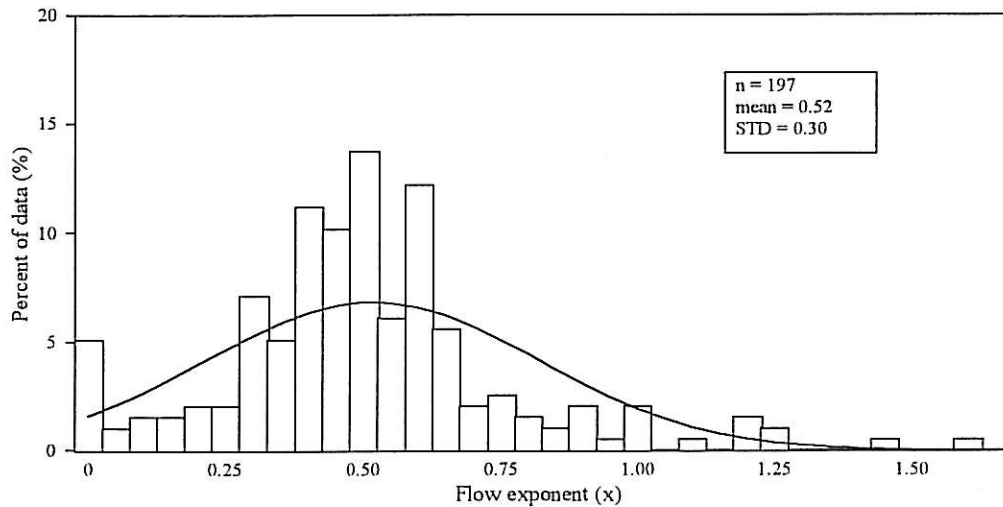


Figure 16: Frequency distribution of flow exponent (x) for all windows

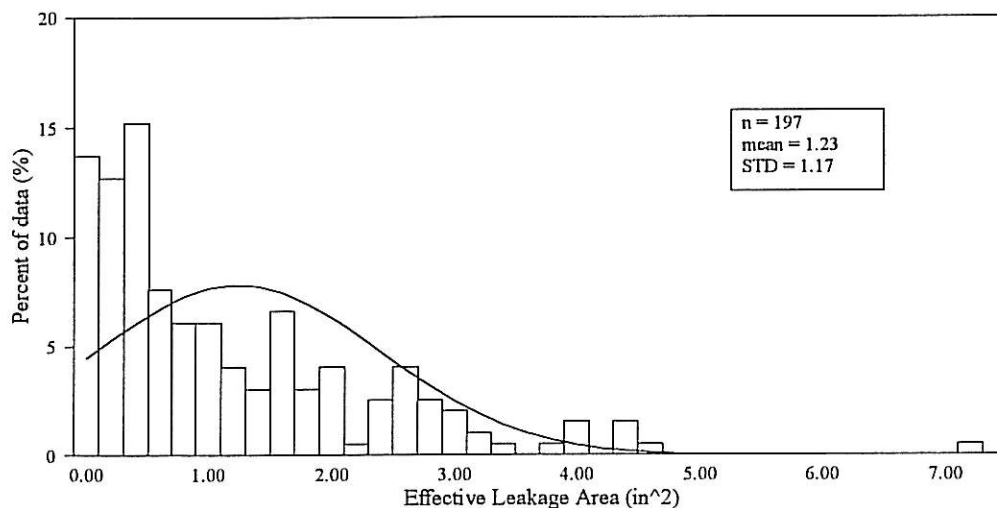


Figure 17: Frequency distribution of $ELA_{t,\alpha}$ for all windows

of the mean value. The underlying cause for the discrepancy between these two flow exponent values is unknown, although it may be the windows are dominated by large cracks as previously discussed, thus leading to flow coefficients approaching 0.50 (turbulent flow).

A frequency distribution of effective leakage areas from the 197 fan pressurization tests reveals a right skew of the data (Figure 17). This was an expected result, as reducing the air leakage through a window would decrease the effective leakage area. Since it is physically impossible to have an effective leakage area less than zero, the effective leakage data should begin to accumulate as the values approach zero, causing a right skew.

5.3 Windows in heating season configurations

Of real interest are upgraded windows in actual heating season configurations, whether those configurations are double-pane insulating glass or single-pane plus a storm window. Sixty windows representing eight general upgrades were tested in what would be

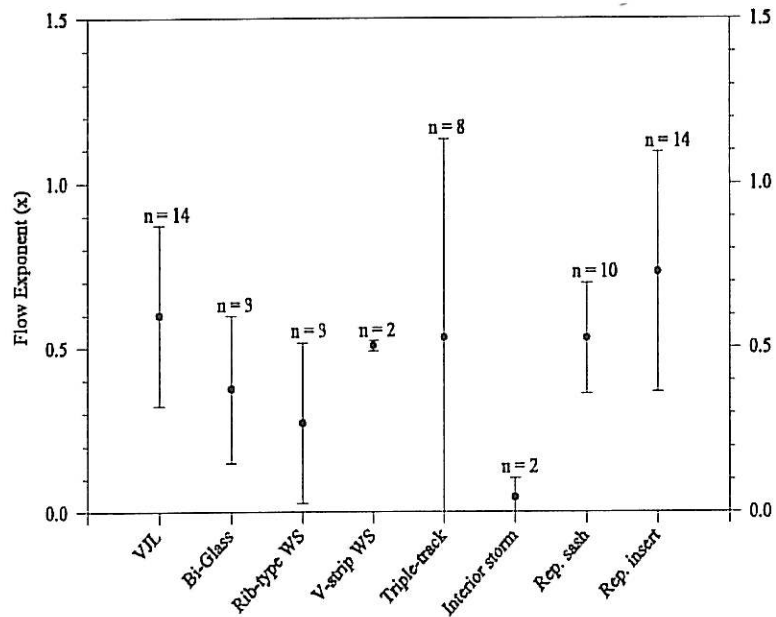


Figure 18: Mean sash leakage flow exponents for eight general upgrade categories, plus/minus one standard deviation

heating season configurations. Figure 18 shows the variability in the mean flow exponents for sash leakage (Q_s) of the eight general upgrades but represents only 56 windows. This is a result of zero sash leakage for three interior storm windows and one replacement sash, none of which allowed calculation of a flow exponent. Figure 19 represents the variability of the total window effective leakage areas (ELA_{tot}) for the eight categories with the bars representing plus and minus one standard deviation.

Very low sample populations lend little statistical significance to the results with n ranging from two to fourteen. However, an approximate idea of the relative effectiveness and variability of upgrades utilizing vinyl jamb liners ($n = 14$), aluminum triple-track storm windows ($n = 8$), replacement sash ($n = 11$), and replacement window inserts ($n = 14$) may be gathered from the figures. As expected, replacement sash and replacement inserts both

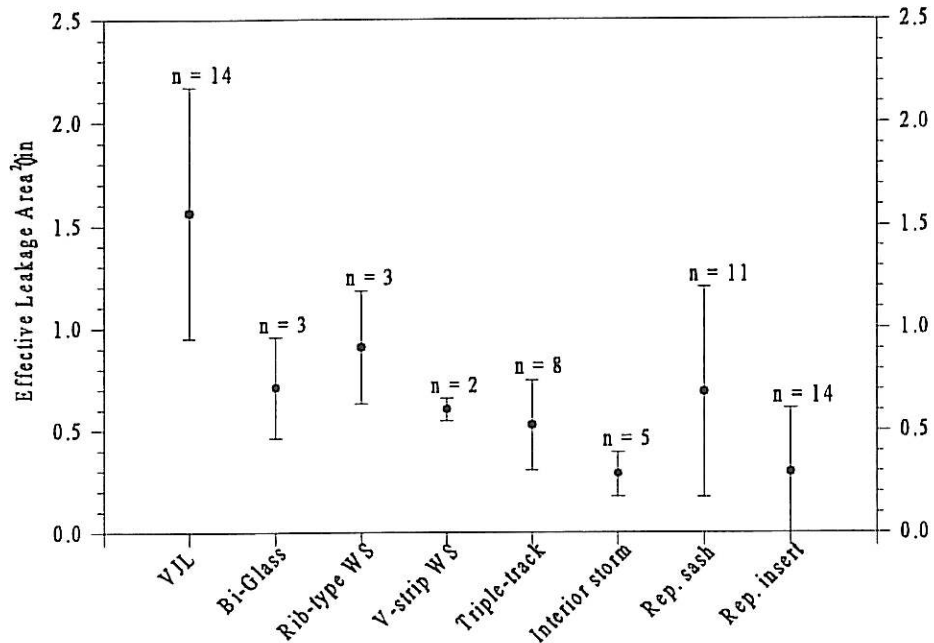


Figure 19: Mean whole window effective leakage area (ELA_{tot}) for eight general upgrade categories, plus/minus one standard deviation

had low mean whole window effective leakage areas (mean $ELA_{tot} = 0.69$ and 0.29 in², respectively) since replacement sash utilized a mated vinyl jamb liner and replacement inserts had an integral frame. Windows fitted with vinyl jamb liners were relatively leaky (mean $ELA_{tot} = 1.56$ in²), perhaps due to each window being routed to accept the jamb liners. However, new, good quality triple-track storm windows were found to be highly effective in reducing whole window leakage when caulked to the exterior trim (mean $ELA_{tot} = 0.52$ in²), even when little other than routine maintenance had been done to the prime windows.

Variability of the whole window effective leakage areas for windows fitted with new aluminum triple-track storms was low when compared to the variability of vinyl jamb liner upgrades and replacement sash and insert upgrades. As discussed previously (Section 4.3.1),

it was unclear as to the underlying cause(s) of the variability in windows fitted with vinyl jamb liners. Variability of replacement sash was largely due to two windows with very low exterior air leakage rates and one replacement sash placed in a non-square frame which allowed excessive sash leakage. Replacement sash variability was largely a result of the one window which allowed an inordinately large amount of exterior air leakage as previously discussed (Section 4.3.3). The total effective leakage area of this window (16G) was 1.32 in², an ELA_{tot} greater than three standard deviations from the mean ($\mu = 0.29$ in², $\sigma = 0.32$ in²).

5.4 Infiltration reduction in windows tested pre- and post-upgrade

A total of 26 windows at six sites were field tested prior to and after window renovations. Four of these original condition windows were of sufficient leakage to prevent maximum pressurization and were not considered. Of the remaining 22 windows, 17 retained the original storm after renovation or had no storm window when tested. The other five windows were fitted with interior storm windows. Average sash and exterior air leakage characteristics for the 17 windows with either the original exterior storm window or no storm are listed by site in Table 22, with storm windows off or open. The same characteristics for the five interior storm windows are also listed, but with storms removed and in place.

All pre- and post-test windows retained the original sash with the exception of site 6. Upgrades at this site were vinyl replacement window inserts and were expected to perform significantly better than the original condition windows, as may be seen by the 95% reduction in whole window leakage. All relative percentages should be viewed with caution, due to the low number of samples in each population.

Interior storm windows showed the greatest reduction in ELA_{tot} as discussed earlier

Table 22: Averaged leakage characteristics of windows prior to and post renovation

Site ID	Window Upgrade	n	Pre-upgrade			Post-upgrade			ELA _{tot} % Dec.
			ELA _{s x 19} (in ²)	ELA _{RO x 19} (in ²)	ELA _{tot} (in ²)	ELA _{s x 19} (in ²)	ELA _{RO x 19} (in ²)	ELA _{tot} (in ²)	
2	Bi-Glass System	3	2.75	0.57	3.32	0.71	0.33	1.04	70%
3	Replacement sash	2	1.07	0.70	1.77	0.32	0.24	0.56	70%
6 *	Vinyl inserts replacement	3	3.42 *	0.63 *	4.05 *	0.04	0.10	0.14	95%
7	Original Sash with vinyl jamb liners	9	2.18	0.55	2.63	0.81	0.32	1.13	60%
	Interior Storm Windows		Interior storm window removed			Interior storm window in place			
10	Spring loaded	1	4.05	0.20	4.25	0.25	0.19	0.44	90%
15	Magnetic stripping	4	1.42	1.67	3.09	0.01	0.23	0.24	90%

* Original windows at Site 6 were single-hung, partially accounting for the relatively large value. As a double-hung window, ELA_{s x 19} would have been 1.96 in² and ELA_{RO x 19} would have equaled 0.36 in² for an ELA_{tot} of 2.32 in².

(Section 4.3.4). Three of the four interior storm windows at site 15 allowed zero sash flow (Q_s) within the limits of resolution of the pressurization device flow meter, largely accounting for the significant reduction in ELA_{s x 19}.

There was a significant reduction in ELA_{tot} between windows in their original condition and any resulting upgrade (mean ELA_{tot} = 3.07 and 0.99 in² respectively, $p < 0.001$). Again, it should be noted that all sample populations are low with the largest site population number of nine windows at site 7. The average reduction in ELA_{tot} for that site was 60%.

Extrapolated values for sash leakage rates (Q_s) at 0.30 inches of water pressure (75 Pa) were also compared, with upgrades again showing significant reductions (mean Q_s = 2.19 and 0.52 scfm/lfc, respectively; $p < 0.001$). Extrapolated values were used due to the leaky

nature of the original windows.

5.5 Improvements due to storm window upgrades

The use of exterior storm windows provided two energy reduction benefits, first by significantly reducing sash leakage when the storm frame was caulked to the exterior trim and secondly, by providing a second glazing layer. The storm window as a second glazing layer had a significant effect on reduction of non-infiltrative thermal loss rates during modeling with WINDOW 4.1 as noted previously (Section 4.3.5), decreasing U-values from 0.92 Btu/hr-ft²-°F for a single-pane window with no storm to 0.51 Btu/hr-ft²-°F for the same window with a closed storm.

A significant improvement was seen with the use of new aluminum triple-track storm windows when frames were caulked to the exterior trim. Four prime windows showed a reduction of 75% in sash leakage when the new storms were closed, while another site with three year old storm windows showed a 35% reduction. It can be assumed the average value for sash leakage reduction is between those bounds. A comparison of 24 original condition windows with aluminum triple-track storms in open and closed positions, showed a 46% reduction in sash leakage. It is likely that the use of new aluminum triple-track storm windows with frames caulked would exceed original window condition sash leakage reduction, being closer to the 75% reduction seen with the use of new storm windows. Differences between new and old storm windows are largely found in the quality of the weatherstripping surrounding the storm sash and the sash/frame fit if frames for both are caulked to the exterior window trim.

5.6 Infiltrative versus non-infiltrative thermal losses

Another factor to consider was the relative importance of infiltrative losses versus non-infiltrative losses. Costs due to infiltrative thermal loss rates (L_{in}) for selected window upgrades were compared to their non-infiltrative loss rate costs (L_u) to gain an understanding of their relative importance (Figure 20). Infiltrative loss rates and costs averaged 16% of non-infiltrative loss rates and costs with only two sites showing an infiltrative/non-infiltrative loss ratio greater than 18%, results supported by the literature (Klems, 1983).

The savings due to a reduction of non-infiltrative thermal loss rates realized by the use of double- versus single-glazed sash were investigated by modeling. Average values from windows with storms closed at three sites were chosen to represent actual loose, typical, and tight windows encountered in the field. Site 19 was chosen to represent tight windows, site

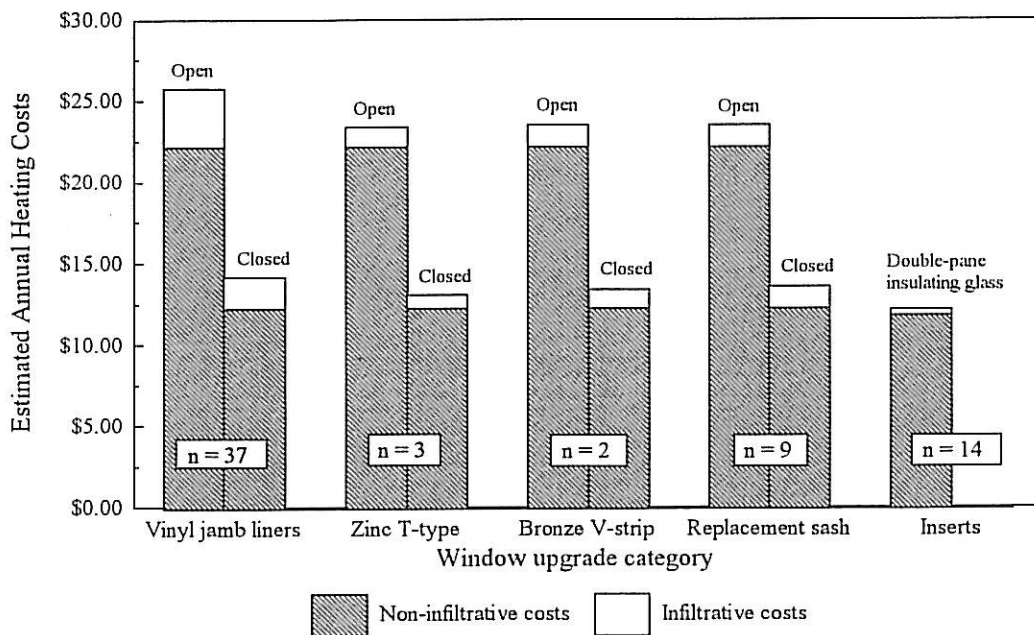


Figure 20: Comparison of costs due to infiltrative and non-infiltrative thermal losses for selected window types, with and without storm windows

Table 23: Comparison of first year energy savings per window from double-versus single-glazed sash ($\pm 25\%$)

Windows from Site:	Single-pane		Double-pane		Difference in Costs
	U-value (Btu/hr-ft ² -°F)	Annual Cost	U-value (Btu/hr-ft ² -°F)	Annual Cost	
19 (Tight)	0.51	\$13.80 ¹	0.49	\$13.30 ³	\$0.50
7 (Typical)	0.51	\$14.30 ¹	0.49	\$13.80 ³	\$0.50
12 (Loose)	0.92	\$25.80 ²	0.49	\$15.40 ³	\$10.40

¹ Storm window closed

² Storm window open

³ Double-paned insulating glass, no storm window

7 to represent typical windows, and site 12 to represent loose windows based on average heating season infiltration rates (Table 19). Results were compared to those costs estimated for baseline typical, tight, and loose windows to determine savings attributable to double-glazing (Table 23).

When replacing a single-pane prime window and storm window combination with double-pane insulating glass (i.e., the tight and typical windows), minimal savings (\$0.50 per window per year) are realized due to the storm window acting as a second glazing layer. Addition of a storm window thus significantly decreased the U-value when compared to a prime window alone, closely mimicking double-pane insulating glass. Significant savings would be incurred if a sash with single-pane glass but no storm window were to be replaced with double-pane insulating glass (\$10.40 per window per year).

However, an additional benefit of double-glazed sash versus a single-glazing and storm window combination arises from occupant behavior. During field testing, buildings were seen with a portion of their storm windows open during the heating season, an obvious result of occupant behavior. Windows with storms in the open position were effectively

windows without storms, thus having greater thermal loss rates due to a single glazing layer. The use of double-glazed sash would negate occupant behavior as no storm window is generally installed if the window is a replacement.

If a double-glazed sash were combined with a storm window (i.e., triple-glazing), a larger portion of savings would arise from reduced non-infiltrative loss rates (U-values) due to the third glazing layer. Benefits of triple-glazing are somewhat reduced from what might be expected however, due to the gap distance between the prime and storm windows (average 2.5 inches). A reduction in U-values occurs until the optimal gap distance of 0.75 inches is exceeded, after which point U-values exhibit a slow rise as gap distance increases. Triple-glazing was not investigated in this study but was shown to be effective in very cold climates (Flanders et al., 1982).

Chapter 6

Conclusions

Over the course of the study, it became apparent that replacing an historic window does not necessarily result in greater energy savings than upgrading that same window. The decision to renovate or replace a window should not be based solely on energy considerations as the differences in estimated first year savings between the upgrade options are small. Other non-energy factors to consider include the historical significance of a window and its role in a building's character, occupant comfort, ease of operation, and life-cycle costing as well as the need for lead abatement, none of which were subjects of this study.

The study addressed the following issues:

- estimate energy savings attributable to existing window retrofits,
- estimate first year savings in heating costs attributable to field tested window retrofits,
- estimate installation and materials costs for existing window retrofits, and
- compare the estimated costs and savings from existing window retrofits to those incurred by replacement windows.

Table 24 summarizes the results of the study by listing estimated purchase and installation costs for grouped upgrades as well as first year energy savings when compared to the baseline tight, typical, and loose windows. Window upgrades were categorized into eight broad groups as follows:

1. retain the original sash using bronze V-strip weatherstripping with a storm window;

Table 24: Estimated costs and first year energy savings ($\pm 25\%$) of categorized upgrades

	Upgrade category	Cost of window with lead abatement*:		First year energy savings per window as compared to baseline ($\pm 25\%$):		
		excluded	included*	Tight window	Typical window	Loose window
Retain original sash	1 ^A	\$76	\$201	\$0.60	\$2.10	\$15.20
	2 ^A	\$175	\$300	\$0.05	\$1.60	\$14.60
	3 ^A	\$225	\$350	\$0.80	\$2.40	\$15.40
	4 ^A	\$70	\$195	\$1.00	\$2.50	\$15.50
	5 ^A	\$115	\$240	\$1.30	\$2.80	\$15.90
Replacement sash	6 ^A	\$214	---	\$0.20	\$1.70	\$14.70
	7 ^B	\$320	---	\$0.70	\$2.30	\$15.30
	8 ^B	\$350	---	\$2.10	\$3.60	\$16.60

^A Storm windows in the closed position

^B No storm windows

* Lead abatement cost assumed to be \$125

2. retain the original sash utilizing vinyl jamb liners and silicone bulb weatherstripping with a storm window;
3. retain the original sash by use of the Bi-Glass System upgrade;
4. retain the original sash utilizing new aluminum triple-track storm windows;
5. retain the original sash utilizing interior storm windows;
6. single-glazed replacement sash utilizing vinyl jamb liners and silicone bulb weatherstripping;
7. double-glazed replacement sash utilizing vinyl jamb liners and silicone bulb weatherstripping; and
8. double-glazed replacement window insert.

Estimated installation and purchase costs are shown with and without costs associated

with lead abatement, assumed to cost \$125. The purchase cost shown for single-glazed replacement sash with vinyl jamb liners (category 6) was for an in-kind replacement (two-over-two true divided lites). The double-glazed replacement sash and replacement window inserts (categories 6 and 7) are one-over-ones as encountered in the field.

It can be seen that bronze V-strip weatherstripping (category 1) compares favorably to the other upgrade options while also being the least expensive option. However, due to the low sample population ($n = 2$), no statistical significance may be associated with this observation. Bronze V-strip is visually unobtrusive as was noted several times during field research, a benefit when preserving the visual facade of a building.

Most windows tested during the study were two-over-two true divided lites. In-kind wood sash when used as replacement sash can help retain the appearance of a building by closely approximating the look of the original sash. One illustrative instance occurred when one face of a building containing six windows was being examined from the exterior. No difference was noted between any windows until inside, when two windows were discovered to be in-kind replacements.

Replacement window inserts may also retain the original appearance of a building while providing the additional benefit of reducing exterior air leakage, making the immediate window environment more comfortable for occupants. Actual window size is decreased when using window inserts due to the integral frame, modifying the building appearance somewhat.

6.1 Estimating savings in other locales

Estimated savings listed in Table 24 are based on Burlington, Vermont climatic data

and typical shielding and terrain parameters for that location. To make the results more universal, savings in other locations may be estimated by dividing the number of heating degree-days for that locale by 7744 (the number of heating degree-days in Burlington) and multiplying the resulting conversion factor by the savings of interest. This method does not fully account for changes in natural infiltration rates due to a new locale and thus will give only a rough approximation of savings for that location. Factors governing natural infiltrative rates include not only interior/exterior temperature differentials (i.e., degree-days) but also humidity levels, wind speeds and directions as well as surrounding terrain and shielding, all of which vary from locale to locale and are accounted for in the LBL correlation model. Table 25 lists heating degree-day units and conversion factors for forty cities spread throughout the United States and Canada. Areas close to those cities may use those conversion factors to approximate savings.

Table 25: Selected cities with heating degree-day units and conversion factors to estimate savings for other climates, based on the Burlington, VT data

Locale	Heating Degree-Days	Conversion Factor
Aberdeen, SD	8570	1.11
Albuquerque, NM	4414	0.57
Anchorage, AK	10816	1.40
Baltimore, MD	4706	0.61
Billings, MT	7212	0.93
Bismark, ND	9075	1.17
Boise, ID	5802	0.75
Boston, MA	5593	0.72
Buffalo, NY	6798	0.88
Calgary, Alberta	9709	1.25
Caribou, ME	9616	1.24
Cheyenne, WY	7310	0.94
Chicago, IL	6455	0.83
Cleveland, OH	6178	0.80
Concord, NH	7482	0.97
Denver, CO	6014	0.78
Des Moines, IA	6554	0.85
Dodge City, KS	5059	0.65
Duluth, MN	9901	1.28
Green Bay, WI	8143	1.05
Halifax, Nova Scotia	7154	0.92
Indianapolis, IN	5650	0.73
Kansas City, MO	5283	0.68
Lansing, MI	6987	0.90
Louisville, KY	4525	0.58
Madison, WI	7642	0.99
Medford, OR	4798	0.62
Minneapolis, MN	8007	1.03
New York, NY	5169	0.67
Ottawa, Ontario	8395	1.08
Pittsburgh, PA	5950	0.77
Portland, ME	7501	0.97
Quebec, Quebec	8687	1.12
Richmond, VA	3960	0.51
Saint John, New Brunswick	8213	1.06
Spokane, WA	6882	0.89
St. Louis, MO	4938	0.64
Vancouver, British Columbia	5329	0.69
Washington, DC	4122	0.53
Winnipeg, Manitoba	10403	1.34

6.2 General observations

The following observations were made during the course of the study.

- The majority of energy costs associated with thermal losses from a window are due to non-infiltrative thermal losses (80-85% versus 15-20%).
- Exterior air infiltrating through the jamb from the rough opening can make a significant contribution to the infiltrative heat load of any window.
- Pulley-type windows allowed significantly more exterior air leakage than pin-type windows, likely due to the window weight cavity acting as a conduit to the rough opening.
- Double-hung windows had lower sash leakage rates than a small sample of single-hung windows.
- Existing aluminum triple-track or fixed panel aluminum storm windows reduced sash leakage by 45% on average.
- New, good quality aluminum triple-track storm windows decreased sash leakage by 75% on average when the frame was caulked to the exterior window trim.
- Caulking the frame of existing exterior aluminum triple-track storm windows to the exterior window trim significantly reduced sash leakage.
- Interior storm windows significantly reduced both sash leakage and exterior air leakage, averaging reductions of approximately 95% and 80% respectively.
- In general, new, good quality storm windows, whether interior or exterior, significantly reduced both infiltrative and non-infiltrative thermal losses.
- A second glazing layer either from using a closed storm window or double-pane

insulating glass is anticipated to significantly reduce non-infiltrative losses, as would low-e glass.

- Original sash fitted with vinyl jamb liners and silicone bulb weatherstripping show significantly reduced sash leakage rates over the original condition windows but were subject to high variability.
- In-kind replacement sash with vinyl jamb liners were effective when placed in a square jamb. Existing jambs utilizing this option should be checked for squareness.
- Replacement window inserts did not always reduce exterior air infiltration as expected, causing the window to perform poorly.
- Thermal performance of all options are subject to variation due to the quality of installation.

The study showed that window replacement will not necessarily reduce energy costs more than an upgrade utilizing the existing sash. The importance of the window frame/rough opening junction as a path for exterior air infiltration was noted throughout the study as well as by others (Louis and Nelson, 1995; Proskiw, 1995). An effective method of sealing this junction can greatly reduce the infiltrative thermal losses associated with any window renovation. Storm windows, either existing or replacements, were found to be effective in reducing both infiltrative and non-infiltrative losses. Many sash-retaining upgrades generally retain existing exterior storm windows, which may be left open by occupants. Consequently, options including double-glazed sash are likely to achieve more consistent energy savings than storm window options. Quantifying those differences was beyond the scope of this study.

6.3 Further work

Further research that would help quantify some of these issues include:

- validate and/or modify the method used to estimate the fraction of extraneous air leakage coming from the outside of the building;
- improve the sample size of the windows tested to achieve more statistically significant results;
- investigate the effects of wind on non-infiltrative losses between prime and exterior storm windows;
- further investigate the leakage response of windows to changing environmental factors to determine the lag time;
- test statistically significant numbers of single- and double-hung pin-type windows for air leakage rates to determine if single-hung windows allow more infiltration than double-hung;
- long-term monitoring of windows to see how energy savings vary over time;
- long-term monitoring of upgrades to investigate the effective life-span of an upgrade;
- perform economic analyses of window upgrade options, including life-cycle costing of installation, financing, maintenance and energy costs; and
- investigate triple-glazing and other upgrade strategies.

References

- Act 165: An Act to Prevent Childhood Lead Poisoning in Rental Housing and Child Care Facilities (Public Act 165, 15 May 1996). Acts and Resolves Passed by the General Assembly of the State of Vermont, 63rd Biennial Session, pp. 354-364.
- ASHRAE 1993. *Handbook of Fundamentals*. Atlanta, GA: American Society of Heating, Refrigerating, and Air-Conditioning Engineers, Inc., 1993. Chapters 6, 22, and 23.
- American Society for Testing and Materials. ASTM E 283-91 "Standard Test Method for Determining the Rate of Air Leakage Through Exterior Windows, Curtain Walls, and Doors Under Specified Pressure Differences Across the Specimen." *1994 Annual Book of ASTM Standards 04.07*: 486-489 (1994a).
- American Society for Testing and Materials. ASTM E 1423-91 "Standard Practice for Determining the Steady State Thermal Transmittance of Fenestration Systems." *1994 Annual Book of ASTM Standards 04.07*: 1160-1164 (1994b).
- American Society for Testing and Materials. ASTM E 779-87 "Standard Test Method for Determining Air Leakage Rate by Fan Pressurization." *1994 Annual Book of ASTM Standards 04.07*: 730-733 (1994c).
- American Society for Testing and Materials. ASTM E 783-93 "Standard Test Method for Field Measurement of Air Leakage Through Installed Exterior Windows and Doors." *1994 Annual Book of ASTM Standards 04.07*: 734-739 (1994d).
- Bassett, M.R.: Building Site Measurements for Predicting Air Infiltration Rates. *Measured Air Leakage of Buildings, ASTM STP 904*: 365-383 (1986).
- Conway, McK. and L.L. Liston: *The Weather Handbook*. 3rd edition. Norcross, GA: Conway Data, Inc., 1990. Chapters 4 and 6.
- Fisher, C.: *Installing Insulating Glass in Existing Wooden Sash Incorporating the Historic Glass*. Preservation Tech Notes, National Park Service, U.S. Department of the Interior, Washington, D.C. (1985).
- Flanders, S.N., J.S. Buska, and S.A. Barrett: *Window Performance in Extreme Cold*. Cold Regions Research and Engineering Laboratory, U.S. Army Corps of Engineers. Report 82-38 (1982).
- Giesbrecht, P.G. and G. Proskiw: An Evaluation of the Effectiveness of Air Leakage Sealing. *Measured Air Leakage of Buildings, ASTM STP 904*: 312-322 (1986).

- Grimsrud, D.T., M.H. Sherman, and R.C. Sonderegger: Calculating Infiltration: Implications for a Construction Quality Standard. *Proceedings, ASHRAE/DOE Conference on Thermal Performance of Exterior Envelopes of Buildings II*: 1-31 (1982).
- Harrje, D.T. and T.A. Mills, Jr.: Air Infiltration Reduction through Retrofitting. *Building Air Change Rate and Infiltration Measurements, ASTM STP 719*: 89-106 (1980).
- Housing and Community Development Act of 1992: Title X - Residential Lead-based Paint Hazard Reduction Act of 1992 (Public Law 102-550, 28 Oct. 1992). 106 *United States Statutes at Large*, pp. 3897-3927.
- Jacobson, D.I., G.S. Dutt, and R.H. Socolow: Pressurization Testing, Infiltration Reduction, and Energy Savings. *Measured Air Leakage of Buildings, ASTM STP 904*: 265-293 (1986).
- Kehrli, D.: Whole House Fenestration Energy Consumption as a Function of Variable Window Air Leakage Rates. *Airflow Performance of Building Envelopes, Components, and Systems, ASTM STP 1255*: 90-107 (1995a).
- Kehrli, David: March 1995b. Personal communication. E.T.C. Laboratories, Inc., 40 Ajax Road, Rochester, New York 14624.
- Kleinbaum, D.G, L.L. Kupper, and K.E. Muller: *Applied Regression Analysis and Other Multivariable Methods*. Belmont, CA: Duxbury Press, 1988. Chapters 3, 5, and 6.
- Kreith, F. and R. Eisenstadt: Pressure Drop and Flow Characteristics of Short Capillary Tubes at Low Reynolds Numbers. *Transactions of the American Society of Mechanical Engineers* 79(5): 1070-1078 (July 1957).
- Klems, J.H.: Methods of Estimating Air Infiltration through Windows. *Energy and Buildings*: 243-251 (1983).
- Lawrence Berkeley Laboratory. Windows and Daylighting Group, Building Technologies Program, Berkeley, California. *RESFEN: Residential Fenestration Performance Analysis Tool, version 1.4*. (1994a).
- Lawrence Berkeley Laboratory. Windows and Daylighting Group, Building Technologies Program, Berkeley, California. *WINDOW 4.1: A PC Program for Analyzing the Thermal Performance of Fenestration Products*. (1994b).
- Levin, P.A., D.J. Wilson, and M.Y. Ackerman: Air Leakage in the Perspective of International Standards. *Airflow Performance of Building Envelopes, Components, and Systems, ASTM STP 1255*: 231-247 (1995).

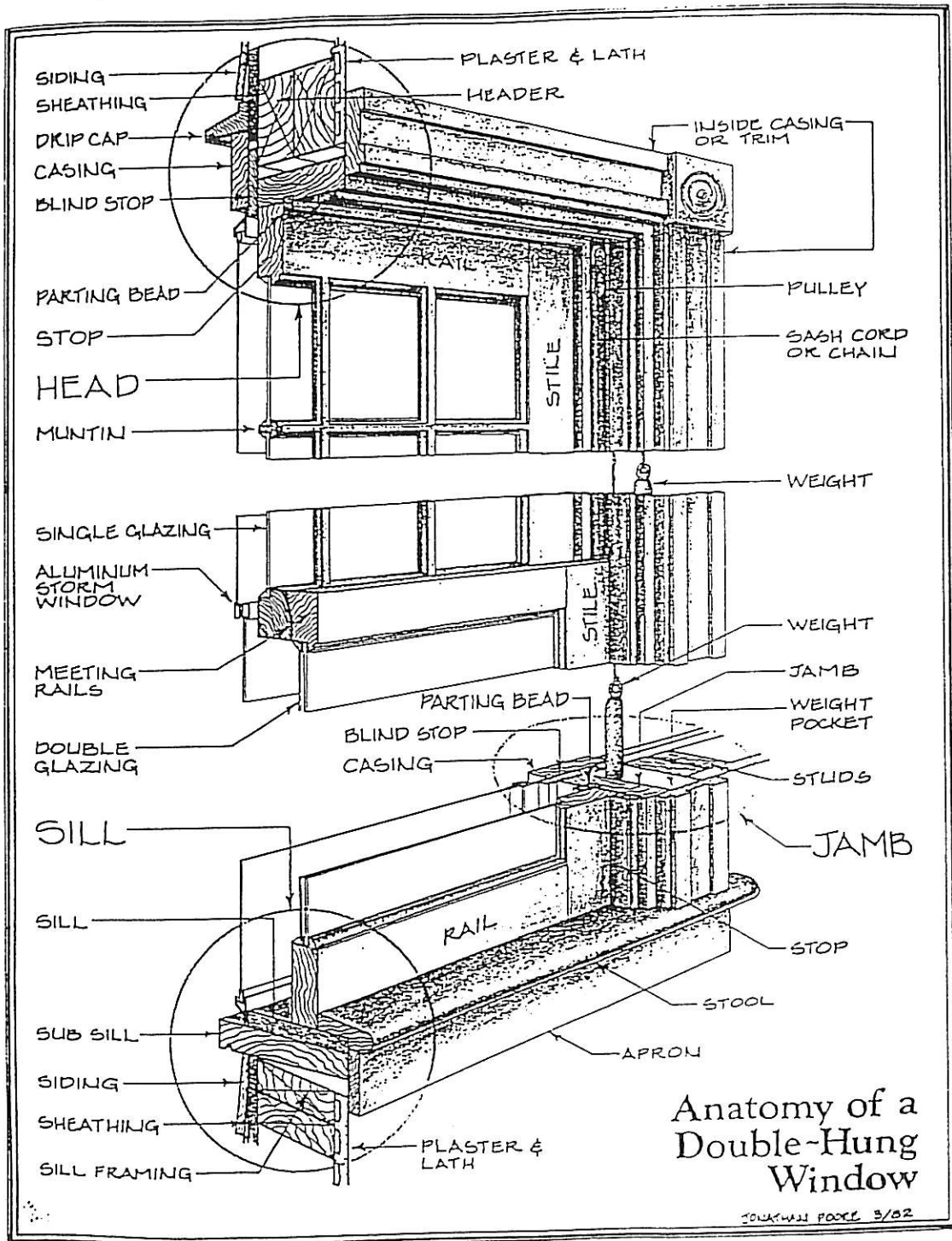
- Louis, M.J. and P.E. Nelson: Extraneous Air Leakage from Window Perimeters. *Airflow Performance of Building Envelopes, Components, and Systems, ASTM STP 1255*: 108-122 (1995).
- Lstiburek, Joseph: March 1995. Personal communication. Building Science Corporation, 273 Russett Road, Chestnut Hill, Massachusetts 02167.
- Lund, C.E. and W.T. Peterson: Air Infiltration through Weatherstripped and Non-Weatherstripped Windows. University of Minnesota. Bulletin no. 35 (1952).
- Montgomery, D.C.: *Design and Analysis of Experiments*. New York, NY: John Wiley and Sons, 1991. pp. 31-33.
- Murphy, W.E, D.G. Colliver, and L.R. Piercy: Repeatability and Reproducibility of Fan Pressurization Devices in Measuring Building Air Leakage. *Indoor Air Quality, ASHRAE Technical Data Bulletin 7(4)*: 36-46 (June 1991).
- Nagda, N.L., D.T. Harrje, M.D. Koontz, and G.G. Purcell: A Detailed Investigation of the Air Infiltration Characteristics of Two Houses. *Measured Air Leakage of Buildings, ASTM STP 904*: 33-45 (1986).
- National Fenestration Rating Council: NFRC 100-91: *Procedure for Determining Fenestration Product Thermal Properties*. Silver Spring, Maryland. (1991).
- National Park Service: *The Windows Handbook: Successful Strategies for Rehabilitating Windows in Historic Buildings*. Preservation Tech Notes, National Park Service, U.S. Department of the Interior, Washington, D.C. (1986).
- Ott, R.L.: *An Introduction to Statistical Methods and Data Analysis*. Belmont, CA: Duxbury Press, 1993. Chapters 5-13.
- Park, S.: *Improving Thermal Efficiency: Historic Wooden Windows: the Colcord Building, Oklahoma City, Oklahoma*. Preservation Tech Notes, National Park Service, U.S. Department of the Interior, Washington, D.C. (1982).
- Persily, A.K. and R.A. Grot: Pressurization Testing of Federal Buildings. *Measured Air Leakage of Buildings, ASTM STP 904*: 184-200 (1986).
- Proskiw, G.: Air Leakage Characteristics of Various Rough-Opening Sealing Methods for Windows and Doors. *Airflow Performance of Building Envelopes, Components, and Systems, ASTM STP 1255*: 123-134 (1995a).
- Proskiw, Gary: March 1995b. Personal communication. Proskiw Engineering Ltd., 1666

Dublin Avenue, Winnipeg, Manitoba R3H 0H1.

- Rayment, R. and K. Morgan: Energy Savings from Secondary Windows. *Building Services Engineering, Research, and Technology*: 95-102 (1985).
- Rayment, R.: Energy Savings from Sealed Double and Heat Reflecting Glazing Units. *Building Services Engineering, Research, and Technology*: 123-127 (1989).
- Sherman, M.H.: "Air Infiltration in Buildings." Ph.D. dissertation, University of California, 1980.
- Sherman, M.H.: Estimation of Infiltration from Leakage and Climate Indicators. *Energy and Buildings 10*: 81-86 (1987).
- Sherman, M.H. and M.P. Modera: Comparison of Measured and Predicted Infiltration Using the LBL Infiltration Model. *Measured Air Leakage of Buildings, ASTM STP 904*: 325-347 (1986).
- Sherman, M.H. and L. Palmiter: Uncertainties in Fan Pressurization Measurements. *Airflow Performance of Building Envelopes, Components, and Systems, ASTM STP 1255*: (1995).
- Sherman, M.H., D.J. Wilson, and D.E. Kiel: Variability in Residential Air Leakage. *Measured Air Leakage of Buildings, ASTM STP 904*: 348-364 (1986).
- Sinden, F.W.: A Two-Thirds Reduction in the Space Heat Requirement of a Twin Rivers Townhouse. *Energy and Buildings*: 243-260 (1978).
- Streeter, V.L. and E.B. Wylie: *Fluid Mechanics*. 8th edition. New York, NY: McGraw-Hill, Inc., 1985. pp. 94-111, 185-216.
- Tamura, G.T.: Measurement of Air Leakage Characteristics of House Enclosures. *ASHRAE Transactions 81*: 202 (1975).
- Warner, J.L. and M. Wilde: DOE Windows and Glazings Research Program. *Selecting Windows for Energy Efficiency*. http://eande.lbl.gov/BTP/DOE/selwind/sel_wind.html#ventilation. (18 November 1996).
- Weidt, John: March 1995. Personal communication. The Weidt Group, 5800 Baker Road, Suite 100, Minnetonka, Minnesota 55345.
- Weidt, J.L., J. Weidt, and S. Selkowitz: "Field Air Leakage of Newly Installed Residential Windows." Presented at the ASHRAE/DOE Conference, Kissimmee, FL, 1979.

Appendix

A. Anatomy of a double-hung window



Reprinted from the Old House Journal, April, 1982

B. Calibration of fan pressurization unit

The DeVac fan pressurization unit was calibrated using a Roots Gas Meter (model 1.5M125), manufactured by Dresser Industries, Inc., Houston, Texas (Figure 22). Data from the two Ametek flow meters exhibited a good fit to a straight line ($R^2 = 0.996$), with the average variation being less than 2% and the largest variation being less than 8% (Table 26). Due to the reasonable fit of the data to the Roots Gas Meter, data from the DeVac fan pressurization unit was read directly from the flow meters as actual cubic feet per minute and corrected to standard cubic feet per minute by using ambient temperature and atmospheric pressure data (Appendix D).

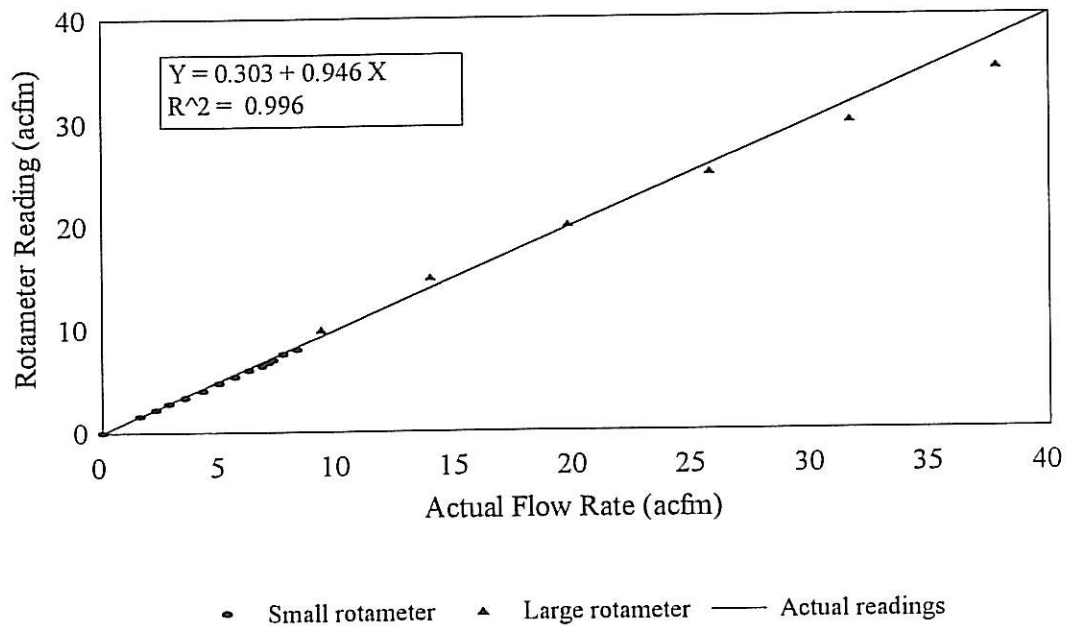


Figure 22: Calibration curve for the DeVac fan pressurization unit

Table 26: Calibration data for the DeVac fan pressurization unit

Large Rotameter Reading (acfm)	Small Rotameter Reading (acfm)	Roots Meter: Actual Flow (acfm)	Percent Difference (%)
	0	0	
	1.6	1.6	-1.72
	2.2	2.3	2.55
	2.8	2.8	0.34
	3.4	3.5	2.94
	4.0	4.3	6.30
	4.8	4.9	3.00
	5.4	5.6	4.28
	6.0	6.2	3.43
	6.4	6.8	5.67
	6.8	7.0	3.52
	7.0	7.2	3.23
	7.6	7.7	1.24
	8.0	8.3	3.67
10		9.3	-7.58
15		13.9	-7.75
20		19.7	-1.42
25		25.7	2.75
30		31.6	5.15
35		37.8	7.34
		40.0	

C. Flow and regression data for field tested windows

C.1 Sash air leakage (Q_s)

Window ID	Storm Window Up or Off							Storm Window Down or On							
	Actual Q 0.30	Reg Q 0.30	Reg Q 0.016	ELA	Constant	R ²	X coef	Actual Q 0.30	Reg Q 0.30	Reg Q 0.016	ELA	Constant	R ²	X coef	
1A		1.19	0.307	0.087	0.7109	0.9564	0.4607		0.92	0.196	0.056	0.5384	0.9404	0.5287	
1B		2.91	0.519	0.147	1.7313	0.9842	0.5992		1.81	0.428	0.121	1.1723	0.9854	0.4961	
1C		1.85	0.498	0.142	1.1103	0.9840	0.4394		1.17	0.286	0.081	0.7739	0.9585	0.5216	
2A		3.51	0.496	0.141	2.0599	1.0000	0.6674		1.68	0.273	0.077	1.2654	0.9869	0.6201	
2B		4.91	0.486	0.138	2.5401	0.9998	0.7887		1.09	0.184	0.053	0.8183	0.9162	0.6072	
2C		3.41	0.551	0.156	1.9762	0.9997	0.6222		2.01	0.059	0.017	2.1494	0.9913	1.2039	
2A2	0.38	0.39	0.089	0.026	-0.3466	0.8692	0.5002	0.18	0.27	0.044	0.013	-0.5850	0.7267	0.6136	
2B2	0.25	0.25	0.056	0.016	-0.7631	0.7543	0.5118	0.06	0.09	0.051	0.014	-2.2793	0.1218	0.1694	
2C2		0.80	0.244	0.070	0.2610	0.8794	0.4039	0.37	0.32	0.118	0.033	-0.7396	0.5091	0.3374	
3A		2.13	0.350	0.099	1.4992	0.9939	0.6164								
3B		2.00	0.461	0.131	1.2938	0.9852	0.5003		0.61	0.097	0.028	0.2630	0.8991	0.6276	
3C		1.22	0.246	0.070	0.8510	0.9708	0.5444								
3D		1.18	0.326	0.093	0.6966	0.8743	0.4397								
3E		0.98	0.138	0.039	0.7843	0.9856	0.6866		0.60	0.091	0.026	0.2646	0.7466	0.6424	
3F		1.01	0.151	0.043	0.7893	0.9771	0.6493								
3G									1.41	0.222	0.063	1.0991	0.9093	0.6298	
3H		3.22	0.477	0.136	1.9531	0.9267	0.6516		1.65	0.367	0.104	1.1106	0.9710	0.5110	
3I		2.73	0.316	0.090	1.8895	0.9703	0.7353		0.0		0.0				
3A2		0.0		0.0					0.40	0.40	0.157	0.044	-0.5546	0.7117	0.3140
3B2	0.45	0.43	0.127	0.037	-0.3479	0.8518	0.4144	0.40	0.40	0.157	0.044	-0.5546	0.7117	0.3140	
3C2	0.12	0.09	0.077	0.022	-2.3620	0.0059	0.0483	0.23	0.16	0.049	0.014	-1.3150	0.3269	0.4082	
3D2	0.11	0.10	0.034	0.010	-1.9017	0.5069	0.3576	0.11	0.10	0.034	0.010	-1.9017	0.5069	0.3576	
3E2									2.14	0.059	0.017	2.2310	0.9139	1.2222	
4A		2.36	0.151	0.043	1.9896	0.9898	0.9387								
4B									1.33	0.084	0.024	1.4202	0.6843	0.9426	
4C		1.78	0.337	0.096	1.2569	0.9712	0.5673		1.10	0.176	0.051	0.8384	0.8952	0.6226	
4D		0.95	0.201	0.057	0.5848	0.9167	0.5290		7.62	0.207	0.059	3.5123	1.0000	1.2306	
4E															
5A								1.64	1.62	0.463	0.131	0.9979	0.9865	0.4279	
5B	1.33	1.36	0.328	0.094	0.8879	0.9971	0.4840	0.40	0.39	0.132	0.038	-0.5061	0.8806	0.3663	
5C	0.56	0.67	0.164	0.046	0.1642	0.8873	0.4776	0.06	0.05	0.019	0.005	-2.4498	0.6088	0.3548	
5D															
5E									0.55	0.59	0.110	0.031	0.1643	0.9330	0.5751
5F								0.00	0.80	0.133	0.038	0.5037	0.9856	0.6081	
5G		0.91	0.186	0.053	0.5586	0.9763	0.5419	0.45	0.37	0.122	0.034	-0.5431	0.7324	0.3775	
5H	0.49	0.47	0.111	0.031	-0.1554	0.9452	0.4954								
6A **		5.94	1.35	0.38	2.3921	0.9994	0.5066		0.62	0.51	0.25	0.07	-0.3890	0.4423	0.2437
6B **															
6C **	1.76	1.76	0.40	0.11	1.1771	0.9456	0.5073								
6D **	1.14	1.29	0.17	0.05	1.0834	0.9032	0.6905								
6A2	0.05	0.05	0.004	0.001	-1.8141	0.9122	0.8550								
6B2	0.06	0.06	0.003	0.001	-1.5161	0.9170	0.9839								
6C2	0.16	0.23	0.003	0.001	0.2827	0.8786	1.4671								
6D2	0.15	0.15	0.016	0.004	-1.0032	0.9627	0.7601								
6E 2	0.36	0.26	0.034	0.010	-0.5375	0.9071	0.6867								
6F2	0.16	0.06	0.005	0.001	-1.7051	0.6208	0.8486								

Sash air leakage (Q_s) continued

Window ID	Storm Window Up or Off							Storm Window Down or On						
	Actual Q 0.30	Reg Q 0.30	Reg Q 0.016	ELA	Constant	R ²	X coef	Actual Q 0.30	Reg Q 0.30	Reg Q 0.016	ELA	Constant	R ²	X coef
7A		0.95	0.061	0.017	1.0780	0.9539	0.9377		0.97	0.008	0.002	1.9446	0.6459	0.6464
7B		0.88	0.609	0.173	0.0189	0.2920	0.1247		4.40	0.112	0.032	2.9878	0.9771	1.2518
7C														
7D		0.80	0.204	0.058	0.3307	0.9360	0.4641							
7E		1.92	0.572	0.162	1.1494	0.9748	0.4131							
7F		1.26	0.509	0.144	0.6059	0.9055	0.3101							
7G														
7H		2.14	0.484	0.138	1.3706	0.9895	0.5066		0.70	0.144	0.041	0.2920	0.7430	0.5390
7I		1.00	0.218	0.062	0.6292	0.9793	0.5205							
7J		0.20	0.333	0.095	-1.8151	0.1921	-0.1730							
7K		4.08	0.636	0.181	2.1690	1.0000	0.6339							
7L														
7 A 2		0.48	0.111	0.031	-0.1066	0.9792	0.5057		1.32	0.226	0.065	1.0029	0.8662	0.6025
7 B 2		2.00	0.315	0.089	1.4499	0.8666	0.6295							
7 C 2	0.43	0.47	0.129	0.037	-0.2156	0.8030	0.4437							
7 D 2		1.61	0.386	0.110	1.0683	0.9986	0.4862							
7 E 2	0.24	0.27	0.023	0.006	-0.3014	0.8412	0.8414							
7 F 2		1.25	0.374	0.107	0.7126	0.9904	0.4102							
7 G 2	0.19	0.19	0.054	0.015	-1.1503	0.8176	0.4291							
7 H 2	0.51	0.57	0.076	0.022	0.2645	0.7120	0.6855							
7 I 2	0.77	0.75	0.145	0.042	0.3957	0.9191	0.5614							
7 J 2	1.07	1.09	0.220	0.062	0.7416	0.9282	0.5454							
7 K 2	0.80	0.85	0.127	0.037	0.6176	0.9425	0.6476							
7 L 2	1.07	1.11	0.152	0.043	0.9246	0.9497	0.6790							
7 M 2	0.90	0.93	0.245	0.070	0.4724	0.9274	0.4536							
7 N 2	0.58	0.56	0.101	0.029	0.1255	0.8453	0.5853							
7 O 2		0.62	0.128	0.037	0.1753	0.8720	0.5387							
7 P 2	1.04	1.04	0.221	0.062	0.6765	0.9758	0.5289							
7 Q 2		0.22	0.109	0.031	-1.2552	0.2597	0.2339							
7 R 2	0.42	0.38	0.081	0.023	-0.3540	0.8162	0.5219							
7 S 2		0.36	0.069	0.019	-0.3556	0.9570	0.5608							
7 T 2	0.05	0.05	0.003	0.001	-1.6521	0.5294	1.0120							
8A		1.75	0.492	0.140	1.0800	0.9917	0.4327							
8B		2.12	0.338	0.096	1.5056	0.7825	0.6268							
8C		3.63	0.861	0.244	1.8786	0.9985	0.4906							
8D								0.05	0.06	0.017	0.004	-2.1401	0.4307	0.4720
8E								0.17	0.17	0.024	0.006	-0.9557	0.5629	0.6788
8F								0.05	0.05	0.056	0.016	-2.8883		
9A		2.38	0.521	0.148	1.4921	0.9927	0.5186		1.46	0.222	0.063	1.1571	0.9889	0.6450
9B		1.98	0.376	0.107	1.3639	0.9905	0.5665		1.59	0.247	0.070	1.2313	0.9618	0.6353
9C		2.80	0.845	0.240	1.5217	1.0000	0.4088							
9D		1.09	0.281	0.080	0.6434	0.9587	0.4630		0.83	0.310	0.088	0.2142	0.9429	0.3350
9E	0.52	0.54	0.097	0.028	0.0764	0.9337	0.5819							
9F		2.46	0.824	0.235	1.3540	1.0000	0.3740		1.47	0.072	0.020	1.6216	0.7085	1.0238
10A1	1.03	1.10	0.751	0.213	0.2514	0.8373	0.1300		0.05	0.05	0.046	0.013	-2.7265	0.3078
10A2														
10B1	1.82	1.80	0.833	0.237	0.8994	0.9916	0.2619		0.84	0.93	0.111	0.031	0.7920	0.9610
10B2														
10C1	1.03	1.10	0.748	0.213	0.2475	0.8373	0.1300							
10C2								0.46	0.48	0.122	0.034	-0.1442	0.9127	0.4754
10D 1		2.64	0.457	0.130	1.6903	1.0000	0.5978		1.62	0.194	0.055	1.3582	0.9390	0.7253
10D 2	0.10	0.10	0.054	0.015	-2.0768	0.1632	0.2052		0.19	0.18	0.071	0.020	-1.3101	0.4986

Sash air leakage (Q_s) continued

Window ID	Storm Window Up or Off							Storm Window Down or On							
	Actual Q 0.30	Reg Q 0.30	Reg Q 0.016	ELA	Constant	R ²	X coef	Actual Q 0.30	Reg Q 0.30	Reg Q 0.016	ELA	Constant	R ²	X coef	
11 A	0.17	0.16	0.014	0.004	-0.7924	0.9208	0.8365								
11 B	0.02	0.04	0.011	0.003	-2.7665	0.3574	0.4252								
11 C	0.14	0.16	0.055	0.015	-1.3799	0.7569	0.3701								
11 D	0.13	0.11	0.085	0.024	-2.0996	0.1170	0.0896								
11 E	0.36	0.36	0.024	0.006	0.0931	0.9757	0.9332								
11 F	0.06	0.06	0.040	0.011	-2.5502	0.2263	0.1646								
12 A		1.98	0.769	0.218	1.0717	0.8445	0.3227		1.02	0.178	0.051	0.7444	0.9631	0.5982	
12 B		0.30	0.082	0.023	-0.6426	0.4569	0.4519		0.28	0.065	0.018	-0.6626	0.6079	0.5014	
12 C	0.37	0.33	0.100	0.029	-0.6003	0.9206	0.4106	0.37	0.31	0.094	0.027	-0.6676	0.9206	0.4106	
12 D		0.15	0.037	0.011	-1.3264	0.8231	0.4781		0.13	0.044	0.013	-1.6486	0.2957	0.3579	
12 E		0.76	0.297	0.085	0.1156	0.7724	0.3213		0.74	0.082	0.024	0.6035	0.9356	0.7523	
12 F	0.34	0.44	0.017	0.005	0.4992	0.9082	1.1012	0.34	0.44	0.011	0.003	0.7483	0.8590	1.2813	
12 G		3.00	0.390	0.111	1.9383	0.9955	0.6966		2.21	0.329	0.094	1.5730	0.9874	0.6490	
12 H		2.10	0.585	0.167	1.2634	0.9895	0.4352		0.69	0.095	0.027	0.4481	0.8661	0.6784	
12 I		2.53	0.703	0.200	1.4541	0.9996	0.4368		0.86	0.312	0.088	0.2745	0.8229	0.3482	
12 J															
13 A		1.54	0.400	0.114	0.9878	0.9425	0.4606		0.58	0.176	0.051	-0.0669	0.7900	0.4027	
13 B		1.22	0.490	0.138	0.5722	0.9390	0.3135		0.73	0.161	0.046	0.2988	0.7637	0.5131	
13 C		1.83	0.557	0.158	1.0962	1.0000	0.4065		1.66	0.088	0.025	1.7111	1.0000	1.0000	
13 D		1.25	0.480	0.137	0.6162	0.8372	0.3264		0.89	0.371	0.105	0.2424	0.5627	0.2981	
13 E		1.82	0.563	0.160	1.0792	0.9757	0.4000		1.31	0.394	0.112	0.7619	0.9751	0.4095	
13 F		0.67	0.291	0.083	-0.0646	0.3062	0.2830		0.45	0.112	0.031	-0.2312	0.9133	0.4744	
13 G		1.08	0.317	0.090	0.5707	0.7640	0.4155		0.74	0.275	0.079	0.1120	0.5868	0.3385	
13 H		1.78	0.211	0.060	1.4457	0.9932	0.7263		1.02	0.165	0.047	0.7654	0.9139	0.6206	
13 I		1.08	0.354	0.101	0.5312	0.9130	0.3795		0.65	0.265	0.075	-0.0765	0.7344	0.3032	
13 J	0.28	0.26	0.067	0.019	-0.7803	0.8136	0.4674	0.23	0.17	0.027	0.008	-0.9569	0.7436	0.6455	
14 A	0.79	0.84	0.166	0.047	0.4830	0.8934	0.5512		0.17	0.26	0.002	0.001	0.6116	0.7771	1.6306
14 B		1.74	0.553	0.157	1.0297	0.8668	0.3922		0.28	0.25	0.053	0.015	-0.7808	0.8531	0.5243
14 C		1.37	0.321	0.091	0.9064	0.9885	0.4939		0.33	0.37	0.077	0.022	-0.3488	0.8197	0.5344
14 D	0.56	0.67	0.099	0.028	0.3612	0.8838	0.6507		0.17	0.18	0.018	0.005	-0.7721	0.8936	0.7878
14 E	1.12	1.04	0.542	0.154	0.3167	0.9600	0.2244		0.03	0.06	0.062	0.017	-2.6487	0.0010	0.0304
14 F		1.18	0.492	0.140	0.5286	0.9889	0.2994		0.02	0.02	0.077	0.022	-4.4737	0.6440	-0.4630
15 A 1									2.11	0.113	0.032	1.9513	1.0000	1.0000	
15 A 2									0.0						
15 B 1		2.16	0.330	0.094	1.5449	0.9956	0.6412		0.36	0.351	0.100	-1.0483		0.0000	
15 B 2								0.01	0.01	0.008	0.002	-4.9564	1.0000	-0.0000	
15 C 1									0.0						
15 C 2								0.70	0.25	0.070	0.007	1.0733	0.3569	0.0300	
15 D 1									0.0						
15 D 2									0.0						
16 A								0.00	0.52	0.213	0.060	-0.3007	1.0000	0.3018	
16 B								0.00	0.01	0.597	0.170	-6.1266	1.0000	-1.3569	
16 C															
16 D															
16 E															
16 F					0.0733										
16 G		0.55	0.054	0.015	0.3624	1.0000	0.7937								
17 A	0.09	0.09	0.087	0.025	-2.4419		0.0000	0.09	0.09	0.087	0.025	-2.4419		0.0000	
17 B	0.17	0.20	0.045	0.013	-0.9981	0.5887	0.5104	0.09	0.12	0.029	0.009	-1.5635	0.7429	0.4752	
17 C	0.26	0.24	0.132	0.038	-1.2320	0.2568	0.1920	0.09	0.13	0.049	0.014	-1.6114	0.4717	0.3356	
18 A	0.33	0.32	0.026	0.008	-0.1134	0.9835	0.8571								
18 B	0.11	0.09	0.014	0.004	-1.6243	0.9208	0.6412								
19 A	0.39	0.41	0.090	0.026	-0.2587	0.8700	0.5183	0.28	0.30	0.070	0.020	-0.6209	0.7986	0.4923	
19 B	0.49	0.57	0.109	0.031	0.1214	0.8937	0.5653	0.33	0.40	0.088	0.025	-0.2964	0.8843	0.5154	

C.2 Extraneous air leakage (Q_e)

	Storm Window Up or Off							Storm Window Down or On							
	Actual Q 0.30	Reg Q 0.30	Reg Q 0.016	ELA	Constant	R ²	X coef	Actual Q 0.30	Reg Q 0.30	Reg Q 0.016	ELA	Constant	R ²	X coef	
1A		1.27	0.159	0.046	1.0857	0.9921	0.7060			1.25	0.168	0.048	1.0517	0.9913	0.6882
1B		0.66	0.072	0.020	0.4890	0.9928	0.7609			0.67	0.176	0.021	0.5036	0.9898	0.7621
1C		1.15	0.130	0.076	1.0195	0.9930	0.7412			1.18	0.136	0.039	1.0484	0.9915	0.7424
2A		1.97	0.306	0.087	1.4430	0.9972	0.6360			2.00	0.352	0.100	1.4077	0.9978	0.5928
2B		2.13	0.330	0.094	1.5188	0.9835	0.6353			2.15	0.322	0.091	1.5497	0.9869	0.6486
2C		2.46	0.424	0.121	1.6231	0.9970	0.6003			2.54	0.441	0.126	1.6494	0.9945	0.5966
2A2	1.37	1.33	0.152	0.043	1.1841	0.9966	0.7429	1.37	1.33	0.151	0.043	1.1893	0.9966	0.7457	
2B2	1.72	1.74	0.244	0.069	1.3629	0.9963	0.6706	1.72	1.76	0.241	0.069	1.3881	0.9940	0.6797	
2C2	1.90	2.03	0.209	0.059	1.6434	0.9818	0.7768	1.90	2.02	0.212	0.060	1.6305	0.9833	0.7690	
3A		2.71	0.406	0.115	1.7755	0.9849	0.6477								
3B	1.52	1.71	0.111	0.031	1.6620	0.9808	0.9336								
3C	1.78	1.79	0.289	0.082	1.3251	0.9980	0.6205	1.83	1.85	0.329	0.094	1.3273	0.9982	0.5900	
3D		2.81	0.550	0.156	1.7023	0.9976	0.5564								
3E	1.93	1.93	0.355	0.101	1.3516	0.9978	0.5769								
3F	2.15	2.13	0.577	0.164	1.2923	0.9978	0.4455	2.15	2.12	0.526	0.150	1.3270	0.9981	0.4763	
3G	1.55	1.59	0.197	0.056	1.3211	0.9937	0.7121								
3H		3.03	0.463	0.131	1.8839	0.9948	0.6420			3.03	0.463	0.131	1.8839	0.9948	0.6420
3I		3.64	0.624	0.178	2.0168	0.9965	0.6018			3.52	0.590	0.168	1.9937	0.9985	0.6098
3A2	1.15	1.19	0.136	0.039	1.0782	0.9975	0.7445	1.15	1.21	0.135	0.038	1.0827	0.9977	0.7476	
3B2	1.02	1.10	0.127	0.036	0.9812	0.9957	0.7374	1.02	1.10	0.131	0.038	0.9659	0.9961	0.7247	
3C2	1.19	1.31	0.151	0.043	1.1661	0.9892	0.7395	1.19	1.32	0.148	0.042	1.1736	0.9866	0.7447	
3D2	1.27	1.31	0.182	0.052	1.0832	0.9969	0.6746	1.27	1.31	0.185	0.053	1.0723	0.9972	0.6679	
3E2															
4A	1.88	1.85	0.480	0.137	1.1725	0.9973	0.4612	1.88	1.81	0.493	0.140	1.1237	0.9818	0.4429	
4B		3.76	0.767	0.218	1.9734	0.9759	0.5412			4.11	0.723	0.206	2.1286	0.9978	0.5931
4C	2.45	2.40	0.386	0.110	1.6288	0.9966	0.6240	2.52	2.44	0.392	0.111	1.6473	0.9956	0.6251	
4D		3.13	0.415	0.118	1.9716	0.9939	0.6892			3.07	0.463	0.131	1.8974	0.9923	0.6450
4E		3.87	0.807	0.229	1.9968	0.9688	0.5347			4.18	0.756	0.215	2.1302	0.9877	0.5827
5A								0.44	0.43	0.061	0.017	-0.0460	0.9922	0.6629	
5B	0.52	0.53	0.081	0.023	0.1207	0.9987	0.6378	0.96	1.00	0.141	0.040	0.8121	0.9954	0.6701	
5C	0.84	0.84	0.140	0.040	0.5679	0.9878	0.6121	0.23	0.24	0.036	0.010	-0.6697	0.9986	0.6486	
5D								0.09	0.09	0.016	0.004	-1.8554	0.9525	0.5433	
5E								1.15	1.16	0.179	0.051	0.9223	0.9937	0.6389	
5F								1.85	1.83	0.334	0.095	1.3010	0.9962	0.5798	
5G	1.89	1.86	0.330	0.094	1.3292	0.9963	0.5890	1.50	1.58	0.197	0.056	1.3139	0.9912	0.7110	
5H	1.55	1.56	0.224	0.063	1.2464	0.9975	0.6629								
6A**		3.96	0.60	0.17	2.1473	0.9985	0.6410								
6B**								2.83	3.13	0.27	0.08	2.1537	0.9780	0.8413	
6C**	2.50	2.56	0.30	0.09	1.8165	0.9951	0.7292								
6D**	2.39	2.49	0.23	0.07	1.8792	0.9976	0.8049								
6A2	0.84	0.87	0.105	0.030	0.7256	0.9942	0.7194								
6B2	0.29	0.29	0.030	0.009	-0.3188	0.9856	0.7683								
6C2	0.34	0.34	0.054	0.015	-0.3061	0.9943	0.6345								
6D2	0.33	0.33	0.041	0.012	-0.2502	0.9803	0.7103								
6E 2	0.33	0.32	0.046	0.013	-0.3236	0.9927	0.6652								
6F2	0.52	0.51	0.091	0.026	0.0122	0.9560	0.5805								

Extraneous air leakage (Q_e) continued

	Storm Window Up or Off							Storm Window Down or On						
	Actual Q 0.30	Reg Q 0.30	Reg Q 0.016	ELA	Constant	R ²	X coef	Actual Q 0.30	Reg Q 0.30	Reg Q 0.016	ELA	Constant	R ²	X coef
7A	1.69	1.67	0.265	0.075	1.2717	0.9899	0.6294	1.69	1.67	0.293	0.083	1.2226	0.9945	0.5929
7B		2.21	0.396	0.113	1.4981	0.9925	0.5863							
7C									1.67	0.298	0.085	1.2221	0.9848	0.5885
7D		3.01	0.513	0.146	1.8274	0.9994	0.6033							
7E	1.58	1.61	0.253	0.072	1.2426	0.9976	0.6325							
7F	1.78	1.84	0.244	0.070	1.4403	0.9923	0.6891							
7G		2.12	0.414	0.117	1.4224	0.9965	0.5574							
7H	1.83	1.85	0.298	0.085	1.3690	0.9940	0.6234							
7I		2.18	0.383	0.109	1.4972	0.9943	0.5940	2.29	0.392	0.112	1.5526	0.9900	0.6019	
7J		3.48	0.577	0.164	1.9832	0.9901	0.6127							
7K	1.58	1.61	0.238	0.068	1.2683	0.9868	0.6535							
7L	1.38	1.40	0.161	0.046	1.2255	0.9923	0.7375							
7A2	1.53	1.59	0.200	0.057	1.3163	0.9920	0.7067							
7B2		2.26	0.312	0.089	1.6265	0.9953	0.6746	2.26	0.312	0.089	1.6265	0.9953	0.6746	
7C2	0.85	0.85	0.057	0.016	0.9516	0.9978	0.9249							
7D2	0.46	0.46	0.042	0.012	0.2270	0.9953	0.8216							
7E2	1.42	1.46	0.222	0.063	1.1556	0.9919	0.6433							
7F2	0.95	0.99	0.108	0.031	0.9065	0.9880	0.7574							
7G2	0.90	0.95	0.072	0.020	1.0035	0.9935	0.8797							
7H2	1.02	1.04	0.112	0.031	0.9632	0.9869	0.7635							
7I2	1.08	1.10	0.135	0.039	0.9511	0.9834	0.7142							
7J2	0.97	1.00	0.124	0.036	0.8600	0.9904	0.7136							
7K2	1.07	1.10	0.118	0.033	1.0024	0.9965	0.7579							
7L2	0.90	0.93	0.121	0.034	0.7547	0.9926	0.6939							
7M2	1.05	1.08	0.136	0.039	0.9248	0.9967	0.7077							
7N2	1.26	0.00	0.173	0.049	1.1022	0.9930	0.6903							
7O2	1.62	1.69	0.212	0.060	1.3774	0.9857	0.7082							
7P2	1.04	1.05	0.119	0.033	0.9556	0.9963	0.7457							
7Q2	2.09	2.12	0.324	0.093	1.5198	0.9940	0.6403							
7R2	1.19	1.28	0.156	0.044	1.1153	0.9900	0.7191							
7S2	1.61	1.66	0.250	0.071	1.2798	0.9904	0.6455							
7T2	0.75	0.73	0.073	0.020	0.6358	0.9980	0.7871							
8A	1.46	1.51	0.230	0.066	1.1803	0.9975	0.6401							
8B	2.06	2.04	0.336	0.096	1.4600	0.9942	0.6168							
8C	1.35	1.40	0.198	0.056	1.1435	0.9972	0.6668	1.33	1.40	0.168	0.047	1.2031	0.9939	0.7221
8D								1.61	1.65	0.179	0.051	1.4105	0.9941	0.7577
8E								1.39	1.45	0.199	0.057	1.1859	0.9951	0.6771
8F								0.62	0.62	0.042	0.012	0.6301	0.9928	0.9176
9A	0.57	0.56	0.054	0.015	0.3686	0.9978	0.8007	1.09	1.14	0.091	0.026	1.1760	0.9916	0.8641
9B	0.94	1.01	0.087	0.025	1.0106	0.9957	0.8330							
9C		2.23	0.305	0.086	1.6215	0.9981	0.6800							
9D	1.67	1.72	0.236	0.067	1.3639	0.9930	0.6798	1.71	1.76	0.241	0.069	1.3863	0.9890	0.6795
9E	1.30	1.37	0.158	0.045	1.1993	0.9884	0.7354							
9F		2.72	0.473	0.135	1.7215	0.9940	0.5972	2.72	0.473	0.135	1.7215	0.9940	0.5972	
10A1	0.81	0.77	0.125	0.036	0.4836	0.9960	0.6194							
10A2								0.36	0.33	0.087	0.025	-0.5333	0.9920	0.4622
10B1	0.19	0.18	0.031	0.009	-0.9695	0.9872	0.6029							
10B2								0.19	0.18	0.031	0.009	-0.9747	0.9743	0.6046
10C1	0.80	0.76	0.125	0.036	0.4797	0.9960	0.6194							
10C2								0.86	0.85	0.133	0.038	0.5954	0.9980	0.6302
10D1		2.26	0.466	0.132	1.4655	0.9960	0.5388	0.00	2.25	0.396	0.113	1.5237	0.9961	0.5925
10D2	1.54	1.55	0.260	0.074	1.1731	0.9974	0.6095	1.54	1.55	0.260	0.074	1.1731	0.9974	0.6095

Extraneous air leakage (Q_e) continued

	Storm Window Up or Off							Storm Window Down or On						
	Actual Q 0.30	Reg Q 0.30	Reg Q 0.016	ELA	Constant	R ²	X coef	Actual Q 0.30	Reg Q 0.30	Reg Q 0.016	ELA	Constant	R ²	X coef
11 A	0.48	0.52	0.044	0.013	0.3375	0.9872	0.8341							
11 B	0.41	0.41	0.061	0.017	-0.1188	0.9989	0.6472							
11 C	0.28	0.28	0.037	0.011	-0.4389	0.9846	0.6957							
11 D	0.42	0.45	0.043	0.012	0.1822	0.9855	0.8040							
11 E	0.54	0.54	0.075	0.022	0.1809	0.9980	0.6698							
11 F	0.33	0.33	0.038	0.011	-0.2132	0.9957	0.7388							
12 A	2.26	2.27	0.362	0.103	1.5757	0.9913	0.6269	2.26	2.30	0.373	0.107	1.5832	0.9943	0.6213
12 B	2.32	2.32	0.315	0.089	1.6806	0.9981	0.6853	2.32	2.34	0.314	0.089	1.6736	0.9976	0.6846
12 C	1.75	1.82	0.192	0.055	1.5231	0.9965	0.7684	1.75	1.82	0.192	0.055	1.5206	0.9966	0.7671
12 D	2.26	2.39	0.242	0.069	1.8093	0.9924	0.7806	2.26	2.38	0.243	0.069	1.8039	0.9932	0.7777
12 E		2.56	0.282	0.080	1.8482	0.9898	0.7534		2.55	0.284	0.081	1.8394	0.9910	0.7487
12 F	1.27	1.33	0.117	0.033	1.2903	0.9966	0.8298	1.27	1.33	0.117	0.033	1.2903	0.9966	0.8298
12 G	1.27	1.37	0.136	0.039	1.2571	0.9925	0.7877	1.27	1.36	0.137	0.039	1.2521	0.9917	0.7850
12 H	2.20	2.26	0.322	0.091	1.6156	0.9914	0.6651	2.20	2.26	0.322	0.091	1.6156	0.9914	0.6651
12 I		2.49	0.311	0.088	1.7670	0.9978	0.7097		2.49	0.311	0.088	1.7670	0.9978	0.7097
12 J		5.65	0.905	0.257	2.4850	0.9993	0.6251		5.65	0.905	0.257	2.4850	0.9993	0.6251
13 A	1.98	2.00	0.337	0.096	1.4234	0.9914	0.6072	1.98	2.00	0.337	0.096	1.4234	0.9914	0.6072
13 B	1.90	1.97	0.242	0.069	1.5404	0.9890	0.7152	1.90	1.97	0.242	0.069	1.5404	0.9890	0.7152
13 C		3.48	0.659	0.187	1.9308	0.9977	0.5678		3.48	0.659	0.187	1.9308	0.9977	0.5678
13 D		2.18	0.302	0.086	1.5903	0.9918	0.6738		2.18	0.302	0.086	1.5903	0.9918	0.6738
13 E	1.22	1.32	0.121	0.034	1.2637	0.9925	0.8176		1.32	0.121	0.034	1.2637	0.9925	0.8176
13 F		2.46	0.428	0.122	1.6216	0.9936	0.5974		2.46	0.428	0.122	1.6216	0.9936	0.5974
13 G	2.17	2.23	0.328	0.094	1.5899	0.9900	0.6539		2.23	0.328	0.094	1.5899	0.9900	0.6539
13 H		2.44	0.341	0.097	1.7049	0.9989	0.6728		2.44	0.341	0.097	1.7049	0.9989	0.6728
13 I		2.29	0.348	0.099	1.6066	0.9936	0.6442		2.29	0.348	0.099	1.6066	0.9936	0.6442
13 J	1.76	1.89	0.208	0.059	1.5433	0.9790	0.7534		1.89	0.208	0.059	1.5433	0.9790	0.7534
14 A	0.96	0.99	0.102	0.029	0.9216	0.9935	0.7749	0.96	0.99	0.102	0.029	0.9216	0.9935	0.7749
14 B	1.41	1.48	0.202	0.057	1.2116	0.9901	0.6794	1.41	1.48	0.202	0.057	1.2116	0.9901	0.6794
14 C	1.35	1.39	0.140	0.040	1.2706	0.9974	0.7828	1.35	1.39	0.140	0.040	1.2706	0.9974	0.7828
14 D	0.85	0.82	0.099	0.028	0.6612	0.9950	0.7200	0.85	0.82	0.099	0.028	0.6612	0.9950	0.7200
14 E	1.12	1.16	0.126	0.036	1.0674	0.9968	0.7601	1.12	1.16	0.126	0.036	1.0674	0.9968	0.7601
14 F	1.05	1.09	0.089	0.026	1.1159	0.9954	0.8539	1.05	1.09	0.089	0.026	1.1159	0.9954	0.8539
15 A 1		4.98	1.117	0.317	2.2213	0.9969	0.5104		4.98	1.117	0.317	2.2213	0.9969	0.5104
15 A 2								0.31	0.32	0.135	0.039	-0.7846	0.9833	0.2954
15 B 1		3.84	0.712	0.202	2.0399	0.9931	0.5754		3.84	0.712	0.202	2.0399	0.9931	0.5754
15 B 2								0.34	0.36	0.145	0.041	-0.6823	0.9693	0.3017
15 C 1		5.44	1.228	0.349	2.3056	1.0000	0.5080		4.98	1.117	0.317	2.2213	0.9969	0.5104
15 C 2								0.42	0.41	0.245	0.070	-0.6771	0.9787	0.1756
15 D 1		5.22	1.059	0.301	2.3074	0.9993	0.5440		3.84	0.712	0.202	2.0399	0.9931	0.5754
15 D 2								0.26	0.26	0.085	0.025	-0.8961	0.9916	0.3785
16 A		4.45	0.616	0.175	2.3079	1.0000	0.6753		4.45	0.616	0.175	2.3079	1.0000	0.6753
16 B		4.19	0.804	0.228	2.1103	1.0000	0.5632		4.19	0.804	0.228	2.1103	1.0000	0.5632
16 C		4.15	0.839	0.239	2.0813	1.0000	0.5456		4.15	0.839	0.239	2.0813	1.0000	0.5456
16 D		4.14	0.795	0.226	2.0991	1.0000	0.5632		4.14	0.795	0.226	2.0991	1.0000	0.5632
16 E		6.41	0.918	0.260	2.6574	0.9980	0.6634							
16 F		4.56	0.915	0.260	2.1769	0.9998	0.5479							
16 G		4.53	0.636	0.181	2.3176	0.9951	0.6701							
17 A	2.35	2.37	0.409	0.116	1.5843	0.9930	0.5995	2.35	2.37	0.409	0.116	1.5843	0.9930	0.5995
17 B	1.90	1.98	0.268	0.076	1.5061	0.9969	0.6827	1.90	1.98	0.268	0.076	1.5061	0.9969	0.6827
17 C	2.40	2.44	0.441	0.126	1.5932	0.9920	0.5833	2.40	2.44	0.441	0.126	1.5932	0.9920	0.5833
18 A	0.54	0.53	0.071	0.020	0.1907	0.9963	0.6860							
18 B	0.58	0.55	0.086	0.025	0.1766	0.9914	0.6372							
19 A	1.27	1.31	0.155	0.044	1.1506	0.9911	0.7288	1.27	1.31	0.155	0.044	1.1506	0.9911	0.7288
19 B	0.77	0.73	0.055	0.016	0.7535	0.9936	0.8835	0.77	0.73	0.055	0.016	0.7535	0.9936	0.8835

C.3 Total air leakage (Q_t)

	Storm Window Up or Off							Storm Window Down or On							
	Actual Q 0.30	Reg Q 0.30	Reg Q 0.016	ELA	Constant	R ²	X coef	Actual Q 0.30	Reg Q 0.30	Reg Q 0.016	ELA	Constant	R ²	X coef	
1A		2.47	0.455	0.129	1.5937	0.9948	0.5765		2.17	0.359	0.102	1.5100	0.9950	0.6140	
1B		3.51	0.569	0.162	1.9677	0.9930	0.6259		2.40	0.473	0.135	1.5370	0.9936	0.5574	
1C		2.89	0.714	0.203	1.6442	0.8773	0.4899		2.34	0.406	0.116	1.5732	0.9917	0.6051	
2A		4.94	0.935	0.266	2.2805	0.9830	0.5678		3.68	0.624	0.178	2.0328	0.9993	0.6054	
2B		6.83	0.822	0.234	2.7923	0.9913	0.7226		3.34	0.499	0.142	1.9856	0.9970	0.6482	
2C		5.96	0.968	0.275	2.5319	0.9981	0.6201		4.24	0.475	0.135	2.3438	0.9995	0.7471	
2A2	1.73	1.72	0.238	0.068	1.3551	0.9915	0.6752	1.55	1.62	0.193	0.055	1.3581	0.9894	0.7262	
2B2	1.97	2.00	0.300	0.085	1.4715	0.9960	0.6468	1.79	1.82	0.281	0.080	1.3618	0.9956	0.6364	
2C2		2.83	0.437	0.124	1.8056	0.9969	0.6371	2.27	2.30	0.327	0.093	1.6376	0.9935	0.6662	
3A		4.98	0.744	0.211	2.3867	0.9698	0.6488								
3B		3.96	0.522	0.148	2.2082	0.9979	0.6913		2.50	0.421	0.119	1.6438	0.9969	0.6066	
3C		3.00	0.534	0.152	1.8101	0.9933	0.5888								
3D		3.80	0.897	0.255	0.2589	0.9884	0.4925								
3E		2.87	0.498	0.142	1.7763	0.9954	0.5979		2.71	0.622	0.176	1.6040	0.9939	0.5027	
3F		3.09	0.727	0.207	1.7228	0.9991	0.4937								
3G									4.45	0.684	0.195	2.2616	0.9909	0.6385	
3H		6.39	0.931	0.265	2.6454	0.9836	0.6571		5.12	0.957	0.272	2.3220	0.9999	0.5722	
3I		6.17	0.953	0.271	2.5861	0.9983	0.6370		1.15	1.19	0.135	0.039	1.0787	0.9971	0.7462
3A2	1.15	1.19	0.137	0.039	1.0696	0.9977	0.7400	1.42	1.48	0.271	0.077	1.0938	0.9869	0.5803	
3B2	1.48	1.52	0.245	0.070	1.1675	0.9876	0.6220	1.42	1.47	0.203	0.058	1.2054	0.9873	0.6762	
3C2	1.31	1.40	0.212	0.060	1.1119	0.9803	0.6439	1.39	1.41	0.216	0.061	1.1099	0.9952	0.6388	
3D2	1.39	1.41	0.213	0.060	1.1192	0.9952	0.6446								
3E2	1.60	1.67	0.251	0.071	1.2935	0.9929	0.6472								
4A		3.80	0.624	0.178	2.0760	0.9914	0.6162		3.25	0.535	0.152	1.9207	0.9992	0.6160	
4B									3.53	0.514	0.146	2.0514	0.9652	0.6566	
4C		3.95	0.748	0.213	2.0578	0.9977	0.5678		4.18	0.639	0.182	2.1995	0.9989	0.6400	
4D		4.19	0.604	0.172	2.2274	0.9910	0.6605		7.82	1.012	0.287	2.8984	1.0000	0.6982	
4E								2.08	2.04	0.520	0.147	1.2777	0.9938	0.4672	
5A															
5B	1.85	1.88	0.407	0.115	1.2592	0.9989	0.5221	1.35	1.39	0.266	0.075	1.0062	0.9949	0.5638	
5C	1.40	1.52	0.301	0.085	1.0802	0.9824	0.5517	0.30	0.29	0.057	0.016	-0.5878	0.9907	0.5518	
5D								0.09	0.09	0.016	0.004	-1.8554	0.9525	0.5433	
5E								1.71	1.75	0.289	0.082	1.3050	0.9924	0.6157	
5F									2.60	0.471	0.133	1.6605	0.9976	0.5837	
5G		2.70	0.527	0.150	1.6625	0.9996	0.5568	1.95	1.92	0.321	0.091	1.3661	0.9956	0.6106	
5H	2.04	2.03	0.335	0.095	1.4487	0.9982	0.6152								
6A **		10.09	1.91	0.54	2.9948	0.9996	0.5673	3.46	3.53	0.48	0.14	2.0770	0.9895	0.6777	
6B **															
6C **	4.26	4.30	0.89	0.20	2.2128	0.9931	0.6250								
6D **	3.53	3.78	0.40	0.12	2.2458	0.9821	0.7619								
6A2	0.89	0.93	0.110	0.031	0.8002	0.9944	0.7268								
6B2	0.36	0.36	0.033	0.010	-0.0663	0.9946	0.8026								
6C2	0.51	0.53	0.055	0.015	0.3022	0.9920	0.7755								
6D2	0.48	0.47	0.057	0.016	0.1319	0.9898	0.7227								
6E 2	0.69	0.58	0.081	0.023	0.2759	0.9759	0.6785								
6F2	0.69	0.58	0.096	0.027	0.1985	0.9550	0.6151								

Total air leakage (Q_t) continued

	Storm Window Up or Off							Storm Window Down or On						
	Actual Q 0.30	Reg Q 0.30	Reg Q 0.016	ELA	Constant	R ²	X coef	Actual Q 0.30	Reg Q 0.30	Reg Q 0.016	ELA	Constant	R ²	X coef
7A		2.59	0.320	0.090	1.8163	0.9810	0.7154		2.22	0.323	0.091	1.5896	0.9933	0.6582
7B		3.05	0.949	0.270	1.5920	0.9852	0.3978							
7C									4.80	0.411	0.117	2.5778	0.9887	0.8386
7D		3.86	0.710	0.202	2.0473	0.9977	0.5779							
7E		3.54	0.807	0.229	1.8735	0.9900	0.5048							
7F		3.17	0.706	0.201	1.7706	0.9992	0.5122							
7G														
7H		4.19	0.758	0.215	2.1344	0.9991	0.5833							
7I		3.19	0.599	0.170	1.8463	0.9933	0.5703	2.98	0.541	0.154	1.7945	0.9946	0.5822	
7J		3.68	0.812	0.231	1.9223	0.9952	0.5151							
7K		5.15	0.893	0.254	2.3594	1.0000	0.5978							
7L														
7A2		2.10	0.307	0.087	1.5335	0.9979	0.6568							
7B2		4.27	0.627	0.179	2.2395	0.9942	0.6545	3.65	0.533	0.152	2.0835	0.9968	0.6559	
7C2	1.28	1.32	0.161	0.046	1.1449	0.9897	0.7176							
7D2		2.09	0.413	0.117	1.4038	0.9978	0.5533							
7E2	1.67	1.72	0.247	0.070	1.3420	0.9854	0.6621							
7F2		2.25	0.462	0.131	1.4600	0.9942	0.5402							
7G2	1.09	1.15	0.107	0.030	1.1236	0.9938	0.8145							
7H2	1.53	1.61	0.199	0.056	1.3368	0.9727	0.7142							
7I2	1.85	1.86	0.279	0.080	1.3975	0.9914	0.6466							
7J2	2.03	2.09	0.342	0.097	1.4808	0.9873	0.6177							
7K2	1.87	1.95	0.245	0.070	1.5169	0.9912	0.7063							
7L2	1.97	2.03	0.274	0.077	1.5369	0.9877	0.6847							
7M2	1.96	2.00	0.372	0.107	1.3819	0.9863	0.5728							
7N2	1.84	1.88	0.275	0.079	1.4178	0.9930	0.6543							
7O2		2.32	0.340	0.097	1.6349	0.9991	0.6560							
7P2	2.09	2.10	0.335	0.095	1.4919	0.9925	0.6254							
7Q2		2.29	0.434	0.124	1.5162	0.9991	0.5688							
7R2	1.61	1.66	0.237	0.068	1.3045	0.9912	0.6636							
7S2		2.03	0.316	0.090	1.4718	0.9949	0.6345							
7T2	0.81	0.81	0.075	0.022	0.7610	0.9924	0.8098							
8A		3.26	0.710	0.202	1.8063	0.9943	0.5194							
8B		4.78	0.601	0.179	2.3976	0.9606	0.6924	1.39	1.46	0.186	0.053	1.2262	0.9911	0.7030
8C		4.94	1.056	0.300	2.2308	0.9994	0.5265	1.79	1.85	0.189	0.054	1.5518	0.9907	0.7772
8D								1.45	1.48	0.195	0.056	1.2307	0.9961	0.6929
8E														
8F														
9A		2.91	0.572	0.162	1.7314	0.9910	0.5538		2.08	0.260	0.074	1.5819	0.9908	0.7081
9B		2.95	0.457	0.130	1.8474	0.9855	0.6360		2.79	0.328	0.094	1.9034	0.9960	0.7301
9C		5.07	1.124	0.320	2.2412	1.0000	0.5136							
9D		2.92	0.495	0.141	1.7980	0.9997	0.6047	2.71	0.513	0.146	1.6825	0.9996	0.5682	
9E	1.82	1.90	0.255	0.072	1.4689	0.9869	0.6857							
9F		4.28	1.377	0.392	1.9217	1.0000	0.3873	3.86	0.558	0.159	2.1457	0.9826	0.6597	
10A1	1.84	1.85	0.820	0.234	0.9481	0.9935	0.2773							
10A2								0.40	0.40	0.127	0.037	-0.4679	0.9932	0.3852
10B1		2.00	1.98	0.850	1.0271	0.9915	0.2877							
10B2								1.03	1.11	0.142	0.041	0.9438	0.9782	0.6999
10C1		1.83	1.84	0.817	0.232	0.9442	0.2773							
10C2								1.31	1.35	0.253	0.072	0.9786	0.9909	0.5694
10D1		4.68	0.946	0.269	2.2004	1.0000	0.5456							
10D2	1.64	1.67	0.279	0.080	1.2487	0.9938	0.6106	1.73	1.73	0.328	0.094	1.2291	0.9965	0.5664

Total air leakage (Q_t) continued

	Storm Window Up or Off							Storm Window Down or On							
	Actual Q 0.30	Reg Q 0.30	Reg Q 0.016	ELA	Constant	R ²	X coef	Actual Q 0.30	Reg Q 0.30	Reg Q 0.016	ELA	Constant	R ²	X coef	
11 A	0.67	0.68	0.059	0.017	0.6196	0.9809	0.8346								
11 B	0.42	0.45	0.071	0.020	-0.0384	0.9915	0.6296								
11 C	0.42	0.44	0.087	0.025	-0.1577	0.9865	0.5505								
11 D	0.56	0.54	0.116	0.033	-0.0039	0.9758	0.5189								
11 E	0.90	0.89	0.097	0.027	0.7947	0.9926	0.7580								
11 F	0.40	0.40	0.070	0.019	-0.2217	0.9876	0.5904								
12 A		4.65	1.051	0.299	2.1488	0.9528	0.5076		3.50	0.533	0.152	2.0234	0.9983	0.6417	
12 B		2.67	0.399	0.113	1.7625	0.9820	0.6486		2.63	0.379	0.108	1.7623	0.9890	0.6606	
12 C	2.12	2.16	0.267	0.076	1.6293	0.9936	0.7134	2.12	2.14	0.283	0.081	1.5924	0.9961	0.6906	
12 D		2.59	0.271	0.077	1.8814	0.9924	0.7710		2.56	0.280	0.080	1.8481	0.9874	0.7548	
12 E		3.31	0.550	0.156	1.9362	0.9978	0.6128		3.50	0.352	0.100	2.1940	0.9866	0.7832	
12 F	1.61	1.75	0.137	0.039	1.6152	0.9915	0.8723	1.61	1.73	0.130	0.037	1.6154	0.9922	0.8832	
12 G		4.32	0.524	0.150	2.3291	0.9944	0.7193		3.67	0.453	0.129	2.1571	0.9978	0.7131	
12 H		4.91	0.832	0.237	2.3192	0.9989	0.6053		3.05	0.409	0.116	1.9369	0.9845	0.6847	
12 I		5.20	0.972	0.277	2.3376	0.9999	0.5722		3.40	0.593	0.169	1.9402	0.9961	0.5956	
12 J															
13 A		3.65	0.718	0.204	1.9619	0.9998	0.5538		2.54	0.519	0.147	1.5831	0.9992	0.5415	
13 B		3.37	0.665	0.189	1.8816	0.9984	0.5537		2.79	0.394	0.112	1.8262	0.9792	0.6668	
13 C		5.42	1.202	0.342	2.3081	1.0000	0.5136		4.73	0.749	0.213	2.3113	0.9987	0.6289	
13 D		3.51	0.742	0.211	1.8930	0.9951	0.5299		3.07	0.650	0.185	1.7562	0.9827	0.5289	
13 E		3.02	0.661	0.188	1.7325	0.9844	0.5191		2.66	0.483	0.138	1.6781	0.9924	0.5820	
13 F		2.96	0.726	0.207	1.6641	0.9665	0.4797		2.91	0.540	0.154	1.7567	0.9964	0.5737	
13 G		3.39	0.627	0.179	1.9115	0.9976	0.5748		3.01	0.586	0.167	1.7767	0.9939	0.5588	
13 H		4.32	0.543	0.155	2.3145	0.9983	0.7072		3.46	0.507	0.144	2.0336	0.9881	0.6564	
13 I		3.43	0.678	0.193	1.9004	0.9984	0.5537		2.93	0.593	0.169	1.7314	0.9966	0.5450	
13 J	2.04	2.13	0.277	0.079	1.5943	0.9928	0.6963	1.99	2.07	0.236	0.067	1.6196	0.9786	0.7411	
14 A	1.74	1.71	0.288	0.070	1.3329	0.9803	0.6631	1.13	1.13	0.096	0.027	1.1369	0.9908	0.8423	
14 B		3.13	0.670	0.190	1.7755	0.9762	0.5260	1.69	1.61	0.238	0.068	1.2681	0.9947	0.6543	
14 C		2.75	0.449	0.127	1.7591	0.9978	0.6194	1.69	1.75	0.215	0.061	1.4260	0.9911	0.7164	
14 D	1.41	1.57	0.158	0.045	1.3896	0.9727	0.7813	1.01	0.99	0.117	0.033	0.8734	0.9947	0.7302	
14 E	2.23	2.16	0.618	0.175	1.2855	0.9950	0.4275	0.57	0.59	0.114	0.032	0.1482	0.9909	0.5618	
14 F		2.16	0.582	0.166	1.3115	0.9785	0.4481	0.42	0.42	0.097	0.028	-0.2657	0.9991	0.4995	
15 A 1									6.16	1.250	0.355	2.4708	1.0000	0.5435	
15 A 2								0.31	0.32	0.135	0.039	-0.7846	0.9833	0.2954	
15 B 1		5.43	1.092	0.311	2.3519	1.0000	0.5474		3.94	1.025	0.292	1.9226	0.9814	0.4588	
15 B 2								0.36	0.36	0.144	0.041	-0.6594	0.9742	0.3097	
15 C 1									0.42	0.41	0.245	0.070	-0.6771	0.9787	0.1756
15 C 2									6.08	1.288	0.366	2.4415	1.0000	0.5291	
15 D 1								0.26	0.26	0.085	0.025	-0.8961	0.9916	0.3785	
15 D 2															
16 A									4.75	0.823	0.235	2.2778	1.0000	0.5978	
16 B									2.97	1.140	0.324	1.4830	1.0000	0.3270	
16 C												0.0733			
16 D												0.0733			
16 E		4.87	1.023	0.291	2.2263	0.9984	0.5329					0.0733			
16 F		5.47	0.985	0.280	2.4033	1.0000	0.5850					0.0733			
16 G		4.30	0.731	0.208	2.1866	0.9995	0.6046					0.0733			
17 A	2.43	2.44	0.477	0.136	1.5617	0.9939	0.5568	2.43	2.49	0.399	0.113	1.6595	0.9946	0.6236	
17 B	2.08	2.20	0.311	0.088	1.5905	0.9930	0.6673	1.99	2.09	0.293	0.083	1.5446	0.9948	0.6711	
17 C	2.66	2.66	0.566	0.160	1.6109	0.9852	0.5273	2.49	2.58	0.468	0.133	1.6527	0.9870	0.5831	
18 A	0.87	0.85	0.096	0.027	0.7280	0.9956	0.7427					0.0733			
18 B	0.70	0.65	0.100	0.028	0.3280	0.9942	0.6364					0.0733			
19 A	1.66	1.72	0.244	0.069	1.3503	0.9903	0.6677	1.54	1.61	0.224	0.063	1.2883	0.9886	0.6738	
19 B	1.27	1.31	0.157	0.044	1.1439	0.9907	0.7247	1.10	1.13	0.136	0.039	0.9985	0.9967	0.7247	

D. Numerical conversions and transformations

D.1 Data standardization

Air flow measurements (Q_t and Q_c) were recorded in "actual cubic feet per minute" (acfm) under ambient conditions. The sash flow difference (Q_s) was converted to "standard cubic feet per minute" (scfm) by the following formula, based on standard reference conditions listed in ASTM E 783-93 (ASTM 1994d):

$$scfm = acfm * \frac{293.8 K}{273 K + \frac{(^{\circ}F - 32) * 5}{9}} * \frac{atm P}{760 mm Hg}$$

The unit scfm was referenced to standard conditions at 20.8°C (293.8 Kelvin) and one atmosphere of pressure (760 mm Hg), meaning readings in scfm would generally be larger than readings in acfm due to the cooler ambient air temperatures. Converting to scfm allowed for valid comparisons of air leakage between windows of equal sizes tested under differing environmental conditions.

D.2 Standard cubic feet per minute per linear foot crack

Windows were found in varying dimensions and comparison of leakage rates through different sized windows was therefore not valid. As an example, the larger of two windows with identical leakage characteristics excepting size, would always show a larger leakage rate at a given pressure differential than the smaller window due to its larger operable crack length. A method of standardizing window size was employed to remove size bias. This was accomplished by expressing Q_s as standard cubic feet per minute per linear foot crack (scfm/lfc) which represented the amount of air flowing through a unit length of operable window crack. Operable crack was defined as the meeting rail and junctures between movable sash and jambs. For a double-hung window, the formula for operable linear foot crack (lfc) was:

$$lfc = \frac{(2 * Height + 3 * Width)}{12 in./ft}$$

where *height* and *width* were the window dimensions in inches. The linear foot crack number (lfc) was divided into the appropriate flow rate (generally Q_s) to obtain scfm/lfc, a number descriptive of the leakage characteristics of the window independent of temperature, pressure, and window size. The standardized flow rates per operable linear crack (scfm/lfc) were listed for the pressure differentials attained for each window and were the numbers normally used for comparative purposes.

D.3 Standard cubic feet per minute per square foot of sash-area

A second method of presenting a standardized leakage rate was as standard cubic feet per minute per square foot of sash area (scfm/ft²). The formula for the sash area of a double-hung window was:

$$\text{Sash Area (ft}^2\text{)} = \frac{(\text{Height} * \text{Width})}{144 \text{ in.}^2/\text{ft}^2}$$

where *height* and *width* were the window dimensions in inches. Once again, this number was divided into the appropriate flow rate to attain the standard flow per square foot of sash area (scfm/ft²).

When more than one type of window is in a house (*ie.*, double-hung and casement windows) and windows are being compared to one another, the flow per sash area (scfm/ft²) may be both more appropriate and accurate. This is due to the operating characteristics of differing window types. Double- and single-hung windows of identical size showing equivalent leakage rates when expressed as scfm/lfc do not have equivalent flows when viewed as total air leakage through the sash. The flow through a double-hung window is approximately 70% greater than the flow through a single-hung window of equal size as an allowance is given for the increased operable crack length in a double-hung window. (Most manufacturers of new windows list air infiltration data in terms of scfm/lfc, however, regardless of the window type.)

D.4 Effective leakage area

A third comparative method and also used in the LBL correlation model was the effective leakage area (ELA). The ELA was used to characterize the natural air infiltration of a building at a pressure differential of 0.016 inches of water pressure. Extrapolation to the reference pressure was based field data fitted to the standard flow formula:

$$Q = c * \Delta P^x$$

where

Q = air leakage in scfm or scfm/lfc

ΔP = pressure differential

c = leakage coefficient

x = leakage exponent

Characterization of the leakage was accomplished by equilibrating the measured air leakage to an opening of a specific area that allows an equivalent leakage. Both x and c are regression coefficients determined from linear regression. ELA calculation is detailed in ASTM E 779-87, *Standard Test Method for Determining Air Leakage Rate by Fan Pressurization*, and was used to characterize air leakage rates through windows for the purposes of this project. Use of an ELA value allowed air openings in a window to be

expressed as one total area for comparative purposes. Flow rates for all windows were converted to standard cubic feet per minute per linear foot crack (scfm/lfc) prior to ELA calculation to facilitate comparisons between windows of differing dimensions and varying environmental conditions.

ASTM E 779-87 lists a conventional reference pressure of 4 Pascals (Pa), equivalent to 0.016 inches of water pressure. Both metric (SI) and conventional (inch-pound, IP) formulations are given by ASTM for calculating ELA with the metric formulation being the preferred format. Calculated ELA's used in the study were based on the IP formula as most data had been recorded in IP units. Both formulations yield equivalent results when converted to common units. The IP formula is given below:

$$ELA = 0.1855 * c * \Delta P^{(x-0.5)} * (\rho_e/2)^{0.5}$$

where

ELA = equivalent leakage area (square inches)

c = leakage coefficient from linear regression

x = leakage exponent from linear regression

ΔP = 0.016 inches of water pressure

ρ_e = 0.07517 lbm/ft³ (the density of air)

0.1855 = conversion factor

E. Field data sheets

E.1 Window data sheet

Date: _____ Time: _____
 Project Name: _____ Location: _____

Orientation: _____
 Temperature (°F) - Interior: T_{dry} - _____ T_{wet} - _____ Exterior: T_{dry} - _____ T_{wet} - _____
 P_{atm} (mm Hg): _____ Wind: speed (mph) - _____ direction - _____

Window type: _____ Single pane: _____ Multipane: _____ x _____
 Pane Size (in.) - _____ x _____

Dimensions (in.): Total Height - _____ Sash Width - _____
 Upper Sash - _____ Sash Depth - _____
 Lower Sash - _____

Window weight cavity: Y N Connected? Y N

Locking mechanism: Y N Operable: Y N NA
 Type: _____ Location(s): _____

Storm Window Type: Aluminum Aluminum Wood Other: _____
 triple double sash _____
 None track track _____

Comments: _____

Storms up or no storms Storms down

ΔP (in H ₂ O)	Q_i (acfm)	Q_e (acfm)	Q_i (acfm)	Q_e (acfm)
0.30				
0.25				
0.20				
0.15				
0.10				
0.07				
0.05				
0.03				

E.2 Physical condition check sheet

Physical Condition		Excellent								Poor	
Upper Sash	Putty condition	10	9	8	7	6	5	4	3	2	1
	Glass tight	10	9	8	7	6	5	4	3	2	1
	Fit to frame	10	9	8	7	6	5	4	3	2	1
	Square in frame	10	9	8	7	6	5	4	3	2	1
Lower Sash	Putty condition	10	9	8	7	6	5	4	3	2	1
	Glass tight	10	9	8	7	6	5	4	3	2	1
	Fit to frame	10	9	8	7	6	5	4	3	2	1
	Square in frame	10	9	8	7	6	5	4	3	2	1
Frame	Stops tight	10	9	8	7	6	5	4	3	2	1
	Tight to trim	10	9	8	7	6	5	4	3	2	1
Meeting Rail	Tight fit	10	9	8	7	6	5	4	3	2	1
Exterior Caulking		10	9	8	7	6	5	4	3	2	1

E.3 Physical condition criteria

Upper and Lower Sash

Putty Condition - Generally, it is the bottom glazing of each sash that weathers most quickly and it is this border that is the primary determinant for putty condition.

10 - Relatively new putty with no cracks.

9-7 - Putty is intact but has varying degrees of cracks.

6-4 - Putty is intact but obviously dried out, large cracks, some flaking apparent.

3-2 - Portions of the putty missing, less than one inch total.

1 - Greater than one aggregate linear inch of putty missing or a gap between the glass and sash is evident.

Glass Tightness - This is very much a function of the putty condition and the putty condition number is considered when determining tightness. Overall tightness is determined by tapping around the perimeter(s) of the glass pane(s). Caution is taken to ensure that only the sash being tapped is causing any vibratory noise.

10-7 - Glass shows little to no vibrations.

6-4 - Glass vibrates and sounds loose.

3-1 - Glass visibly moves under slight pressure. A putty condition of 1 by definition has a glass tightness of 1.

Fit to Frame - This is a combination of visual and physical inspections. The sash is visually inspected for gaps between the jambs and sash and the lower sash is viewed from above for gap symmetry on either edge. Each sash is physically moved from side to side and front to back while unlatched to subjectively determine play.

10-8 - No gaps, fairly symmetrical, little play in either direction.

7-5 - No gaps, somewhat asymmetrical, play in either direction is becoming pronounced.

4-3 - Small gaps are apparent, sash may be asymmetrical, significant lateral play.

2-1 - Easily noticeable gaps, sash readily moves laterally.

Square in Frame - Squareness is also incorporated in Fit to Frame but is also important enough to warrant its own category and is visually determined relative to the jambs and parting beads if present.

10-8 - Sash appears square with exposed stiles being symmetrical and rails being horizontal.

7-4 - Sash is skewed up to 1/4 inch with exposed stiles being asymmetrical.

3-1 - Sash is skewed more than 1/4 inch.

Frame

Stops Tight - This is determined both visually and physically by tapping the stops and listening for vibrations. Paint also is a consideration. Stops are not considered individually but as a unit.

10-8 - Stops are flush to jambs with no discernable vibration when tapped. Wood may be painted with little to no cracking of the paint along the

stop edge.

7-5 - Stops vibrate when tapped and have visible cracks up to approximately 1/16 inch for 1/4 aggregate stop length.

4-2 - Stops vibrate freely when tapped and have cracks up to approximately 1/8 inch for 1/4 to 1/2 aggregate stop length.

1 - Stops are missing or not held in place and may fall when tapped. Gaps greater than 1/8 inch are present.

Tight to Trim - Determined by visual inspection of the trim to wall juncture.

10-8 - No visible crack to a hairline crack being apparent around any portion of the trim.

7-5 - Narrow crack around 1/4 to 1/2 of trim.

4-3 - Crack extends around entire frame and varies in width.

2-1 - Crack is large (1/8 inch); frame is not flush with the wall.

Meeting Rail

Tight Fit - The meeting rail is examined while sashes are latched (when latches are present and operable) as this is the expected normal winter operating mode. The interface of the sashes is examined for tightness and whether the upper and lower sashes are horizontal and flush in the vertical direction or are skewed.

10-8 - Horizontal, flush, and with a tight interface.

7-4 - Horizontal but not flush and/or slightly skewed with an interface that is not tight for the entire length.

3-1 - Meeting rail is neither horizontal nor flush with an interface that does not fully meet or exhibits poor juncture.

Exterior Caulking - A visual inspection is done to ensure all exterior portions of the window unit are present as well as the window unit/exterior wall caulking.

10-8 - Caulking appears to be intact and in good condition.

7-5 - Caulking appears dry and weathered with cracks and minor flaking apparent.

4-2 - Caulking is crumbling, flaky, and missing in areas.

1 - Some exterior window segments are missing as well as large amounts of caulking.

F. Data sheet interpretation

An example of the transformed air leakage data for an individual window is found on the page *Reference Data Sheet*. Window identification and a brief description are found on line 17. Above that are the relevant parameters necessary for standardization of the air flow. Block B22 through B29 are the pressure differentials in inches of water pressure used during a test run. Block B 30 (0.016 in. H₂O) is equivalent to 4 Pa, the standard reference pressure for ELA's. The 0.016 inches of water pressure differential was assumed to be the annual average heating season differential between interior and exterior pressures and was assumed to be the driving force for natural infiltration. This value was used to compute the effective leakage area (ELA). Window manufacturers report test results at 0.30 inches of water pressure for new windows, equivalent to 75 Pascals. This pressure, 0.30 inches of water, is the reference pressure used in this summation so as to allow comparison with replacement windows.

Blocks C22-29 and D22-29 are the total air flows and extraneous air flows respectively with the storm window open, both expressed as actual cubic feet per minute (acfm). Block E22-29 is the sash flow in standard cubic feet per minute (scfm). Block F22 through H29 shows the same flows for the window with the storm window closed.

Window dimensions are found in block I22 to J23 and were used to standardize the sash flows (Q_s) to standard cubic foot per minute per linear foot crack (scfm/lfc) or per square foot (scfm/ft²). Standardized sash flow per linear foot crack data are found in block K22 to N29 for windows with storm windows both open and closed.

The mathematical model used to describe the induced flow of air through the window is a widely used model for air flow:

$$Q_s = c * \Delta P^x$$

where

ΔP = pressure differential

c = leakage coefficient

x = leakage exponent.

The variables x and c need to be determined, but the model as written mathematically describes half a parabola. A natural logarithmic transformation linearizes the data, allowing x and c to be determined by linear regression. Linear regression compares data to a straight line. This transformation linearizes the data in the following manner:

$$Q_s = c * \Delta P^x$$

$$\ln Q_s = \ln c + x * \ln \Delta P$$

which is analogous to the straight line equation:

$$y = b + mx$$

where

ln c = constant, b (the y intercept)

x = x coefficient, m (the slope)

Blocks B34-42, D34-42, and J34-42 are respectively, the natural logarithms of the pressure differentials and scfm/lfc's for windows with storms open and closed. Linear regression was performed on these data to determine c (Constant) and x (X Coefficient), found in block E33 to H41. Linear regression also provided an estimate of how well the data fit the model, known as the goodness-of-fit value (R^2). The closer this value is to 1.000, the better the data fit the model.

The x and c values, along with the pressure differentials, were used to determine "best fit" data based on the mathematical model. It was these data that were usually used for comparative purposes as opposed to the raw data, due to the leaky nature of many windows tested. These data are found in block P22 to Q30, with P30 and Q30 being the values at 0.016 inches of water pressure (4 Pa).

The regression coefficients x and c were used with the reference pressure 0.016 inches of water to calculate the effective leakage area in square inches (ELA) as previously described. This value is found in block P34 to Q34. To gain a better understanding of the size of the effective leakage area, the ELA was assumed to be a square with the length of one side given in block P37 to Q37.

G. Exterior air

G.1 Determination of percent exterior air in Q_e

Infiltration of exterior air not only occurred through the window sash and sash/frame junction (Q_s), but also through the rough opening as extraneous air (Q_e), adding to the heating load. Quantifying the volume of exterior air is important in understanding the total heat load due to a window. The following field method was devised and implemented to approximate the volume of exterior air contained in the induced extraneous air leakage.

An estimate of the volume of exterior air coming through the rough opening may be calculated by knowing the temperature between the two sheets of plastic while testing for extraneous air (Q_e) along with the ambient exterior and interior air temperatures. Knowing these three data points and any measured value of Q_{ext} , a mass balance on temperature and air flow may be performed to estimate the volume of exterior air in Q_e . The volume of exterior air in Q_e was determined by the following formula:

$$Q_{ext} = \frac{Q_e * (T_{win} - T_{int})}{(T_{ext} - T_{int})}$$

where:

Q_{ext} = the volume of exterior air (acfm)

Q_e = the volume of air chosen from extraneous air test data (acfm)

T_{win} = the temperature between the two plastic sheets during the test (°F)

T_{int} = ambient interior air temperature (°F)

T_{ext} = ambient exterior air temperature (°F)

The volume of exterior air (Q_{ext}) was converted to a percentage by dividing through by Q_e . If the percentage of interior air (Q_{int}) in Q_e is desired, it may be calculated by subtracting the Q_{ext} percentage from 100%, or directly by the following formula if Q_{ext} is not known:

$$Q_{int} = \frac{Q_e * (T_{win} - T_{ext})}{(T_{int} - T_{ext})}$$

where the variables are the same as those in the previous equation.

The amount of exterior air entering through the rough opening was calculated for 36 windows at five different locales. Data from three windows in Irasburg (windows 16E, 16F, and 16G) were not included in an average value as direct sunlight had been heating the wall during the early to mid-morning period prior to testing. Testing of these three windows occurred while the wall was shaded but the calculated exterior air percentages (88%, 88%, and 67%) appeared abnormally large when compared to the other 33 windows. The assumption was made that the wall had not returned to the ambient air temperature prior to testing, and the data was discounted.

The average percentage of exterior air entering the buildings through the rough openings of 33 windows was 29%, meaning approximately 30% of the measured air in the

The average percentage of exterior air entering the buildings through the rough openings of 33 windows was 29%, meaning approximately 30% of the measured air in the Q_c test must be heated during the heating season and must count towards the heating load of a typical window. The percentage of exterior air in Q_c for the 33 windows is summarized in the following table:

Table 27: Percentage of Q_{ext} in Q_c for 33 windows

Average value of Q_{ext}	28.6%
Maximum value of Q_{ext}	54.5%
Minimum value of Q_{ext}	7.7%

Both pin- and pulley-type windows were included in the 33 windows, with pin type windows averaging 26% exterior air passing through the rough opening versus 31% for the pulley-type windows.

Of the 33 windows used to estimate a typical value for the percentage of exterior air in Q_c , all but two were the original sash after refurbishing. Windows 12B and 12C were both in-kind replacement sash with vinyl jamb liners. Both replacement windows have low exterior air percentages (12.5% and 13.2%), although some original sash windows (7B2, 7O2, 12F, 13B, 14B, 14C, and 14D) are of equivalent tightness in terms of Q_{ext} .

This method of estimating the volume of exterior air entering the test zone during testing periods has severe limitations and values thus derived should not be assumed to be accurate. Temperatures in the test zone stabilized within a minute, but it is unknown whether steady state conditions had been reached within the building walls. No attempt was made to determine the actual air path through the wall cavities while a window was under pressure. Exterior air likely increased its temperature as it passed through walls warmer than the ambient exterior atmospheric temperature, raising questions as to the accuracy of the temperature readings in the test zone. The method was used to determine a rough approximation of the contribution of extraneous air to the overall heating load.

G.2 Experimental data used to determine percentage exterior air

Window ID	T _{int} (°F)	T _{win} (°F)	T _{ext} (°F)	Q _e (acfm)	Q _{ext} (acfm)	Percent Ext. Air
7A 2	62	58	48	32	9.1	28.6
7B 2	61	60	48	42	3.2	7.7
7C 2	65	61	53	18	6.0	33.3
7D 2	65	59	53	9.7	4.9	50.0
7E 2	63	59	52	30	10.9	36.4
7F 2	60	57	52	20	7.5	37.5
7G 2	60	58	54	19	6.3	33.3
7J 2	58	51	38	18	6.3	35.0
7K 2	62	56	39	20	5.2	26.1
7L 2	62	55	41	17	5.7	33.3
7M 2	61	56	44	20	5.9	29.4
7N 2	62	57	46	25	7.8	31.3
7O 2	60	58	48	31	5.2	16.7
7P 2	61	57	51	20	8.0	40.0
7Q 2	60	58	51	40	8.9	22.2
12A	70	61	51	40	18.9	47.4
12B	72	69	48	40	5.0	12.5
12C	71	66	33	29	3.8	13.2
12F	71	68	51	22	3.3	15.0
12G	69	60	46	22	8.6	39.1
12H	71	62	46	38	13.7	36.0
12 I	72	63	45	37	12.3	33.3
12 J	71	66	44	39	7.2	18.5
13A	71	66	54	35	10.3	29.4
13B	70	68	56	34	4.9	14.3
13G	69	64	50	38	10.0	26.3
14B	65	63	50	25	3.3	13.3
14C	64	62	52	24	4.0	16.7
14D	64	62	50	15	2.1	14.3
14E	62	57	49	20	7.7	38.5
14F	62	56	51	19	10.4	54.5
14F 2	60	58	51	7.56	1.7	22.2
16B	54	57	62	36	13.5	37.5
16E**	63	68	69	33	27.5	83.3
16F**	65	70	71	31	25.8	83.3
16G**	65	69	71	39	26.0	66.7

**Wall may still be retaining heat from direct sunlight. Data excluded.

H. Equations for weather parameters based on psychrometric data

H.1 Determining dew point temperature and partial water vapor pressure

Calculations to determine dew point temperature (t_d) and partial water vapor pressure (p_w) given field measurements of weather parameters dry-bulb temperature (t), wet-bulb temperature (t^*), and atmospheric pressure (p):

Absolute temperature, T_{abs} or T^*_{abs} (in degrees Rankine):

$$T_{abs} = t + 459.67$$

or

$$T^*_{abs} = t^* + 459.67$$

where

t = dry-bulb temperature ($^{\circ}\text{F}$)

t^* = wet-bulb temperature ($^{\circ}\text{F}$)

Natural logarithm of the saturation water vapor pressure, p^*_{ws} , at T^*_{abs} :

$$\ln(p^*_{ws}) = \frac{C_1}{T^*_{abs}} + C_2 + C_3 * T^*_{abs} + C_4 * (T^*_{abs})^2 + C_5 * (T^*_{abs})^3 + C_6 * (\ln T^*_{abs})$$

where

$$C_1 = -1.044\ 039\ 708 * 10^4$$

$$C_2 = -1.129\ 464\ 96 * 10^1$$

$$C_3 = -2.702\ 235\ 5 * 10^{-2}$$

$$C_4 = 1.289\ 036\ 0 * 10^{-5}$$

$$C_5 = -2.478\ 068 * 10^{-9}$$

$$C_6 = 6.545\ 967\ 3$$

Saturation humidity ratio, W^*_s , at the wet-bulb temperature, t^* :

$$W^*_s = 0.62198 * \frac{p^*_{ws}}{p - p^*_{ws}}$$

where

p^*_{ws} = saturation vapor pressure

p = atmospheric pressure (psia)

Humidity ratio, W :

$$W = \frac{(1093 - 0.556t^*) W_s^* - 0.240(t - t^*)}{1093 + 0.444t - t^*}$$

where

W_s^* = saturation humidity ratio

t = dry-bulb temperature

t^* = wet-bulb temperature ($^{\circ}\text{F}$)

Partial pressure of water vapor, p_w , for moist air:

$$p_w = \frac{p * W}{0.62198 + W}$$

where

p = atmospheric pressure (psia)

W = humidity ratio

Dew point temperature, t_d :

$$t_d = 100.45 + 33.193 * (\ln p_w) + 2.319 * (\ln p_w)^2 + 0.17074 * (\ln p_w)^3 + 1.2063 * (p_w)^{0.1984}$$

where

p_w = partial water vapor pressure

H.2 Determining relative humidity

Calculations to determine relative humidity (ϕ) given field measurements of weather parameters dry-bulb temperature (t), wet-bulb temperature (t^*), and atmospheric pressure (p):

Natural logarithm of the saturation water vapor pressure, p_{ws} , at T_{abs} :

$$\ln(p_{ws}) = \frac{C_1}{T_{abs}} + C_2 + C_3 * T_{abs} + C_4 * T_{abs}^2 + C_5 * T_{abs}^3 + C_6 * (\ln T_{abs})$$

where

$$C_1 = -1.044\ 039\ 708 * 10^4$$

$$C_2 = -1.129\ 464\ 96 * 10^1$$

$$C_3 = -2.702\ 235\ 5 * 10^{-2}$$

$$C_4 = 1.289\ 036\ 0 * 10^{-5}$$

$$C_5 = -2.478\ 068 * 10^{-9}$$

$$C_6 = 6.545\ 967\ 3$$

Saturation humidity ratio, W_s , at the dry-bulb temperature, t :

$$W_s = 0.62198 * \frac{p_{ws}}{p - p_{ws}}$$

where

p_{ws} = saturation water vapor pressure at the dry-bulb temperature

p = atmospheric pressure (psia)

Degree of saturation, μ , at a given temperature and pressure (t, p):

$$\mu = \frac{W}{W_s}$$

where

W = humidity ratio

W_s = saturation humidity ratio

Relative humidity, ϕ :

$$\phi = \frac{\mu}{1 - (1 - \mu) \frac{p_{ws}}{p}}$$

where

μ = degree of saturation

p = atmospheric pressure (psia)

p_{ws} = saturation water vapor pressure at the dry-bulb temperature

I. Assumptions for using WINDOW 4.1

All windows modeled are double-hung (vertical sliders) measuring 36 x 60 inches. Interior and exterior temperatures were 70°F and 0°F respectively, with a 15 mph wind blowing.

Assumed typical and tight window parameters:

1. wood sash;
2. double-glazed with second layer consisting of a storm window 2.5 inches from primary sash (average distance between storm and upper and lower primary sash).
Glass is clear with air between glazing layers.

Assumed loose window parameters:

1. wood sash;
2. single-glazed with no storm window. Glass is clear.

In-kind, two over two replacement sash parameters:

1. wood sash;
2. double-glazed with second layer consisting of a storm window 2.5 inches from primary sash (average distance between storm and upper and lower primary sash).
Glass is clear with air between glazing layers.

Double-pane insulating glass, replacement window insert parameters:

- 1a. wood sash;
- 2a. double-glazed with second layer 0.500 inches from primary sash. Glass is clear with air between glazing layers.

1b. vinyl sash;

- 2b. double-glazed with second layer 0.500 inches from primary sash. Glass is clear with air between glazing layers.

The following windows were modeled using WINDOW 4.1 but were not encountered in the field:

1. low-e replacement sash with standard storm window;
2. standard replacement sash with low-e storm window;
3. replacement sash with double-glazed low-e insulating glass; and
4. replacement window inserts with low-e double-glazed insulating glass.

J. LBL Correlation Model Computer Printout

01/17/97

Historic Window Project
 Average Heating Season Infiltration Rate, Based on Equivalent Leakage Area (ELA)
 Based on LBL Blower Door Data/ Infiltration Rate Correlation

Volume 30,000 22,900
 Pressure 4 Pa
 4 Pa ELA 1.480 (in²) 0.588
 A_o 0.000955 total leakage area (m²)
 A_c 0.000315 leakage area in the ceiling (m²)
 A_f 0.000315 leakage area in the floor (m²)
 R 0.6600
 X 0.0000
 H 5.7912 height of the roof (m)
 y 0.23 terrain parameter #1 (see table)
 a 0.73 terrain parameter #2 (see table)
 Γ 0.757 terrain factor
 C' 0.24 shielding coefficient (see table)
 Γ_W 0.1675 wind parameter
 Γ_W' 0.1269 reduced wind parameter
 f_s 0.4433 stack parameter
 Volume 30000 (ft³)
 Volume 849.6 (m³)
 T_i 68 Winter Indoor Avg. Temp. (°F)

Q_{nat} value at C7.

Site 12, storm windows closed

ELA_{tot} = 1.48 in²

Q_{nat} = 2.069 scfm

Month	ACH	Q _{tot} (m ³ /se)	Q _{wind} (m ³ /sec)	Q _{stack} (m ³ /sec)	VT-wind		f _s	VT-temp			Burlington						
					v'	v's		TIF	ToF	TIK	ToK	Avg Tem	Avg DDays				
JAN	0.0047	0.0011	0.0005	0.0010	4.25	1.04	0.20	68	17	293.2	264.9	15	1,494	0.19292	JAN		
FEB	0.0046	0.0011	0.0005	0.0010	4.11	1.02	0.20	68	19	293.2	266.0	17	1,299	0.16774	FEB		
MAR	0.0043	0.0010	0.0005	0.0009	4.20	0.91	0.20	68	29	293.2	271.5	19	1,113	0.14372	MAR		
APR	0.0036	0.0009	0.0005	0.0007	4.16	0.73	0.20	68	43	293.2	279.3	29	660	0.08523	APR		
MAY	0.0029	0.0007	0.0005	0.0005	3.93	0.52	0.20	68	55	293.2	286.0	43	331	0.04274	MAY		
JUN	0.0023	0.0005	0.0004	0.0003	3.71	0.32	0.19	70	65	294.3	291.5			0	JUN		
JUL	0.0022	0.0005	0.0004	0.0003	3.53	0.32	0.19	75	70	297.1	294.3			0	JUL		
AUG	0.0021	0.0005	0.0004	0.0003	3.31	0.32	0.19	72	67	295.4	292.6			0	AUG		
SEP	0.0026	0.0006	0.0004	0.0004	3.62	0.44	0.20	68	59	293.2	288.2	59	191	0.02466	SEP		
OCT	0.0032	0.0008	0.0005	0.0006	3.84	0.63	0.20	68	49	293.2	282.6	49	502	0.06482	OCT		
NOV	0.0039	0.0009	0.0005	0.0008	4.25	0.81	0.20	68	37	293.2	276.0	37	840	0.10847	NOV		
DEC	0.0045	0.0011	0.0005	0.0009	4.38	0.98	0.20	68	23	293.2	268.2	23	1314	0.16968	DEC		
Average Annual	0.0034	0.0008	0.0005	0.0006												7744	0.00421
Oct-Apr Average	0.0041	0.0010	0.0005	0.0008												DDay weighted avg	

AVERAGE PREDICTED INFILTRATION RATES		
TEST DATE: 06/28/94		
	Air Changes per Hour	Average cfm
Average Annual	0.0034	1.715
Oct-Apr Average	0.0041	2.069
	Wind-Driven	Stack-Driven
Average Annual	43%	57%
Oct-Apr Average	38%	62%